University
of Ljubljana
Faculty
for Civil and Geodetic
Engineering

JASNA DONEVSKA

ANALYSIS OF UNCERTAINTIES IN THE PROCESS OF FLOOD HAZARD MAPS ELABORATION

MASTER'S THESIS

MASTER STUDY PROGRAMME FLOOD RISK MANAGEMENT

Ljubljana, 2022

University
of Ljubljana
Faculty
for Civil and Geodetic Engineering

Candidate
JASNA DONEVSKA

ANALYSIS OF UNCERTAINTIES IN THE PROCESS OF FLOOD HAZARD MAPS ELABORATION

Master's thesis no.:

Mentor:
Assist. Prof. Simon Rusjan, PhD

Co-mentor:
Prof. Matjaž Mikoš, PhD

Commission member:
Prof. Mojca Šraj, PhD

Chairman of the Commission:
Assoc. Prof. Nataša Atanasova, PhD

IHE examiner:
Assoc. Prof. Shreedhar Maskey, PhD

Ljubljana, 2022

"This page is intentionally blank"

ERRATA

Error page	Error bar	Instead	Let it be

ACKOWLEDGEMENTS

"Every accomplishment begins with the decision to try." – John F. Kennedy

I would like to express my sincere gratitude to the following individuals, whose personal and professional support and help were extremely helpful in the completion of this master's thesis.

First and foremost, I am deeply indebted to my mentors, Dr. Simon Rusjan and Dr. Matjaž Mikoš for their professional guidance, valuable support, and encouragement during the planning and development of this research work. I would like to express my deepest appreciation to Dr. Simon Rusjan for all of his invaluable patience, devoted engagement, and untiring help, especially for sharing his knowledge and expertise in every stage of my master's thesis completion. I consider myself extremely fortunate to have a mentor that genuinely cared about my work and who always responded to my inquiries and concerns very quickly. His willingness to give his time so generously has been very much appreciated. Also, I am particularly grateful to Dr. Matjaž Mikoš for his valuable suggestions, constructive comments, and feedback on certain aspects of my thesis, which gave me a better understanding of the topic.

I would like to extend my sincere thanks to the European Commission and the Joint Scholarship Selection Committee for providing me the opportunity to study this interdisciplinary international master's in Flood Risk Management through the Erasmus Mundus Joint Master's Degree scholarship. This master's program allowed me to gain a lot of insight and a significant amount of knowledge from leading experts at four European universities and develop myself personally and professionally.

I am also grateful to my classmates and friends for their emotional support during all of the ups and downs of my studies, and to all those who have contributed directly or indirectly to successfully completing this master's degree.

Lastly, I would like to thank my family for their continuous belief, care, love, and support. They have a big part to play in where I am today.

Jasna Donevska
Ljubljana, Slovenia

BIBLIOGRAPHIC-DOCUMENTALISTIC INFORMATION AND ABSTRACT

UDC: 556.166:711.1(497.4)(043.3)
Author: Jasna Donevska
Supervisor: Assist. Prof. Simon Rusjan, PhD
Co-supervisor: Prof. Matjaž Mikoš, PhD
Title: Analysis of uncertainties in the process of flood hazard maps elaboration
Document type: Master thesis
Notes: 57 p., 6 tab., 40 fig., 1 ann., 84 ref.
Keywords: flood hazard mapping, flow hydrograph, hydraulic modelling, Manning's roughness coefficient, sensitivity analysis, uncertainty analysis, Vipava river

Abstract

Flood hazard mapping is an essential component of flood risk assessment, providing valuable information for preventive pre-impact hazard reduction, largely employed in spatial planning, risk management, and raising public awareness about flood hazards. Spatial and temporal variation of the natural processes, limited knowledge about the system's physical properties, and insufficient data introduce uncertainties in the modelling chain used to produce flood inundation and hazard maps, hampering flood risk management.

This master's thesis investigates the impact of uncertainties in hydrological and hydraulic parameterization and the related sensitivity of hydrological and hydraulic calculations and modelling on flood hazard mapping. Specifically, uncertainties related to the flow hydrograph shape and peak discharge value and variations in the channel and floodplain Manning's roughness coefficients were propagated through a combined 1D/2D hydraulic model using LiDAR Digital Terrain Model (DTM) combined with geodesy data of the Vipava river channel and detailed land use data. The uncertainty analysis was applied to the case study of the Vipava river, a transboundary river catchment shared between Slovenia and Italy, by comparing the flood extension and spatial distribution of flood hazard classes by performing hydraulic simulations associated with 10-, 100-, and 500-year return periods as specified in the Slovenian legislation.

The analysis points out the greatest sensitivity of the results associated with variations in the channel Manning's coefficients for a 10-year return period event, depicting an increase in the flood extent of 45%. The increase in the inundated areas is smaller for 100- and 500-year floods, amounting to 15% and 11%, respectively. Furthermore, the modelling results confirm the higher impact of the uncertainty in the peak discharge with respect to the impact of varying floodplain Manning's values, denoting an increase in the flood extension of 9-12% between the 10% and 90% confidence interval values for the different flood occurrence probabilities. The maximum increase in the flood-prone area with the floodplain Manning's coefficients amounts to 4-6%. Lastly, the impact of the flow hydrograph shape variations appears to be the lowest, depicting a maximum variation in the flood inundation area of 2-3%. All these changes in the overall flood extent are further reflected in variations of flood hazard classes, which are not uniform and not equally distributed for all but depend on the water depth distribution which is considered the dominant criterion for flood hazard classification.

BIBLIOGRAFSKO – DOKUMENTACIJSKA STRAN IN IZVLEČEK

UDK: 556.166:711.1(497.4)(043.3)
Avtor: Jasna Donevska
Mentor: doc. dr. Simon Rusjan
Somentor: prof. dr. Matjaž Mikoš
Naslov: Ocena negotovosti pri izdelavi kart poplavne nevarnosti
Tip dokumenta: magistrsko delo
Obseg in oprema: 57 str., 6 pregl., 40 sl., 1 pril., 84 ref.
Ključne besede: kartiranje poplavne nevarnosti, hidrogram odtoka, hidravlično modeliranje, Manningov koeficient hrapavosti, občutljivostna analiza, analiza negotovosti, reka Vipava

Izvleček:

Izdelava kart poplavne nevarnosti je bistvena sestavina v postopku izdelave ocene poplavne ogroženosti, saj zagotavlja ključne informacije za preventivno zmanjševanje poplavne ogroženosti, ki se v veliki meri uporablja pri prostorskem načrtovanju, obvladovanju poplavnih tveganja in ozaveščanju javnosti o nevarnosti poplav. Prostorske in časovne spremembe naravnih procesov, omejeno poznavanje fizikalnih procesov in nezadostni podatki vnašajo negotovosti v proces modeliranja poplavnih dogodkov, ki se uporablja za izdelavo kart obsega poplav in analizo poplavne nevarnosti, kar ovira obvladovanje tveganja zaradi poplav.

To magistrsko delo raziskuje vpliv negotovosti v hidrološki in hidravlični parametrizaciji ter s tem povezano občutljivost hidroloških in hidravličnih izračunov in rezultatov modeliranja na kartiranje poplavne nevarnosti. Natančneje je preučen vpliv negotovosti, povezanih z obliko hidrograma pretoka in oceno konice visokovodnega pretoka ter spremenljivostjo vrednosti Manningovega koeficienta hrapavosti struge reke Vipave in poplavnega območja, na rezultate kombiniranega 1D/2D hidravličnega modela z uporabo LiDAR digitalnega modela terena v kombinaciji z geodetskimi podatki rečne struge in podrobnimi podatki o rabi tal. Analiza negotovosti in občutljivosti je bila izdelana za odsek reke Vipave, čezmejne reke, ki teče skozi Slovenijo in Italijo. Izdelana je bila primerjava obsegov poplav in prostorske porazdelitve razredov poplavne nevarnosti s hidravličnimi simulacijami območij razlivanja poplavnih voda povezanih z 10-, 100- in 500-letno povratno dobo, kot jih določa slovenska zakonodaja.

Analiza je pokazala največjo občutljivost rezultatov modeliranja na spremenljivost vrednosti Manningovega koeficienta hrapavosti glavne struge v primeru 10-letne povratne dobe, ki se odraža v povečanju obsega poplavljenih površin za 45%. Pri 100- in 500-letnih poplavah je povečanje poplavljenih območij manjše in znaša 15% oziroma 11%. Poleg tega rezultati modeliranja potrjujejo velik vpliv negotovosti pri oceni visokovodne konice pretoka v primerjavi z vplivom spremenljivih vrednosti Manningovega koeficienta hrapavosti na poplavnih območjih. Ugotovljeno je bilo povečanje poplavnega območja za 9-12% ob upoštevanju vrednosti intervala zaupanja 10% in 90% statistično izvrednotenih konic pretokov za različne verjetnosti pojava poplav. V primeru spremenljivih vrednosti koeficientov hrapavosti na poplavnih območjih je bilo povečanje obsega poplavljenih območij 4-6%. Vpliv oblike hidrograma toka se je izkazal kot najmanj pomemben dejavnik pri določitvi obsega poplavljenih površin, spremenljivost obsega poplavljenih površin je znašala 2-3%. Vse zgoraj omenjene spremembe skupnega obsega poplav se odražajo v spremenljivosti prostorskega obsega razredov poplavne nevarnosti, ki niso enotne in enakomerno porazdeljene za vse razrede poplavne nevarnosti, ampak so odvisne od porazdelitev globine vode na poplavnih območjih kot prevladujočega kriterija za razvrščanje v razrede poplavne nevarnosti.

TABLE OF CONTENTS

LIST OF FIGURES

LIST OF TABLES

ABBREVIATIONS AND SYMBOLS

Q	Discharge
ARSO	Agencija Republike Slovenije za okolje (Slovenian Environment Agency)
CI	Confidence Interval
DRSV	Direkcija Republike Slovenije za vode (Slovenian Water Agency)
DTM	Digital Terrain Model
FFA	Flood Frequency Analysis
FGG	Fakulteta za gradbeništvo in geodezijo (Faculty of Civil and Geodetic Engineering)
FRMRC	Flood Risk Management Research Consortium
GEV	Generalized Extreme Value
GIS	Geographic Information System
GURS	Geodetska uprava Republike Slovenije (Surveying and Mapping Authority)
HEC-RAS	Hydrological Engineering Centre – River Analysis System
LHS	Latin Hypercube Sampling
LiDAR	Light Detection and Ranging
Manning's n	Manning's Roughness Coefficient
m.a.s.l.	Meters above sea level
MKGP	Ministrstvo za kmetijstvo, gozdarstvo in prehrano (Ministry of Agriculture, Forestry and Food)
MOP	Ministrstvo za okolje in prostor (Ministry of the Environment and Spatial Planning)
RP	Return Period
UL	Univerza v Ljubljani (University of Ljubljana)

1 INTRODUCTION

This chapter provides a brief overview of the topic, the motivation of the study, followed by the relevant objectives and research questions to be addressed. Moreover, a short description of the case study area in Slovenia is presented, as well as the scientific and practical significance of the research.

1.1 Motivation

Floods are among the most common and destructive natural disasters that affect humans and society, causing significant losses and damages every year (Zahmatkesh, Han, & Coulibaly, 2021). Nowadays, flood mapping is a widely used measure for preventive pre-impact flood hazard reduction (Baghel, 2018). Various advanced tools and modelling approaches are used for the estimation of flood hazard maps which are then incorporated into spatial planning (Alfonso, Mukolwe, & Di Baldassarre, 2016). However, these tools and approaches are impacted by significant uncertainties due to the spatial and temporal variation of the hydrological and hydraulic processes such as precipitation, land use, and river channels characteristics, limited knowledge about the system's physical properties, as well as insufficient data, posing challenges for flood risk management (Alfonso et al., 2016; Stephens & Bledsoe, 2020). Conventional deterministic approaches for estimating flood hazards rely on the nonstationary assumption of stationarity and do not take into account the uncertainties, resulting in underestimated or overestimated flood hazards and risks (Ahmadisharaf, Kalyanapu, & Bates, 2018; Stephens & Bledsoe, 2020). Recent studies show that flood inundation and flood hazard maps, which present different kinds of associated uncertainties, provide a more thorough assessment of flood hazards, thus allowing more informed decision-making and enhanced flood risk management (Simões et al., 2015; Zahmatkesh et al., 2021).

The Floods Directive (2007/60/EC) has developed a framework for the assessment and management of flood risks with the goal to reduce the negative impacts of flooding on human health, economy, environment, and cultural heritage in the European Union (European Commission, 2007). The adoption of the Floods Directive was triggered by more frequent and severe flood events observed in Europe, which have caused increased human and economic losses, intensifying the necessity for European collaboration in flood management (Eleftheriadou, Giannopoulou, & Yannopoulos, 2015). Accordingly, in the territory of each Member State, the flood hazard maps and flood risk maps have to be prepared, which are essential for the development and assessment of flood risk management strategies (European Commission, 2007).

Flood inundation and flood hazard mapping, underpinning the flood risk assessment, require hydraulic modelling to simulate flow dynamics and derive flood characteristics (water depths and velocities) (Ahmadisharaf et al., 2018). While inundation models allow for better capacity and performance, the scientific problem of translating such complex modelling results into easy-to-use information is becoming increasingly vital for flood risk management and mitigation. This issue is closely correlated to the identification, quantification, and comprehension of the uncertainties that influence hydrological and hydraulic modelling and, as a result, flood inundation and flood hazard maps, which are the most commonly used strategy for managing flood risk (Annis et al., 2020). To assess different uncertainties, sensitivity analysis is usually applied, which provides an inundation extension corresponding to the worst-case scenario (Glas et al., 2016). Nonetheless, this sensitivity analysis is typically produced using event-based flood simulations linked with predetermined scenarios, such as changing the design discharge values for a specified return period and ignoring the uncertainties inherent in the return-period design hydrograph concepts. Consequently, the hydrological uncertainty's impact on inundation mapping is frequently underestimated (Annis et al., 2020).

Given the possibility of multiple runs with varying different input data and parameter settings, hydraulic models have been successfully applied for assessing various sources of uncertainties affecting flood hazard and flood risk assessments. A detailed flood risk assessment incorporating the uncertainties will be particularly important when such assessment could substantially influence a decision, whether it is to mitigate the risk to life, reduce the property damage, spatial planning, or some other flood mitigation measure. For instance, some critical existing or planned infrastructure (e.g., hospitals, schools, etc.) could be outside of the flood extent mapped deterministically for a certain flood return period, however, might be inside the probabilistic inundation map boundaries for the same return period, with a certain probability to be flooded. Expert knowledge and site-specific conditions will then be crucial for the decision-making about the project, and accounting for the uncertainties in the flood assessment will be vital for the transparency of such decisions (McCarthy, Beven, & Leedal, 2014). Additionally, flood hazard maps derived deterministically and ignoring the related uncertainties, have often been proven as wrong estimates of the flood extension, and a large number of insurance claims have occurred outside these deterministic boundaries of flood inundation areas. As this deterministic approach to flood hazard assessment does not usually give an accurate representation of the flooded areas, there is a need for quantifying the related uncertainties (Stephens & Bledsoe, 2020).

The Vipava river, flowing through western Slovenia and northeast Italy, frequently causes flood-related problems owing to its hydrological characteristics as well as the topography and land use in the floodplain areas. Due to the development of urban infrastructure in floodplains, flood-related issues have become worse in the last decades. Most flood mitigation measures are spatially constrained, implemented on small scales, and primarily located where local needs and interests necessitated effective flood protection interventions. Without a comprehensive and coordinated approach, the effectiveness of such interventions is relatively limited. Furthermore, the land use in the floodplain areas is predominantly agricultural, and quite intensively exploited for farming during the last few decades (Rusjan, Vidmar, & Brilly, 2012). Given the flood-related problems and the importance of agriculture in the region, the valley was profoundly influenced by human interventions in the past aiming for the improvement of the agricultural land and flood protection, thus, changing the channel morphology through river engineering works and also the land use (Magjar et al., 2016). Apart from the spatial variability in precipitation which makes it difficult to estimate the flood magnitude with high accuracy, the seasonal changes in land use, as well as man-made interventions, introduce additional uncertainties in the flood inundation predictions in the Vipava river valley.

Past studies have investigated and developed different approaches to assess the impacts of hydrological and hydraulic uncertainties in flood hazard assessments through hydraulic simulations. Given the successful practical application of hydraulic models in assessing uncertainties and the available high-quality data for the study area, this research aims to evaluate the sensitivity of flood hazard mapping on the uncertainties in hydrological and hydraulic input data and parameters through 1D/2D hydraulic modelling approach utilizing the HEC-RAS software. Considering uncertainties in the process of flood inundation and flood hazard maps elaboration allows for a more critical and process-based delineation of flood inundation areas and hazard classification. These flood hazard scenarios allow for credible incorporation of the flood hazard mapping in spatial planning and estimation of direct economic damages and the associated uncertainties, which may be useful for planning future flood mitigation measures, facilitating more informed decision-making. For instance, the insurance policies can be adjusted, correlating the probability of risk with the insurance coverage. Additionally, flood mapping that incorporates uncertainties is very helpful for spatial planning since it encourages the gradation of different land use types (Garrote, Peña, & Díez-Herrero, 2021; Merwade et al., 2008).

1.2 Objectives

The main objective of the master's thesis is to evaluate the potential impact of uncertainties in hydrological and hydraulic input data and related uncertainties in hydrological and hydraulic calculations and modelling on the elaboration of flood inundation and flood hazard maps. Furthermore, this research was performed to meet the following specific objectives:

a. Literature review of different sources of uncertainties affecting the flood hazard assessment and approaches for the elaboration of flood inundation and flood hazard maps by considering uncertainty aspects;
b. Uncertainty analysis of the impact of hydrological data (flow hydrograph shape and peak discharge) and hydraulic parameters (channel and floodplain Manning's roughness coefficients) for specific flood return periods on the elaboration of flood inundation and flood hazard maps;
c. Proposing flood inundation and flood hazard maps elaboration procedure by considering uncertainty aspects based on the hydraulic modelling results.

1.3 Research questions

In relation to the problem definition, the following research questions will be addressed:

a. What are the uncertainties affecting the flood hazard assessment?
b. What are the commonly used approaches for the elaboration of flood inundation and flood hazard maps by considering uncertainty aspects?
c. How do variations in hydrological data (flow hydrograph shape and peak discharge) and hydraulic parameters (channel and floodplain Manning's roughness coefficients) affect the spatial extension of flooded areas and elaboration of flood hazard classes?

1.4 Scientific innovation and practical value

The study area, the Vipava river catchment on the Slovenian-Italian border, which will be further described in more detail, faces flood problems due to its hydrological characteristics, topography, and land use. The majority of flood protection measures are spatially relatively limited, implemented on small scales, and largely positioned where local needs and interests necessitated effective flood protection intervention measures. Such interventions have a relatively limited impact without a complete and integrated approach (Rusjan et al., 2012).

Flood hazard mapping is an essential component of flood risk assessment, largely employed in spatial planning, risk management, and awareness building (EXCIMAP, 2007). As the initial step to flood risk assessment, this study works on the assessment of spatial extension of the areas that are most likely to be flooded from different scenarios of varying model input data and parameters. Therefore, the novelty of this study lies in assessing the sensitivity of flood extension and spatial distribution of flood hazard classes on different uncertainties for different flood exceedance probabilities according to the Slovenian legislation for the selected case study of the Vipava river catchment. The study also adds to the scientific body of knowledge the successful application of a combined 1D/2D hydraulic modelling approach employing a LiDAR DTM in mapping the potentially inundated areas considering uncertainty aspects by using different sets of input data and hydraulic parameterization.

The outcomes of this study can help for a more comprehensive and systematic approach to the assessment of areas exposed to flood hazards and further spatial planning, estimation of direct economic

damages, water management, and flood mitigation measures planning, facilitating more informed decision-making. It may also serve as a jumping-off point for future researchers to consider the impact of the uncertainties in the hydrological and hydraulic monitoring and modelling on flood inundation and flood hazard mapping.

2 LITERATURE REVIEW

This chapter provides a review of existing literature on flood hazard assessment and related uncertainties in hydrological and hydraulic parameterization, which are relevant to this research. The material from past studies will be used as a backdrop and help in developing a suitable methodology to meet the study's research objectives.

2.1 Flood hazard assessment

A flood hazard is defined as the probability of a flood event with a certain magnitude that may impact a particular area and cause possible harm (Apel, Merz, & Thieken, 2008). Flood hazard assessment, which includes creating flood inundation and flood hazard maps, is one of the essential input information for the development and assessment of flood risk management strategies. Hazard assessment focuses on the estimation of the flood magnitude and potential flood extension for a certain exceedance probability. It is based on available data and expertise about hazards and their possible impacts on the communities (Grünthal et al., 2006). Flood extent, floodwater depth, and flow velocity all play a role in determining how and how far floodwaters can spread through floodplains. Estimating the magnitude, frequency, and spatial extension of flood events in a certain area is required for assessing flood hazards, which necessitates information and understanding of the area's hydrometeorological characteristics. Rainfall, water level, and discharge are some of the important parameters that must be closely monitored in order to assess flood hazards. Apart from the hydrological data, floodplain topography, river geometry, location of hydraulic structures, and land use data are among the main data requirements (Poljansek et al., 2021).

In the case of observations with sufficient spatial and temporal coverage, extreme value analysis approaches can be used to directly estimate flood magnitudes and frequencies (Poljansek et al., 2021). The estimation of the flood magnitude is usually based on flood frequency analysis (FFA) of recorded discharge data for a certain area of interest, followed by statistical data analysis, aiming to determine the peak discharge value for a particular return period. Generally, flood hazard estimations are characterized by a high level of uncertainty due to trends in flood magnitude and frequency, limited available data required for the FFA, and possible problems while performing hydrometric measurements during flood events. Various available distribution functions and estimation methods exist to address this issue, and many countries issued guidelines, suggesting different distributions for design discharge estimation (Grünthal et al., 2006; Kidson & Richards, 2005).

Since floods as a natural phenomenon vary greatly depending on the site-specific hydrometeorological conditions and hydraulic properties, there is illusional to expect that a united methodology for assessment of flood hazard and flood risk would be suitable for properly addressing the flood-related processes. Therefore, many countries published guidelines and recommendations for flood hazard and flood risk assessment and associated uncertainties in flood hazard and flood risk mapping. For example, the Framework for assessing uncertainty in fluvial flood risk mapping developed by the UK Flood Risk Management Research Consortium (FRMRC) is one notable guide for the assessment of uncertainty in fluvial flood risk mapping (McCarthy et al., 2014).

2.2 Sources of uncertainty in flood hazard assessment

Flood inundation boundaries are typically depicted as sharp lines in the flood maps based on deterministic model results, indicating the expected inundation borders for predefined flood return periods. However, these maps are subject to various sources of uncertainty including: the estimated design discharge for chosen return period; the floodplain topography and river cross-sections; the choice

of effective hydraulic roughness coefficients; the choice of a hydraulic model and its physical representation; the consideration of floodplain infrastructure and flood defences performance; and the possibility of non-stationarity due to catchment and climate changes (Bales & Wagner, 2009; Beven et al., 2014; McCarthy et al., 2014). Those sources can be classified into two categories: (a) aleatory uncertainties, which are random uncertainties related to the variability of the natural processes such as temporal and spatial variability of precipitation, and cannot be decreased; and (b) epistemic uncertainties, which are linked to the limited understanding of the physics (model uncertainty), or insufficient data (statistical uncertainty), and can be decreased by acquiring more knowledge (Garrote et al., 2021; Vojinović, 2012). The aleatory uncertainties are usually estimated using statistical analysis approaches, whereas the epistemic uncertainties are not easy to be quantified statistically due to their spatial and temporal variability. However, in practice, both aleatory and epistemic uncertainties are often quantified using statistical methods, and transparent assumptions about uncertainties affecting the hydraulic modelling and their impacts on flood hazard estimations are advised (Stephens & Bledsoe, 2020).

Furthermore, the Framework for assessing uncertainty in fluvial flood risk mapping developed by the UK FRMRC (2014) classifies the sources of uncertainty according to the source-pathway-receptor system, as follows: (a) uncertainties in flood sources, which include uncertainties in design flood magnitude and impacts of climate and catchment changes, (b) uncertainties in pathways, which include uncertainties in hydraulic model structure, channel morphology/conveyance/rating curve, effects of floodplain infrastructure, and performance of flood defences, and (c) uncertainties in receptors, which are uncertainties in consequences/vulnerabilities (McCarthy et al., 2014).

2.3 Uncertainty in design flood magnitude

Hydrological uncertainties affecting flood hazard assessment are mainly focused on rating curves relating floodwater levels to discharges, flow hydrograph shape, and flood frequency analysis, which is used to estimate the design discharge for preselected return periods (Annis et al., 2020). From the engineering hydrology point of view, determining the design discharge is very important for designing hydraulic structures, such as dams, reservoirs, flood embankments, etc. Furthermore, discharge estimates are widely employed in environmental engineering, assessment and management of sediment transport, and planning of flood mitigation measures (Sharifi, Majdzadeh Tabatabai, & Ghoreishi Najafabadi, 2020). However, estimation of the design discharge is a complex task due to the uncertainty linked to the limited available time series and/or the limited representativeness of the measured discharge data with regard to its global behaviour. This lack of knowledge leads to epistemic uncertainties, which as previously described, arise either from incomplete knowledge of the physics or simplifications related to the chosen modelling approach and parameterizations (Garrote et al., 2021).

Uncertainty in the magnitude of a design flood presents a statistical issue, requiring the selection of a specific distribution for a selected exceedance probability. Post-flood analyses show that the uncertainty in the design flood discharge estimates is often overlooked, but it can be substantial. An example is the Carlisle flood in January 2005, when, the performed post-flood analysis showed about 60% higher peak discharge value compared to the design discharge estimated from the rating curve (McCarthy et al., 2014). Moreover, a study of the Douro river reach in the Spanish city of Zamora done by Garrote et al. (2021) revealed an uncertainty associated with the FFA of about 40%. Nevertheless, past experiences show that there is no guarantee that any of the statistical methods will always produce design discharges that are similar to the observed values. As a result, determining the design flood magnitude for a certain location involves significant knowledge uncertainty, which should be incorporated into the flood mapping, thus allowing more informed decision-making (McCarthy et al., 2014).

Where discharge data series are available, uncertainty estimations are dependent on the sample size, variability, and choice of the probability distribution. However, at ungauged catchments where measured discharge data lack, the design flood discharge can be estimated through different methods such as hydrological modelling, gauge extrapolation, or regional regression equations, and the uncertainty will be conditioned on the choice of the method (Haberlandt & Radtke, 2014; Stephens & Bledsoe, 2020). Furthermore, determining the design discharge for a particular return period can be more challenging due to trends in flood magnitude and frequency (Stephens & Bledsoe, 2020).

Flood Frequency Analysis (FFA) is one of the factors causing uncertainty in flood hazard and risk assessments (Sharafati et al., 2020). FFA is a popular method for estimating design discharges for specific probabilities of occurrence in gauged catchments by fitting a probability distribution to historically recorded discharge data. The Gumbel, log-normal, log-Pearson, log-Pearson type III, and generalized extreme value (GEV) are all commonly used distributions for FFA, and the choice depends on the site-specific characteristics and availability of hydrological data (Garrote et al., 2021; Mateo-Lázaro et al., 2016). Lack of sufficiently long time series of discharge (Apel et al., 2004), biases in extreme value estimation (Makkonen, 2008), and non-stationarity due to climate change (Khaliq et al., 2006) introduce uncertainties in the FFA (Koivumäki et al., 2010). Longer hydrological data series can generally improve the accuracy of the FFA. However, longer data series are not always available for many catchments around the world. Moreover, the existence of wet and dry seasons might impact maximum yearly peak discharge, causing uncertainty in the flood hazard and risk assessment, and future management and planning. This uncertainty is usually accounted for by computing confidence intervals of the design flood discharges associated with a certain probability of occurrence (Garrote et al., 2021).

Field measurements of discharge pose a real challenge, especially during flood events, hence, the discharge data used for the FFA is usually not measured directly but estimated through a rating curve, which represents a stage-discharge relationship at a specific river section. Consequently, discharge data is subject to uncertainty because the true rating curve is unknown, and defined rating curves are often linked to some degree of error, which consequently affects the results of FFA and brings uncertainty in the estimated flood quantiles. The uncertainties in river discharge data due to rating curve errors can be significant and can highly impact the results of hydrological and hydraulic studies (Haque, Rahman, & Haddad, 2014; Westerberg & McMillan, 2015). Some of the factors causing uncertainties in the estimate of discharge from a rating curve are: (a) errors in stage and discharge measurements; (b) the number of gaugings to develop the rating curve; (c) the assumptions about a suitable form of stage-discharge relationship and the quality of the curve fit; (d) extrapolation of the curves beyond the maximum gauging points; (e) hysteresis in the rating curve; and (f) changes in the channel cross-section because of vegetation growth or bed movement due to erosion or deposition (Haque et al., 2014; Holmes, 2016; McMahon & Peel, 2019).

2.4 Uncertainty in Manning's roughness coefficient

Manning's roughness coefficient is widely employed to represent floodplain and channel hydraulic roughness in hydrological and hydraulic modelling. According to previous studies, the runoff response is highly sensitive to variations in Manning's coefficient values (Foster & Maxwell, 2018; Govers, Takken, & Helming, 2000; Kalyanapu, Burian, & McPherson, 2009; Mustaffa, Ahmad, & Razi, 2016; Sanz-Ramos et al., 2021). Therefore, hydrological and hydraulic models would perform better if Manning's roughness coefficient estimates are more accurate. Nevertheless, a variety of challenges arise while estimating Manning's roughness coefficient due to its empirical nature and lack of descriptive knowledge, causing uncertainties in its estimates (Caro Camargo, Pacheco-Merchán, & Sánchez-Tueros, 2019; Kalyanapu et al., 2009; Stephens & Bledsoe, 2020). Moreover, the spatial and temporal variability as well as time-consuming measurements make it more difficult to determine the surface

roughness (Darboux, 2011). Generally, land use data are employed to define Manning's roughness coefficients according to land use classification. Manning's coefficient is also linked to the surface physical characteristics such as hydraulic conductivity, friction resistance, moisture content, granular structure, vegetation density, etc., making its estimation more complex (Kalyanapu et al., 2009). Furthermore, the land use and vegetation in a particular area vary through the year, which also introduces uncertainties in the inundation parameters estimates (Stephens & Bledsoe, 2020).

As reported in many studies, current practice allows for the determination of acceptable roughness coefficients based on hydraulic considerations and relevant expertise applied in a standardized approach (Kalyanapu et al., 2009; McCarthy et al., 2014). However, since there is no theoretical method for its calculation but it is determined empirically, based on engineering knowledge and experience, Manning's coefficient estimates are relatively subjective (Stephens & Bledsoe, 2020). In actual practice, values from previous best estimates are frequently changed to assess how sensitive the model predictions are to the roughness coefficient. More extensive analyses of uncertainty in the roughness coefficient, on the other hand, have largely been ignored because of the assumption that uncertainty in the roughness coefficient, due to its physical nature, is dominated by other uncertainties in flood modelling. However, when inundation modelling results are compared to observations, there is a significant difference, denoting considerable uncertainty in the roughness coefficient. This is partially due to the fact that the roughness coefficient is model reliant and associated with the degree of representation of the system's behaviour in the model. A more detailed physical representation of the system, such as a full 2D inundation model, may reduce the uncertainty related to the roughness parameter. Another factor is that the estimated roughness coefficient compensates for additional sources of uncertainty, such as the floodplain topography and infrastructure, channel morphology, boundary conditions, and so on. As a result, the roughness coefficient values needed for more accurate flood inundation estimates will be determined by the inundation model chosen and implemented as well as the data available (McCarthy et al., 2014).

Nowadays, with the increased availability of satellite data and GIS mapping tools, new methods for estimating Manning's roughness coefficient have arisen, utilizing mathematical correlations, lookup tables, and inference. For large-scale applications, extracting surface roughness data based on GIS and remote sensing is highly suggested. Current practice in hydrological and hydraulic modelling is to obtain a digitized land use dataset and to apply Manning's roughness coefficient values in a GIS using recommended literature values (Arcement & Schneider, 1989; Kalyanapu et al., 2009). Then, the roughness uncertainty is mostly represented as a uniform distribution between two roughness values – upper and lower limit (Annis et al., 2020; Seewig, 2013).

Furthermore, Manning's roughness coefficient is an important parameter to consider when constructing rating curves. However, as previously stated, there might be considerable uncertainties associated with determining this parameter, which will then propagate in the rating curves, largely affecting the discharge estimates. Seasonal variations of the vegetation and changes in land use may cause discharge values to correlate with the same water level. Accordingly, a good estimate of Manning's roughness coefficient can help decrease uncertainties in stage-discharge estimation (Vatanchi & Maghrebi, 2019).

It is evident that the determination of Manning's roughness coefficient and rating curves is characterized by knowledge uncertainty, and the roughness has a significant effect on the flood extent and depth. As a result, some assumptions regarding the expected uncertainty nature will have to be made beforehand. In general, this uncertainty is lessened by calibrating against observations, albeit this does not ensure accurate inundation predictions throughout the whole floodplain (McCarthy et al., 2014).

2.5 Implementing an uncertainty analysis

In the flood modelling process, expert decisions about different sources of uncertainty for a specific site should be made in order to propagate these uncertainties through inundation models, and further analyze and evaluate them. Implementation of an uncertainty analysis generally consists of two steps: (1) assessing the interaction between different sources of uncertainty and (2) propagation of the assumptions about the different sources of uncertainty through uncertain flood maps (McCarthy et al., 2014).

Historically, the "freeboard" concept was used in flood defense design to indirectly address assumptions about various sources of uncertainty. Also, a common practice is performing a sensitivity analysis of the inundation model to assess how sensitive are the flood maps to variations in the assumptions about the different uncertainties. The Framework for assessing uncertainty in fluvial flood risk mapping developed by the UK FRMRC (2014) provides a more thorough analysis of the propagation of uncertainties through an inundation model (McCarthy et al., 2014).

2.5.1 Assessing interactions between sources of uncertainty

About the relationships between different sources of uncertainties, there are two types of assumptions that might be made (McCarthy et al., 2014):

1) *Explicit interactions.* Explicit interactions are most suitable when dealing with parameters that have obvious interactions, such as the uncertainties in the design discharge for a particular flood return period at nearby locations. The nature of the interaction between locations can be analyzed in the case of available data, or specified by assumption if data is not available. Interactions between channel and floodplain roughness in different areas of the floodplain, or model grid size and effective roughness values, are two examples of explicit interactions (McCarthy et al., 2014).
2) *Scenario interactions.* Scenario interactions are most suitable when knowledge uncertainties make it difficult to define the interaction. In many cases, due to insufficient knowledge, multiple sources of uncertainty are presumed to be unrelated. For instance, a constant values of the channel and floodplain roughness coefficients may be assumed throughout the whole floodplain area, which is not correct but is appropriate simplification for the modelling process (McCarthy et al., 2014).

2.5.2 Defining an uncertainty propagation process

To quantify the uncertainties affecting the whole modelling chain of flood hazard assessment usually requires an evaluation of a large number of uncertainty scenarios, which can be computationally highly complex and demanding (Dottori, Martina, & Figueiredo, 2018). Most of the existing hydraulic modelling tools and commonly used computer hardwares are not developed to run numerous simulations for assessing uncertainties. Given the nonlinearity of these hydraulic models in space and time and the complexity to apply analytical methods for the uncertainty propagation, approximate approaches are widely employed to assess different uncertain parameters. Monte Carlo simulation is one of the approaches used for propagating the various sources of uncertainty in flood inundation models. The method includes randomly sampling a set of uncertain model inputs within a range of probable values and propagating the model outcomes to generate an ensemble of the required results (Bessar, Matte, & Anctil, 2020; McCarthy et al., 2014). In more detail, hydraulic model simulations are being performed for each generated value of possible uncertain model input/parameter. Then, for each cell of the

modelling domain, the number of simulations when a particular criterion is being reached (e.g., water depth above a certain threshold) is divided by the total number of model simulations. As a result, the frequency of inundation or reaching a certain inundation parameter (e.g., depth, velocity) value of each modelling cell is obtained. The results are usually expressed in the range 0-1, where 0 depicts no probability and 1 depicts a 100% probability of a particular cell being inundated or reaching some inundation parameter threshold (McCarthy et al., 2014).

Given the various sources of uncertainty, the Monte Carlo sampling approach can be too computationally demanding, requiring a significant number of runs of a particular model to propagate the uncertainties into flood maps, and even a single simulation could take a long computational time for complex floodplains and larger computational grids. Therefore, parallel computing solutions, such as multiple PCs, multi-core processors, or graphics processing unit systems can help with the necessary model runs, reducing the simulation time and making the development of uncertain flood maps more commonplace. However, the Monte Carlo method is not very suitable for a larger number of uncertain input variables, especially if the distribution and interactions of those variables are well-known (McCarthy et al., 2014). For such cases, Latin Hypercube Sampling (LHS), as a more controlled method of sampling data, is used to save some computational time when running Monte Carlo simulations. LHS is based on randomly generating samples with a better distribution in a particular domain of uncertainty (Bessar et al., 2020; Glen, 2018). Specifically, the probabilistic distribution of each uncertain parameter is divided into a set of increments with equal probabilities. Accounting for interactions between the parameters, samples are then created in such a way that each increment is not used more than once. Further, each simulation is run, generating a set of outputs with equal probabilities (McCarthy et al., 2014).

These probabilistic approaches to quantifying the uncertainties allow more detailed and informative uncertainty assessments in terms of the statistical analysis, however, usually require a large amount of input data in order to choose the appropriate probability density functions. As a result, a simpler approach to uncertainty assessment is the three-point estimation method, where the uncertainty inputs/parameters are presented as three values (best-case value, the most likely value, and the worst-case value), determined subjectively. Furthermore, a bit more extended approach to evaluating uncertainties is the interval analysis, which considers a specified range of probable inputs and parameters, and the upper and lower limits are defined based on an expert judgement which might be subjective. The assumption that any value inside the range has an equal probability allows capturing the maximum input/parameter variation, however, it does not provide additional information about the uncertainty as the probabilistic approaches (Komatina & Branisavljević, 2005). In this study, due to the complexity of the hydraulic model computational domain, the uncertainties were quantified using the three-point estimation technique. The flow hydrograph uncertainty was accounted for by comparing different hydrograph shapes (narrow, middle, and wide) and the uncertainty in the peak discharge was delimited through the 10% and 90% confidence interval values, defined in previous hydrological studies and FFA. The floodplain Manning's roughness values were specified according to the actual land use classification, based on value ranges suggested in the literature – minimum, maximum, and recommended value.

2.6 Probabilistic floodplain mapping

Flood hazard assessment has historically relied on a deterministic technique of producing flood inundation maps. A design flow hydrograph corresponding to a peak discharge of a certain return period is generated using statistical analyses of past observations and hydrological models that combine meteorological data and catchment properties, which is then routed through the floodplain using a hydraulic model to estimate flood extension and other inundation parameters such as floodwater levels,

flow velocities, etc. (Gangadhara & Vemavarapu, 2020). Deterministic flood inundation maps divide floodplains into two sections of inundated and dry zones (Figure 1a). However, many studies have shown that flood prediction using hydraulic models is influenced by considerable uncertainties (Aronica, Bates, & Horritt, 2002; Aronica, Hankin, & Beven, 1998; Bates et al., 2004; Beven et al., 2014; Di Baldassarre et al., 2010; Leedal et al., 2010; Merz, Thieken, & Gocht, 2007; Neal et al., 2013; Pappenberger et al., 2007; Pappenberger et al., 2005; Pappenberger, Frodsham, et al., 2006; Pappenberger, Matgen, et al., 2006; Romanowicz & Beven, 2003). Subsequently, all flood hazard and risk assessments suffer from a certain degree of uncertainty due to multiple factors, such as inaccurate input data (e.g., topographic data, boundary conditions) (Alfonso & Tefferi, 2015), inappropriate model structure and parameterization (Aronica et al., 1998; Bates et al., 2004; Di Baldassarre & Claps, 2010; Hall et al., 2005; Pappenberger et al., 2005; Romanowicz & Beven, 2003), etc. As the deterministic mapping represents the flood extent as a single best-fit polygon for a particular return period event, it does not allow for the inclusion of the uncertainties. Accordingly, the flood extension is fixed in space and may consequently seem inaccurately certain (Alfonso et al., 2016).

Probabilistic inundation maps, on the other hand, which also include information on the degree of uncertainty associated with the flood extension, are a more comprehensive approach to presenting flood hazards (Gangadhara & Vemavarapu, 2020). Accounting for uncertainties, the probabilistic maps are less likely to be wrong for any specific flood event, allowing for more informed decision-making. Probabilistic flood inundation mapping involves a large number of hydraulic model runs for different scenarios of probable uncertain inputs and parameters. These datasets of uncertain model inputs and parameters can be generated using the previously described Monte Carlo approach or other data sampling methods. The hydraulic model is then run ”n” number of times for each scenario of uncertain model input/parameter until a statistical convergence is reached. As outputs from the model, ”n” number of inundation maps are generated, for each considered scenario, which are then combined into a probabilistic flood inundation map. This inundation map depicts the probability of a certain location being flooded and usually ranges from 0 (no probability of inundation) to 1 (100% probability of inundation), as shown in Figure 1b (Alfonso et al., 2016).

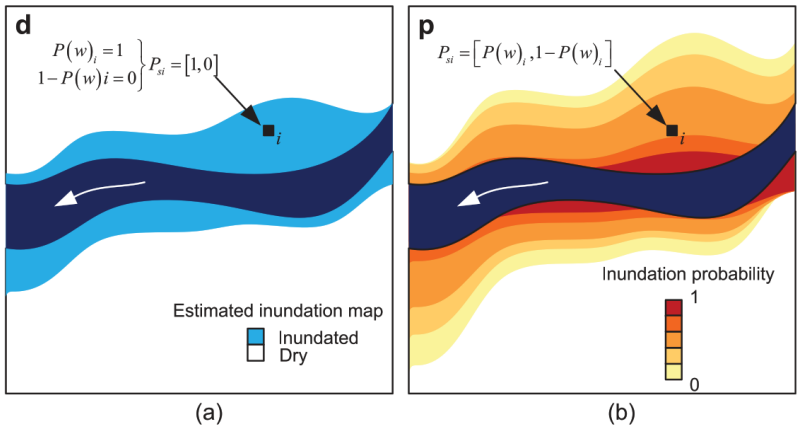

Figure 1. (a) Deterministic and (b) probabilistic flood inundation maps (Alfonso et al., 2016)

The key benefit of probabilistic mapping is its flexibility, as it allows a wide variety of potential hydrological and hydraulic uncertainties to be incorporated into intervals of probabilities and presented visually. From a practical standpoint, probability mapping's flexibility allows it to be applied to flood risk management and the implementation of flood mitigation measures. Given the limited knowledge, the probabilistic flood mapping should be selected over the deterministic approach due to several reasons: (a) uncertainty in hydrological and hydraulic parameterization, input data, and modelling approaches always exists; (b) a correct representation of the modelling outputs and associated

uncertainties can only be done using a probabilistic approach; and (c) decision-makers and different stakeholders can only guide, support, and make decisions for flood mitigation measures based on the best knowledge of flood hazards and risks (Alfonso et al., 2016; Domeneghetti et al., 2013; Garrote et al., 2021).

3 CASE STUDY AREA

The study area is the Vipava river which flows through western Slovenia and northeast Italy. The river has a total length of 49 km, out of which 45 km in Slovenia, and an average annual discharge of 17.3 m^3/s (data period 1971–2000). It flows into the Soča river near the Municipality of Savogna d'Isonzo after entering Italy (Wikipedia, 2021). The domain of interest for this study is represented by the last 21 km of the river before it enters Italy, depicted in Figure 2.

The Vipava river's hydrographic basin is part of the Soča river basin area. It is stretched across the hill slopes of the Nanos and Hrušica hills, covering an area of about 600 km^2, and a population of about 52,000 inhabitants. The region has a sub-Mediterranean climate, characterized by hot summers and mild winters (Magjar et al., 2016). The Soča river basin is among the wettest places in the Eastern Alps, with a mean annual rainfall of above 3,000 mm and approximately 4,000 mm locally (Brilly, Mikoš, & Šraj, 1999). The mean annual rainfall in the upper part of the Vipava valley is approximately 2,000 mm and in the lower part and the hilly areas about 1,500 mm (Magjar et al., 2016).

The rich natural and cultural heritage, breathtaking landscapes, and many attractions such as hiking, cycling, canoeing, gastronomy, and wine tasting bring a lot of tourists to the area every year (Magjar et al., 2016).

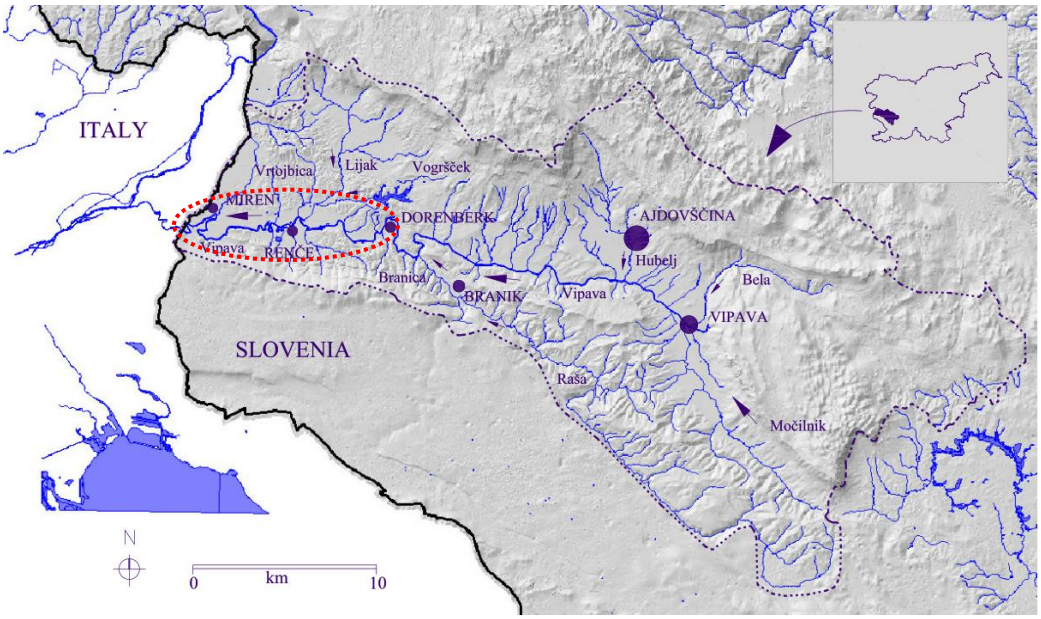

Figure 2. Location of the study area (Suhadolnik, 2016)

3.1 Hydrographic characteristics

Vipava river rises beneath the Nanos plateau's slopes, on a geological contact between flysch and limestone. Vipava is a distinct river with springs that originate in the watershed's headwaters. The number of springs is determined by the amount of rain that falls in the karstic headwaters. Because some karstic springs do not dry out even after protracted dry seasons, the Vipava river, while having a karstic character, never dries out. The most abundant springs in the town of Vipava are located at 98 m.a.s.l., nevertheless, during seasons of heavy rainfall, springs from the karstic cracks can reach up to 125 m.a.s.l. The springs of the river are connected to deep, subsurface waters of the Nanos plateau and the Postojna basin. As a result, the water temperature at the springs is rather constant throughout the year, creating unique physical conditions for aquatic biodiversity. Furthermore, the Vipava river has a delta-shaped mouth, which is another unique feature (Rusjan et al., 2012).

The Vipava river's major tributaries are Močilnik, Bela, and the stream Hubelj near the town of Ajdovščina, which discharges water from the Trnovo Forest Plateau with typical karst characteristics. Further downstream, other major tributaries are the Branica creek which flows into the Vipava river in the vicinity of Saksida, and the rivers Lijak and Vrtojbica (Rusjan et al., 2012). The Vipava river exits Slovenia and enters Italy near the town of Miren, where it drains into the Soča river. Flowing through a long, narrow valley with steep slopes and tremendous falls, the Soča river is known for its fast-growing and decreasing flows (Brilly et al., 2014). Despite its torrential tributaries, the Vipava river is in general a slow-moving river with incredible meanders in the downstream part.

Because of the karstic and also torrential character of its tributaries, the water level in the Vipava river fluctuates significantly. The ratio of the Vipava river's minimum, middle, and maximum discharges is 1:10:100 (Rusjan et al., 2012). Due to snowmelt in the mountains, the river experiences a short-lasting low flow in the late winter season and a longer and continuous low flow in the summer. Two high flows can be observed throughout the year, in the early spring and the late autumn period. In late autumn, small-scale flooding events are common in the downstream part, and larger-scale flooding events happen every few years (Magjar et al., 2016). The Vipava river is a lowland river throughout its entire length, with an average channel bed slope of 1.5 ‰ (Rusjan et al., 2012).

3.2 Overview of past flood events

Due to its hydrological characteristics, particular topography, and land use, the areas extending along the Vipava river face frequent floods. The largest historically recorded discharge was observed in 1965 at water station Miren, amounting to 353 m^3/s. During the previous decades, major flood events happened in 1998 and 2010. In the flooding event in November 1998, the measured peak flow at the water station Vipava (headwater section of the river near the main karst spring) was 74.9 m^3/s. Furthermore, during the floods of September 2010, the towns of Renče and Miren were entirely cut off from the valley. The water levels surpassed those of the previous flooding in April 2009, which was classified as a 100-year flood event. Some estimations showed that the water level was about 70 cm above the previously recorded highest water level. Vipava river flooded almost all the roads, fields, vineyards, and orchards in the valley. Furthermore, many houses and industrial areas were inundated as well (Rusjan et al., 2012).

3.3 River regulation works

There were several efforts to regulate the Vipava river channel course in the past. Many river sections were straightened, however, the main reason was obtaining land for agricultural purposes. Flood protection was a less important issue, therefore some flood protection measures have been implemented only in some relatively spatially limited sections. In more detail, there were some water management interventions along both Soča and Vipava rivers, and some of their tributaries in the years leading up to and following World War I, mainly due to local damages to the water infrastructure during flood events. After 1950, water management initiatives became increasingly structured as a sequence of smaller, required actions targeted largely at flood protection (Rusjan et al., 2012). Moreover, in the lowland areas of the Soča valley, and particularly along the Vipava valley, land has become extensively exploited for farming during the previous four decades, necessitating increased effort in river maintenance, stabilization, and control (Rusjan et al., 2012). Since the largest portion of the land use in the floodplain area is agricultural, which is very important for the region, some measures were undertaken to increase the area of arable land (Magjar et al., 2016). A network of drainage ditches was used to improve about 9,000 hectares of agricultural land in the 1980s. The main river channel was enlarged, and the middle river section's meanders were straightened and disconnected from the main channel. Furthermore, on

the mouths of tributaries, some minor widening and regulation works were carried out. The water regime, on the other hand, remained more or less unchanged, and the flood-control measures were generally ineffective (Rusjan et al., 2012).

As a result of the river channel straightening, flood-prone areas have expanded due to quicker run-off, particularly in the lower parts of the river near Renče and Miren towns (Brilly et al., 2014). There, the river channel was recently cleaned and widened by excavating the deposited sediments in order to increase the river channel hydraulic conveyance and prevent the water to propagate through the floodplain. However, the majority of flood protection measures are spatially relatively limited, implemented on small scales, and largely positioned where local needs necessitated effective flood protection intervention measures. Without a comprehensive and integrated approach, such interventions have very limited impact (Rusjan et al., 2012).

4 RESEARCH METHODOLOGY

This chapter presents the research methodology which was implemented in this study to achieve the aforementioned objectives. The following subsections provide an overview of the methodological framework, followed by a detailed description of each research phase, including the relevant datasets.

4.1 Methodological framework

The methodological framework in Figure 3 outlines the steps involved in the research process. The research started with a review of scientific literature on potential uncertainties impacting the flood hazard assessment, followed by commonly used approaches and methodologies for the assessment of flood hazards by considering uncertainty aspects (Chapter 2). The framework includes the experimental part of the master's thesis and is structured into three phases: (1) data acquisition; (2) hydraulic modelling; and (3) flood inundation and flood hazard mapping.

First, the required data for the hydraulic modelling and uncertainty analysis was collected from different sources. Design flow hydrographs and peak discharge values for different return periods are obtained from previous hydrological studies and statistical analysis for the study area. Other data required for building the hydraulic model are DTM, river channel cross-sectional data, and land use data, which are gathered from different governmental entities of Slovenia. After collecting the data, a combined 1D/2D hydraulic model of the study area was built up, followed by multiple hydraulic model simulations, thus, accounting for uncertainties in different model inputs and parameters. In particular, uncertainties related to the flow hydrograph shape and peak discharge as potential sources of hydrological data uncertainties and the choice of Manning's roughness coefficients as uncertain hydraulic parameters were investigated. The outputs of the hydraulic model (water depth, water velocity, and product of water depth and water velocity) were used for creating flood inundation maps for different return periods and flood hazard maps for each simulation scenario. Finally, the impact of the uncertainties on flood extent and spatial distribution of flood hazard classes was analyzed.

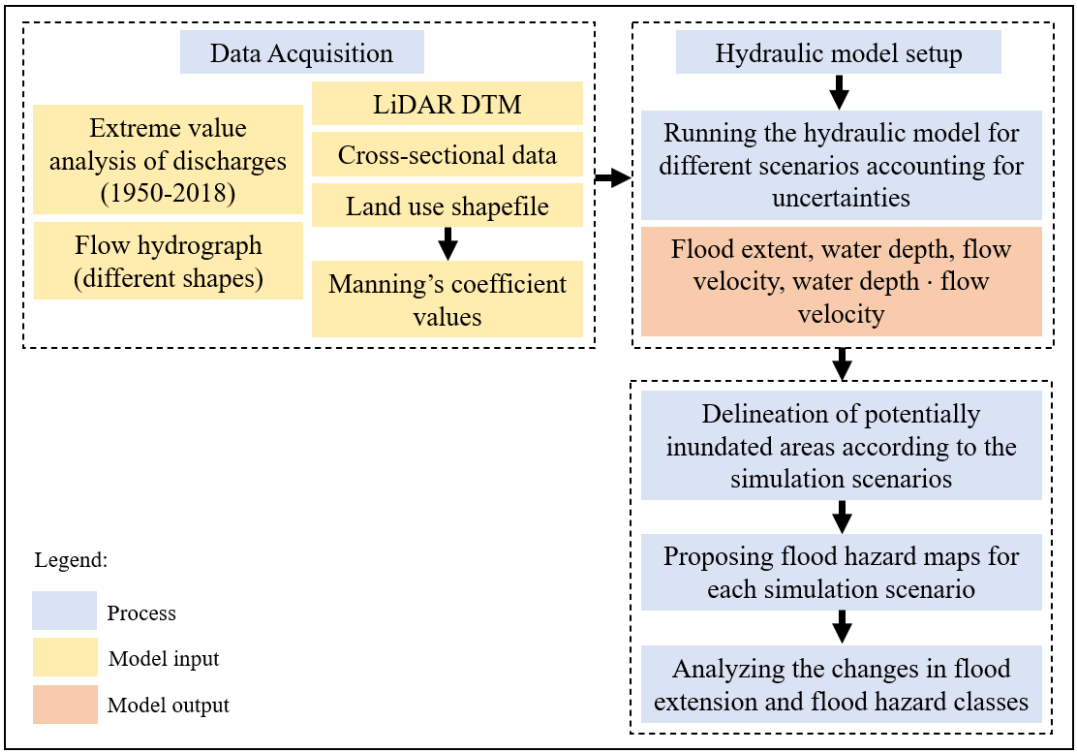

Figure 3. Methodological flowchart

4.2 Data acquisition

Available data for the study area were gathered from different governmental entities of Slovenia. Table 1 summarizes the required datasets for this study, along with the data type, resolution/scale, and source, which are then briefly described in the following subheadings.

As the main source of terrain elevation, a high-resolution LiDAR DTM was used to simulate the flow propagation through the floodplain area. Other geometric data are cross-sectional measurements of the main river channel, which were made available upon request. Furthermore, a land use map of the study area was also required for the hydraulic modelling and flood hazard assessment. The floodplain Manning's roughness coefficient values were defined according to the actual land use classification, based on values available in the literature – upper and lower limits as well as recommended values for each land use type.

The hydrological data used to conduct this study includes design flow hydrographs (three shapes) provided by the Slovenian Water Agency (DRSV) (Anzeljc, 2021) and peak discharge values (10%, middle, and 90% confidence intervals) from FFA done in the scope of a master's thesis at FGG, University of Ljubljana (Piry, 2020), for 10-, 100-, and 500-year return period flood events.

Table 1. Datasets used in the study

Dataset	Data type	Resolution / Scale	Source
LiDAR DTM	Raster	Original: 1 m Converted: 5 m	MOP
Orthophoto	Raster	0.25 m	MOP (GURS)
River channel cross-sectional data	Vector	/	DRSV
Land use shapefile	Vector	1: 5,000	MKGP
Design flow hydrographs (narrow, middle, and wide shape)	Hydrological	Hourly	DRSV
Peak discharge values (10%, middle, and 90% confidence intervals)	Hydrological	Yearly	MSc thesis from UL FGG
Floodplain Manning's roughness coefficient values	Hydraulic	/	Literature

4.2.1 Topographic data

Detailed and highly accurate topographic data is a prerequisite for reliable hydraulic modelling, which is essential for a credible prediction of flooding. The topographic data used to build up the hydraulic model consists of high-resolution LiDAR data and surveyed cross-sections of the main river channel. Light Detection and Ranging (LiDAR) is a remote sensing method used to measure the elevation of an area accurately and economically (Vojinović, 2012). The methodology consists of computing the distances to certain objects by emitting light beams and measuring the time it takes for the sensor to detect them. It can provide exceptionally high accuracy and high point density due to its data collection techniques, allowing for the creation of a precise, realistic three-dimensional representation of infrastructure, buildings, etc. Moreover, it can uniformly and precisely cover large areas very fast, thus, having a wide variety of applications (NOAA, 2012).

For this study, 1m-LiDAR DTM was provided by the Ministry of the Environment and Spatial Planning (MOP) through the project National aerial laser scanning of Slovenia, performed in the period 2014-2015. The data was gathered by employing the LiDAR technique to obtain high-density terrain elevation data (5-10 points per m^2 and 2 points per m^2 in some forest areas). The DTM was corrected from all errors due to interpolation of the areas with fewer ground points, except for errors on water

surfaces and water surface borders. A quality check of the obtained data proved a vertical accuracy of 15 cm and a horizontal accuracy of 30 cm. The results of the project are freely accessible on the web portal: http://gis.arso.gov.si/evode/profile.aspx?id=atlas_voda_Lidar@Arso&culture=en-US, enabling better water and flood risk management in the country (Triglav Čekada et al., 2015). The DTM for the study area was converted into 5m-resolution DTM in order to make it more manageable for the hydraulic modelling. It is stored in the ETRS89 / UTM zone 33N coordinate system and is available as a raster file in GeoTiff (.tif) format. Furthermore, due to the low reflectance of the water, the light beams that are being emitted are usually not able to reach the riverbed and the river channel lacks accurate LiDAR data (Garrote et al., 2021). Hence, another essential input for the hydraulic model is cross-sectional measurements of the river channel. The cross-sectional data of the study area consists of 217 cross-sections and 3 inline structures. The channel's cross-sections are spaced apart on average by around 100 m, whereas they are more closely spaced in the downstream part, where measurements were recently made, with an average distance of 40-50 m.

Figure 4 shows the elevation map of the study area, where a high variation in the elevation can be observed (from 393.2 m.a.s.l. to 35.7 m.a.s.l. downstream where the river enters Italy). Moreover, it is noticeable that the valley has a specific topography with a variable span of floodplains. In some parts, the river channel is constrained by steep hillsides, therefore, there are no extensive floodplains where floodwaters could spread. On the contrary, certain areas have sizable floodplains. Therefore, it is quite a challenge to estimate the flood extent with high accuracy.

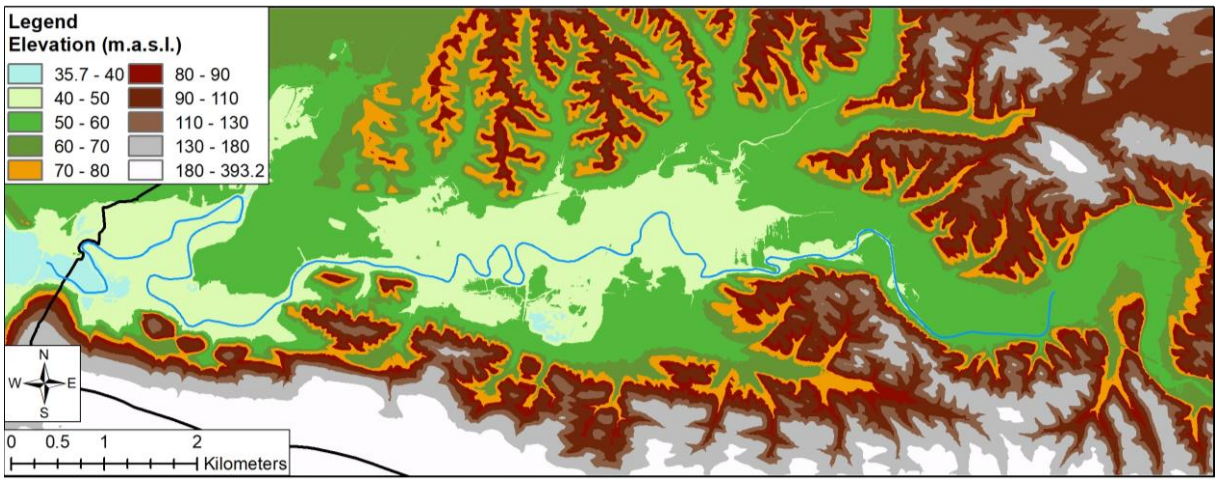

Figure 4. DTM of the study area (source: MOP)

4.2.2 Land use data

Land use data plays an important role in flood hazard assessment, as the flood extension and other inundation parameters depend on its roughness and other characteristics. Detailed land use classification of the study area is obtained from the land use database by the Ministry of Agriculture, Forestry and Food of Slovenia (MKGP), which is publicly available at https://rkg.gov.si/vstop/ as a vector layer. The national study of land use is based on orthophoto data and is very detailed, categorizing the actual land use data into 25 land use classes (MKGP, 2006). For the area of interest, the land use layer consists of 21 actual land use classes and "other" land use class which is not defined because it is on the Italian side. For each class of land use, the range and recommended value of Manning's roughness and the percent impervious value were taken from different literature (NOAA, 2016; USACE, 2022a; USDA, 2016) and summarized in Table 2. As shown in Table 2, the land use data consists of various agricultural land use types which in terms of the hydraulic roughness do not differ significantly. Hence, some different land use classes have the same Manning's values according to information from the literature.

Table 2. Land use classes and associated Manning's coefficients (MKGP, 2006; NOAA, 2016; USACE, 2022a; USDA, 2016)

Land use ID	Land use type	Manning's n range	Recommended Manning's n	Percent impervious
1100	Field or garden	0.02 – 0.05	0.05	0
1180	Perennial plants in arable land	0.02 – 0.05	0.05	0
1190	Greenhouse	0.07 – 0.16	0.08	0
1211	Vineyard	0.07 – 0.16	0.08	0
1221	Intensive orchard	0.07 – 0.16	0.08	0
1222	Extensive orchard	0.07 – 0.16	0.08	0
1230	Olive grove	0.07 – 0.16	0.08	0
1240	Other perennial crops	0.02 – 0.05	0.05	0
1300	Permanent grassland	0.025 – 0.05	0.04	0
1410	Overgrown land	0.025 – 0.05	0.04	0
1420	Forest tree plantation	0.08 – 0.20	0.12	0
1500	Trees and shrubs	0.07 – 0.16	0.08	0
1600	Uncultivated agricultural land	0.025 – 0.05	0.045	0
1800	Agricultural land overgrown with forest trees	0.08 – 0.20	0.12	0
2000	Forest	0.08 – 0.20	0.12	0
3000	Built-up and related land	0.06 – 0.20	0.12	65
4210	Reeds	0.05 – 0.085	0.06	0
4220	Other marshy lands	0.05 – 0.085	0.06	0
5000	Dry open land with special vegetation cover	0.023 – 0.03	0.03	0
6000	Open land without or with insignificant vegetation cover	0.023 – 0.03	0.03	0
7000	Water	0.025 – 0.05	0.035	100
0	Other	0.025 – 0.05	0.04	0

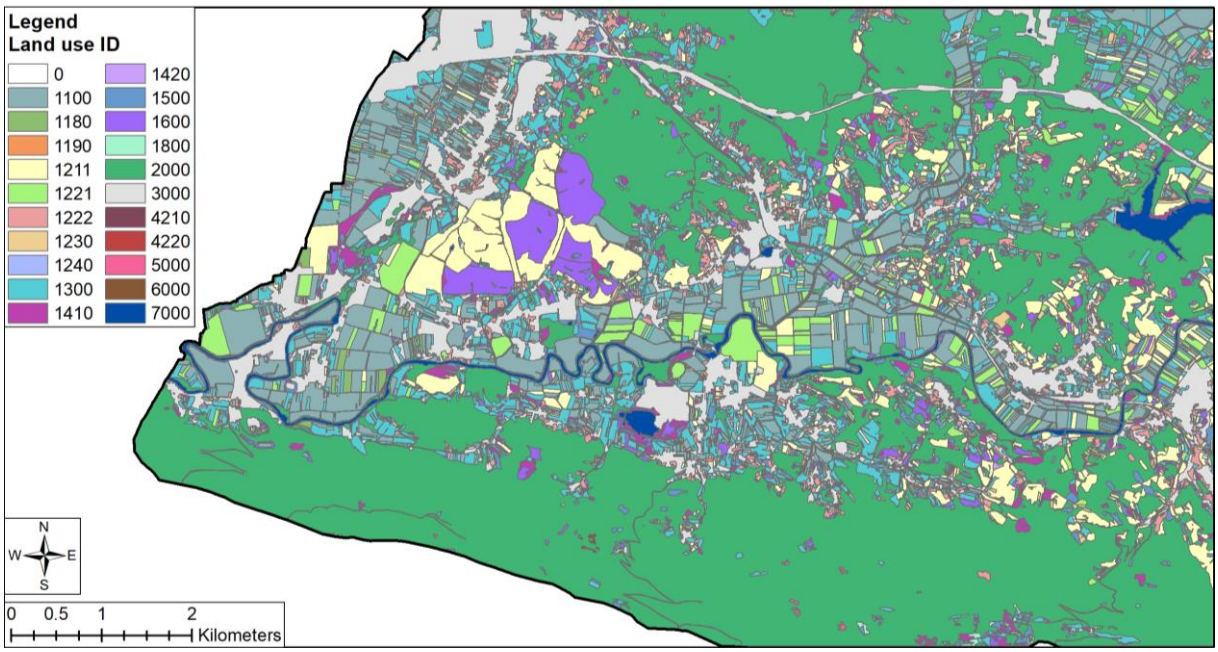

Figure 5. Land use map of the study area (source: MKGP)

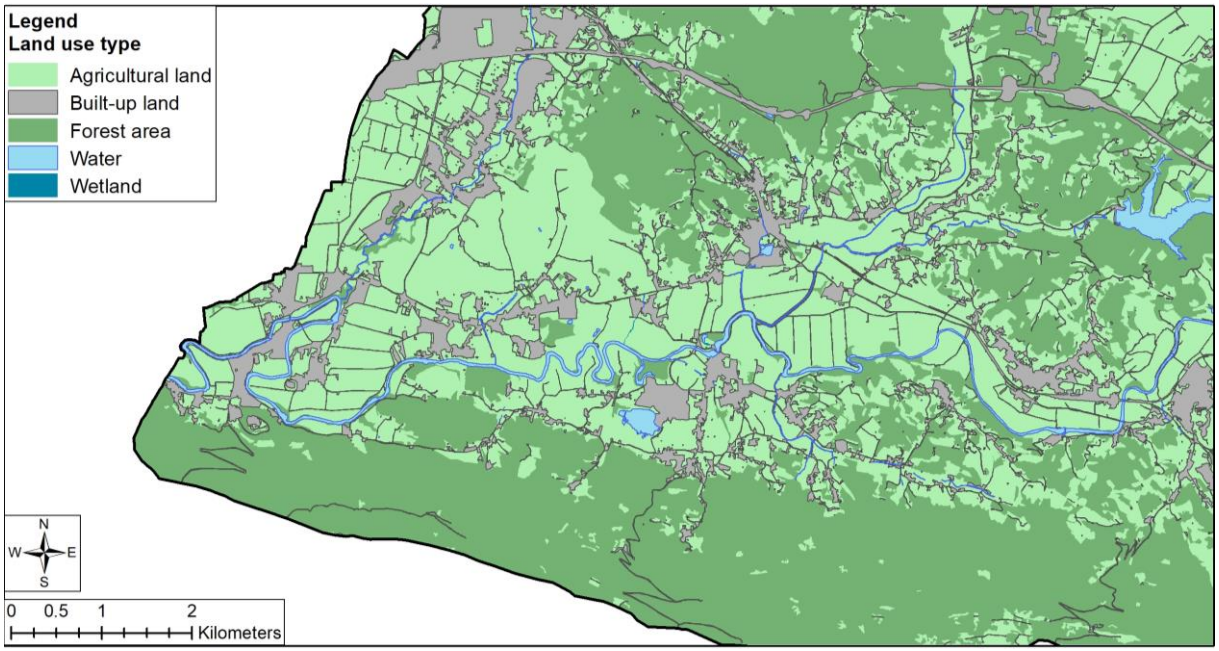

Figure 6. Reclassified land use map of the study area (source: MKGP)

The detailed land use was reclassified into five categories, shown in Figure 6, in order to better represent the land use distribution along the valley. The largest part of the area is covered by forest (44%), mostly on the hillsides around the valley and the south part of the downstream area, and agricultural land (43%), mostly in the low-lying area along the river and its tributaries. Less dominant and highly spatially dispersed is the built-up land, constituting about 11% of the area. The built-up area in the immediate vicinity of the river is mainly downstream before the Vipava river enters Italy, where the town of Miren is located.

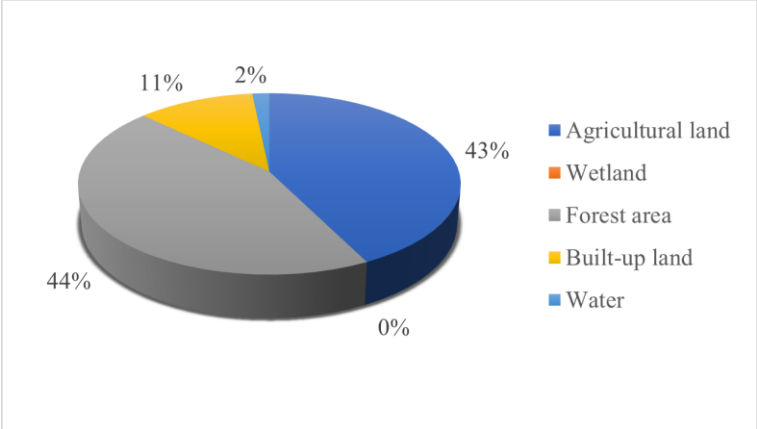

Figure 7. Percentage of land use in the study area (source: MKGP)

Land use in the valley changed noticeably between 2002 and 2015. About 2.1% of the river basin's arable land was converted to grassland and urbanized land, and about 3.5% of the grassland was transformed into shrubland and forests (Magjar et al., 2016). Therefore, assessment of the impact of the land use roughness variations on the flood extension and flood hazard mapping is particularly useful for flood risk management in the area.

4.2.3 Hydrological data

The hydrological data were obtained from previous hydrological studies and statistical analyses for the study area. In the statistical analyses, the measured discharge data from the state hydrometeorological monitoring system operated by ARSO at water station Miren I were used. The design flow hydrographs (narrow, middle, and wide shape) were acquired from a hydrological study of the Vipava river (Anzeljc, 2021), and the different values of peak discharge (10%, middle, and 90% confidence intervals) were taken from a master's thesis at FGG, University of Ljubljana (Piry, 2020).

a) Design flow hydrographs and SCS dimensionless unit hydrograph

While steady flow modelling requires the peak discharge as an input, for the unsteady simulation, the full flow hydrograph is needed as the upstream boundary condition (Ahmadisharaf et al., 2018). The probabilistic analysis makes it possible to determine the maximum flow for a certain exceedance probability but does not give the time variation of the flow, i.e., the flow hydrograph. Design flow hydrographs, which represent the rate of flow in m^3/s versus time, are often determined by hydrological models based on rainfall data and observed flood waves. For the Vipava watercourse, an approach based on observed flood waves was used for defining the flow hydrograph. Based on the grouping of individual waves, three basic shapes of the flow hydrograph were determined in the scope of the hydrological study: narrow, middle, and wide (Figures 8-10) (Anzeljc, 2021), which were further used in this research as indicators of uncertainty in the hydrograph shape. Moreover, the SCS dimensionless hydrograph of 48 hours (Figure 11) was compared to the narrow, middle, and wide hydrographs and, given the similarity in the results, was used for the other simulations to reduce the simulation times.

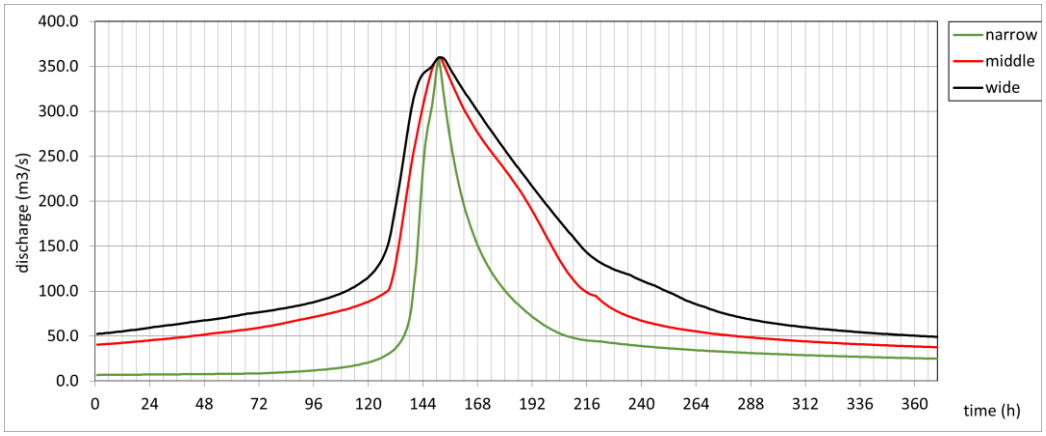

Figure 8. Design flow hydrographs for a 10-year return period flood (Anzeljc, 2021)

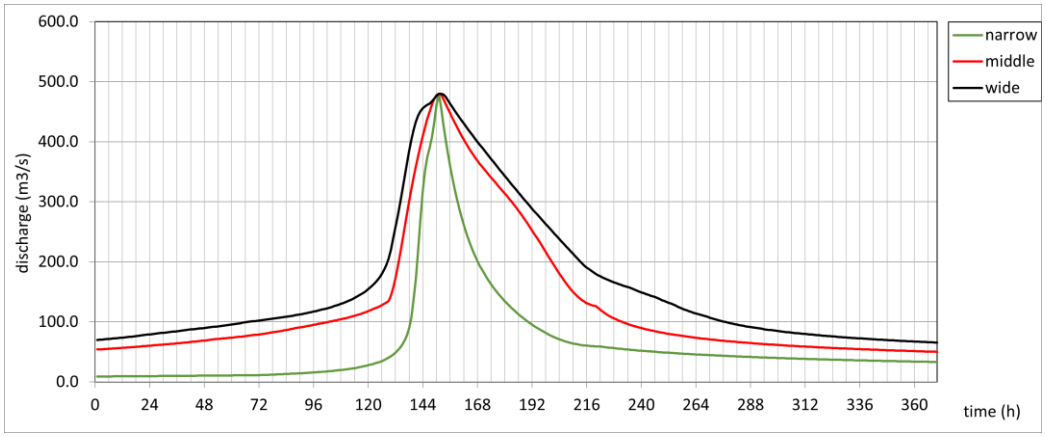

Figure 9. Design flow hydrographs for a 100-year return period flood (Anzeljc, 2021)

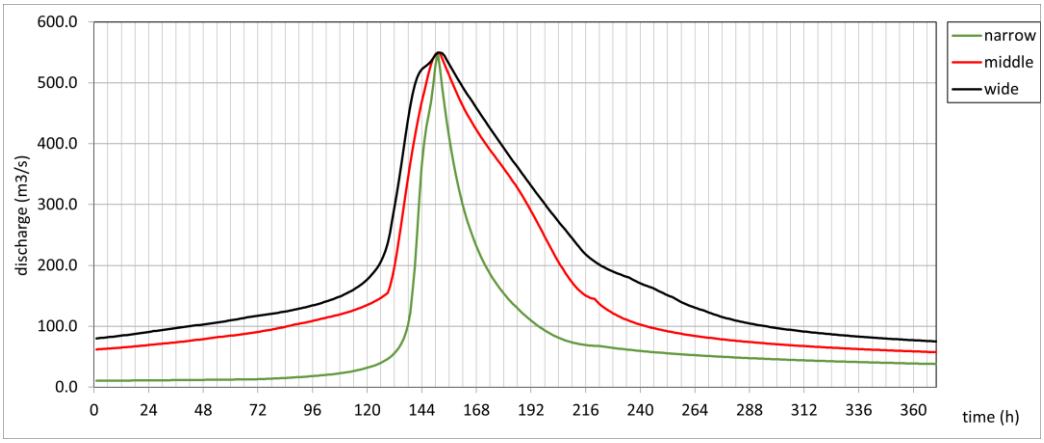

Figure 10. Design flow hydrographs for a 500-year return period flood (Anzeljc, 2021)

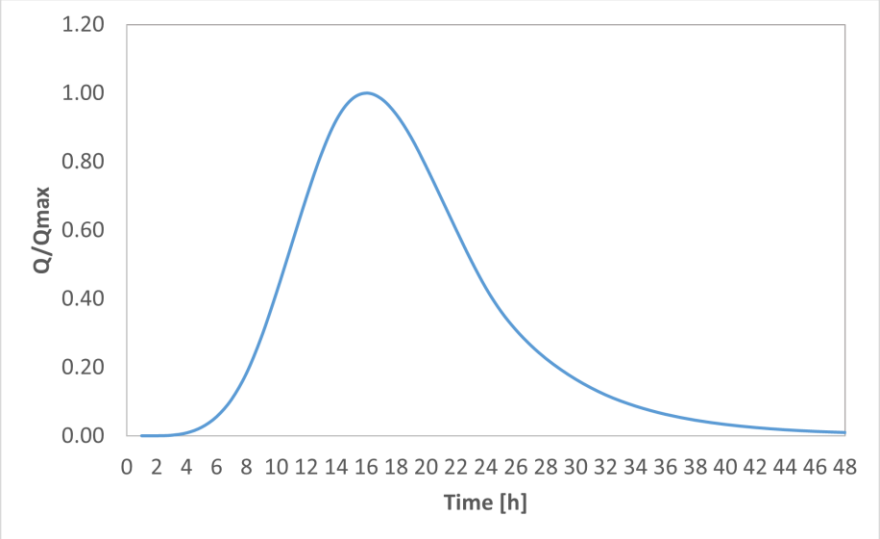

Figure 11. 48-hour SCS dimensionless unit hydrograph

b) Statistical analysis of peak discharges

For the uncertainty analysis in the peak discharge, results from an extreme value analysis of discharges done in the scope of a master's thesis at UL FGG (Piry, 2020) were used. The analysis includes discharge data measured in the period 1950-2018 at the water station Miren I, which was fitted into three distributions: GEV, Pearson III, and log-Pearson III, and taking into account uncertainties through confidence intervals. When determining the confidence intervals, the value α = 10% was used to determine the upper and lower limits. As a result, the estimated peak discharge value for different return periods and the corresponding lower and upper confidence limits for the three distributions were obtained. The results of the probabilistic analysis of discharges are shown in Table 3 and Figure 12.

From this probability analysis, the computed confidence intervals of 10% and 90% were considered as uncertainty indicators for each return period peak discharge value. The maximum design discharge values and confidence intervals from all three distribution analyses (depicted in red in Table 3) were selected as uncertainty measures.

Table 3. Results of the statistical analysis of peak discharges for selected return periods (m^3/s) (Piry, 2020)

Peak discharge	Distribution	10-year RP	100-year RP	500-year RP
10% CI	GEV	318	380	403
	Pearson III	318	386	420
	Log-Pearson III	318	379	402
Qdesign	GEV	340	428	473
	Pearson III	339	431	485
	Log-Pearson III	340	428	476
90% CI	GEV	361	482	566
	Pearson III	362	481	558
	Log-Pearson III	363	487	577

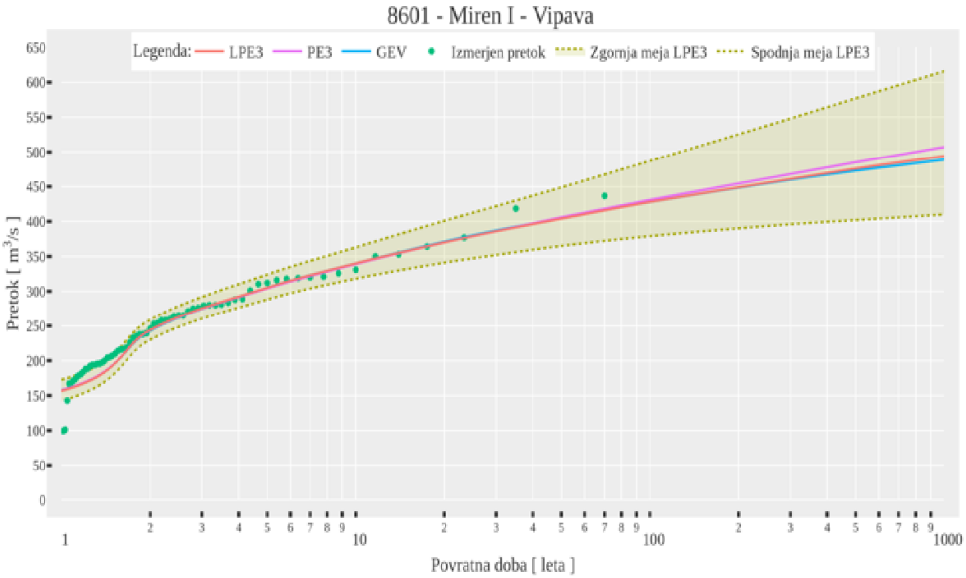

Figure 12. Graphical representation of the probabilistic analysis results (Piry, 2020)

4.3 Hydraulic model setup

From the data obtained in the previous step, it was proceeded to the hydraulic modelling to derive flood parameters (water depth and flow velocity) and produce flood inundation and flood hazard maps. A combined one-dimensional and two-dimensional (1D/2D) unsteady flow simulation for a river reach length of approximately 21 km was performed in HEC-RAS 6.2 to simulate the flood propagation in the floodplain area. This approach allows a 1D flow of the water through the river channel and a 2D flow from one cell to another in the overbank areas. Considering the lateral interactions between the river channel and the floodplain, the 1D/2D approach allows for a more detailed and more accurate representation of the flood characteristics (Pasquier et al., 2019).

The input data used to build the hydraulic model are the LiDAR-derived DTM, surveyed cross-sections, and detailed vector layer (shapefile) with the actual land use, which were previously described in more detail. This land use layer is then used to associate Manning's coefficient values and percent impervious values with each land use type for the 2D modelling domain to account for energy friction losses of overland flow (Sanz-Ramos et al., 2021). The Manning's roughness coefficient values of the river channel were previously calibrated against observed flood events. Figure 13 and Figure 14 show the modelling domain with underlying DTM and land use map, respectively.

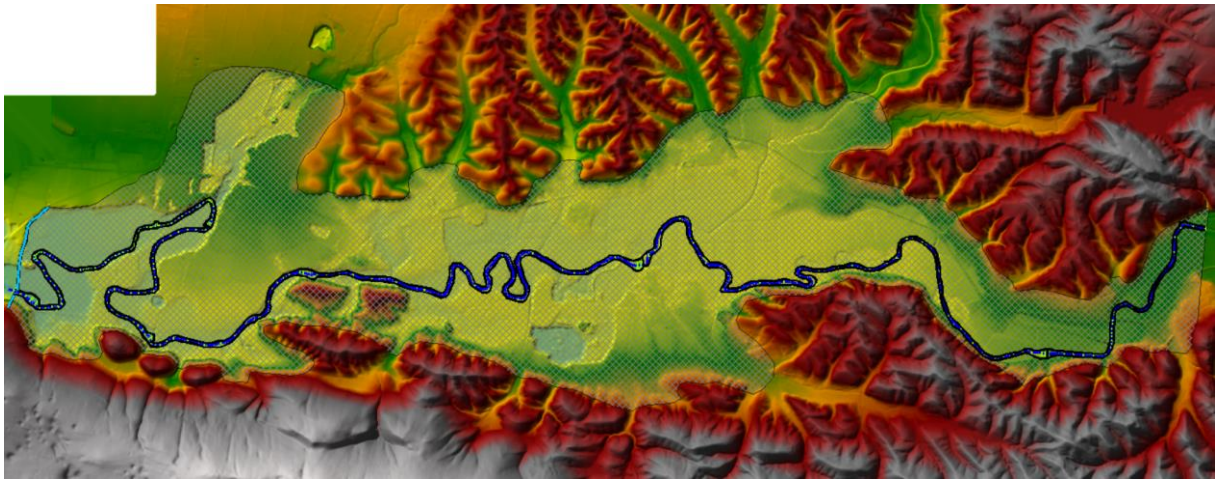

Figure 13. Model domain with underlying DTM (source: MOP)

Figure 14. Model domain with underlying land use map (source: MKGP)

The first step in the modelling process was the development of a 2D computational mesh. Two 2D flow areas (on the left and the right river bank) were created by drawing detailed polygons of the areas based on the actual DTM and a computational mesh with square cells of 20 m was generated over an area of approximately 19 km^2, comprising of 45,362 cells. The size and shape of the boundary cells differ as they follow the polygons' boundaries (Azizian, 2018). The 2D computation mesh was pre-processed, creating detailed hydraulic property tables for each cell (elevation versus volume) and cell face (elevation versus wetted perimeter, area, and roughness) according to the underlying terrain and land cover. This capability of HEC-RAS allows using large computational cells while keeping the underlying topography details, therefore decreasing the computational cost. As a result, more detailed outputs at a cell level are generated when compared to models which use a single elevation for each cell and cell face (Azizian, 2018).

The 2D flow areas were then connected to the 1D river system through lateral structures representing the levees, which allow flow transfer between the river channel and the overbank area. As overflow computational method, weir equation was selected. The weir width was set to 5 m and the weir coefficient was set to Cd=0.2. The option "Default Computed Weir Stationing" was selected for both headwater (1D river cross sections) and tailwater (2D area face points) connections, which automatically links the lateral structure to the 1D cross sections and to the face points of the 2D flow area (USACE, 2022a). The inflow hydrograph was assigned as an upstream boundary condition of the 1D river channel. The downstream boundary condition of the 1D river channel and the 2D flow area is the normal depth

which was set to 0.002, the value which corresponds to the Vipava river channel slope in the further downstream section.

In the computational settings, Finite Difference was selected as the 1D numerical solution, and the Diffusion Wave equation was set for the 2D flow areas. A computation interval of 1 sec was chosen, with an adjustable time step based on the Courant number (0.45-1) to ensure the stability of the simulation and minimize the percent error (USACE, 2022b). In the scenarios which analyze the uncertainty in the hydrograph shapes, the official flow hydrographs with a simulation time of 120 hours were used. In all other scenarios, the SCS dimensionless unit hydrograph with a simulation time of 48 hours was used to optimize the computational complexity and reduce the simulation time.

4.4 Hydraulic model multiple runs for different scenarios

In actual practice, high computational cost often limits a large number of hydraulic model simulations. Therefore, for the purpose of this study, only a few selected scenarios were simulated to account for the impact of the uncertain model inputs/parameters – peak discharge, flow hydrograph, and floodplain and channel Manning's coefficients, considering the full most probable ranges defined in previous studies and literature. Accordingly, four groups of different scenarios (S1a, S1b, S2, and S3), i.e., 12 scenarios were defined, which are summarized in Table 4. Scenario groups S1a and S1b account for hydrological uncertainties, where scenarios S1a present the uncertainty in the flow hydrograph shape, and scenarios S1b present the uncertainty in the peak discharge values derived from three different distributions. The hydraulic uncertainties were assessed in scenario groups S2 and S3, focusing on Manning's roughness coefficient values of the floodplain and the main river channel.

Table 4. Uncertainty analysis scenarios

Scenario group	Uncertainty parameter	Scenario	Varying model input
S1a	Flow hydrograph shape	I	Narrow flow hydrograph
		II	Middle flow hydrograph
		III	Wide flow hydrograph
		IV	48-hour SCS unit flow hydrograph
S1b	Peak discharge	I	10% confidence interval value
		II	Design value
		III	90% confidence interval value
S2	Floodplain Manning's roughness coefficients	I	Minimum floodplain Manning's values
		II	Recommended floodplain Manning's values
		III	Maximum floodplain Manning's values
S3	Channel Manning's roughness coefficient	I	Foreseen channel Manning's value = 0.035
		II	Calibrated channel Manning's values

The hydraulic model was run for each scenario based on 10-, 100-, and 500-year hydrograph peak discharges which are considered in the Slovenian legislation related to flood hazard assessment, totalling 36 simulations. First simulations were performed for the four scenarios of varying the flow hydrograph as the model upstream boundary condition: S1aI (narrow hydrograph), S1aII (middle hydrograph), S1aIII (wide hydrograph), and S1aIV (SCS unit hydrograph) for each return period. The second analysis

considers the uncertainty in the peak discharge, which was delimited through the 10% and 90% confidence interval values. Accordingly, three scenarios were analyzed: design peak discharge value (S1bII) and peak discharge values associated with 10% and 90% confidence intervals (S1bI and S1bIII, respectively), for all three return periods, using the SCS dimensionless unit hydrograph of 48 hours to optimize the hydraulic simulations and reduce the simulation times.

Furthermore, as the roughness coefficient of floodplains and river cross-sections often represents a significant uncertainty source impacting hydraulic modelling results (Annis et al., 2020), the sensitivity analysis in hydraulic modelling parameterization focuses on the floodplain and channel Manning's roughness coefficients. Based on the literature recommended Manning's values, three scenarios were selected to be analyzed: minimum, recommended, and maximum value (S2I, S2II, and S2III, respectively). Lastly, the channel Manning's coefficient calibrated from past flood events (S3II) was compared with Manning's coefficient of the channel when it was designed back in the 1970s, amounting to approximately 0.035 (S3I). In these scenarios, the 48-hour SCS unit flow hydrograph shape using the peak discharge values from the official hydrological study of the Vipava river (Anzeljc, 2021) was assigned as the upstream boundary condition.

From the hydraulic modelling, some inundation parameters – flood extension, water depth, and water velocity were defined for each simulation scenario, which were used for further flood inundation and flood hazard mapping.

4.5 Flood hazard mapping

As mentioned previously, according to the EU Floods Directive (2007/60/EC), each Member State has to determine which areas are exposed to flood risk, map the extent of the flood, identify any potential negative impacts of future flood events, and implement sufficient flood risk reduction measures (Wernhart et al., 2021). EU Floods Directive requires the Member States to prepare flood hazard maps, classifying the potential flood inundation areas into at least three hazard classes depicting low, medium, and high probabilities of occurrence (EXCIMAP, 2007). However, the flood hazard assessment is not integrated and harmonized in all EU Member States, allowing the countries to apply different criteria for hazard classification (Wernhart et al., 2021).

In this section, the flood hazard assessment for three EU Member States – Slovenia, Italy, and Austria are summarized to show the differences in the flood hazard areas definitions. This comparison is also interesting since the Vipava river catchment spreads over the territory of Slovenia and Italy. Generally, all three countries follow a general probabilistic approach for flood hazard assessment based on hydrological and hydraulic modelling. However, there are some important differences in the methodology for flood hazard classification. In Slovenia, flood events with return periods of 10, 100, and 500 years are considered, whereas, in Austria and Italy, 30-, 100- and 300-year flood return periods are considered for the delineation of flood hazard classes (Wernhart et al., 2021).

As for another significant difference, in Slovenia, the flood hazard is divided into four classes (low, medium, high, and other), and a combination of the water depth and flow velocity associated with a 100-year return period flood is considered for flood hazard classification. Moreover, the spatial flood extent for return periods of 10 and 500 years is accounted as an additional component. In Austria and Italy, the flood hazard maps comprise three hazard classes (low, medium, and high), which are defined according to the water depth and flow velocity by considering the abovementioned return periods (Wernhart et al., 2021). Table 5 summarizes the basic components of the flood hazard assessment approaches for the three countries.

Table 5. Comparison of flood hazard assessment in Slovenia, Austria, and Italy (fluvial flooding) (Wernhart et al., 2021)

Country	Intensity parameter	Return periods	Scenario considered
Slovenia	discharge (Q), water level (G), flow velocity (v), product of flow velocity and water depth (where v > 1 m/s at Q_{100})	10 years, 100 years, 500 years	Four hazard classes: low, medium, high, other
Austria	water level, flow velocity, flood extension, product of flow velocity and water depth	30 years, 100 years, 300 years	Three hazard classes: low, medium, high
Italy	water level, flow velocity	30 years, 100 years, 300 years	Three hazard classes: low, medium, high

The flood hazard data for Slovenia are publicly freely available on the website "eVode" (http://evode.arso.gov.si/) utilizing the publicly accessible web GIS viewer based in the state computer cloud, "Atlas Voda", in accordance with the EU INSPIRE Directive (2007) (Wernhart et al., 2021).

For this research, due to the availability of hydrological data, it was decided to apply the Slovenian national approach for the flood hazard mapping and criteria for flood hazard classes determination, which includes both water depth and flow velocity as components of flood hazard. A more detailed overview of the specific criteria used for flood hazard classification according to the Slovenian legislation is given in Table 6.

Table 6. Comparison of criteria for determination of flood hazard classes in Slovenia (fluvial flooding) (Wernhart et al., 2021)

High	Medium	Low	Other
At discharge Q_{100} or water level G_{100}, water depth ≥ 1.5 m OR water depth · water velocity ≥ 1.5 m²/s	At discharge Q_{100} or water level G_{100}, 1.5 m > water depth ≥ 0.5 m OR 1.5 m²/s > water depth · water velocity ≥ 0.5 m²/s OR where at discharge Q_{10} or water level G_{10}, water depth > 0 m.	At discharge Q_{100} or water level G_{100}, water depth < 0.5 m OR water depth · water velocity < 0.5 m²/s	At discharge Q_{500}, water depth ≥ 0 m OR where flooding occurs due to extraordinary natural or man-made events

The flow depth and flow velocity propagation do not differ much when considering the different simulation scenarios. As an illustration of the water depth and velocity propagation along the valley, the results from Scenario S2II – recommended floodplain Manning's coefficients and SCS unit flow hydrograph are illustrated in Figure 15 and Figure 16 and further used as criteria for flood hazard delineation. The maximum water depth is detected in the river channel and amounts to 4.5 m, 5.4 m, and 5.7 m for 10-, 100-, and 500-year floods, respectively. The flow velocity in the floodplain is in order 0-1.2 m/s in most areas, due to the gentler longitudinal slope of the riverbed and along the river. Consequently, the water depth criterion for flood hazard delineation dominates in most floodplain areas, and the flow velocity is not the relevant criterion to consider for flood hazard mapping of the area. It may be the dominant criterion in cases of torrential streams with developed floodplains, which are characterized by much higher velocities when compared to lowland catchments (Ordoñez, 2019).

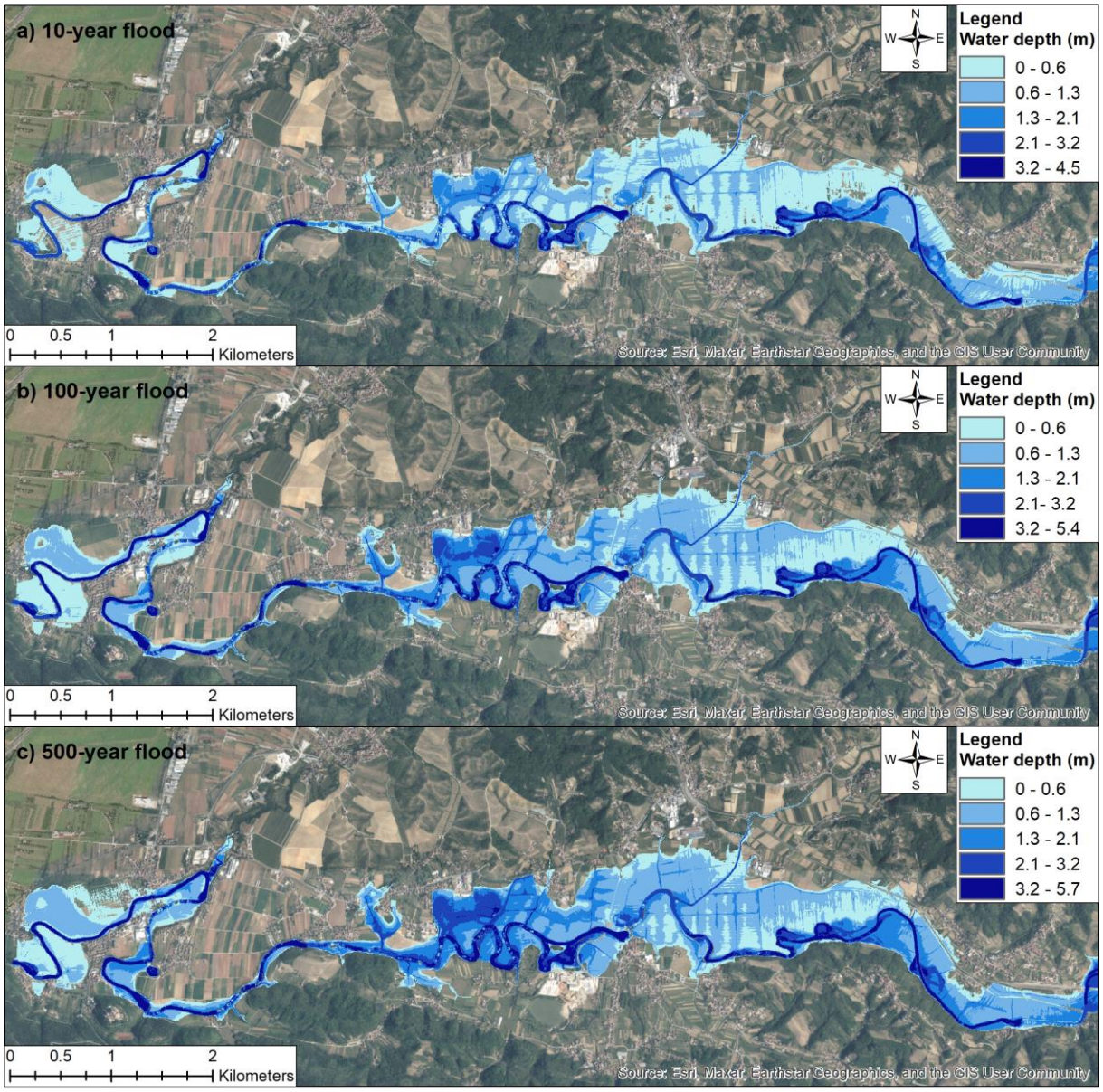

Figure 15. Water depth map for Scenario S2II

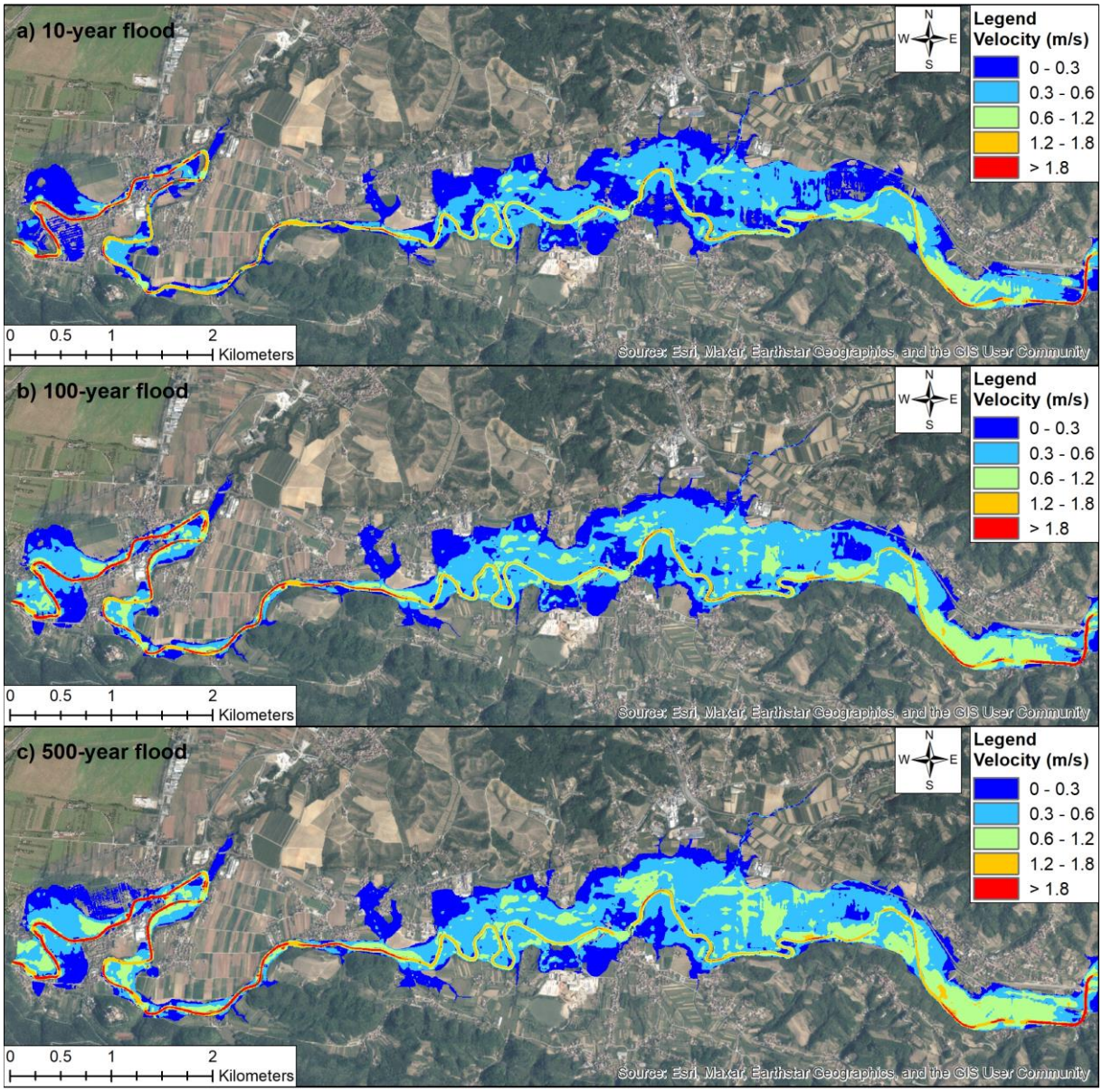

Figure 16. Flow velocity map for Scenario S2II

The final phase of this research was proposing flood inundation and flood hazard maps according to the simulated scenarios accounting for uncertainties, and further analysis of the results. First, flood inundation maps were created for flood recurrence intervals of 10, 100, and 500 years, presenting the related uncertainties. Then, according to Slovenian criteria for the determination of flood hazard classes summarized in Table 6, flood hazard maps were developed and compared for each scenario. Given its features and capabilities, ArcGIS 10.8 was used to visualize the maps.

5 RESULTS AND DISCUSSION

This chapter presents and discusses the outcomes of the uncertainty and sensitivity analysis targeting the flood propagation and spatial distribution of flood hazard classes. The results are structured according to the different scenarios which are included in the analysis, starting with the uncertainty analysis of the hydrological input data, followed by the uncertainties and sensitivity of the hydraulic modelling results on the variable floodplain and channel roughness coefficients.

5.1 S1) Uncertainty in hydrological input data

a) Different hydrograph shapes

This section shows the results of the sensitivity analysis considering the different shapes of the design flow hydrograph (narrow, middle, and wide) and the 48-hour SCS dimensionless unit flow hydrograph in order to argue its further use for the other simulations. Figure 17 shows the comparison of flood inundation maps for the different scenarios S1a, for 10-, 100-, and 500-year floods. All these changes in the flood-prone areas are also reflected in the spatial distribution of the different flood hazard classes. In all analyses, two trends in the area occupied by a particular flood hazard class can be perceived: increasing trend and decreasing trend, depending on the water depth distribution as the dominant criterion for flood hazard classification. Figure 18 shows the flood hazard maps for the scenarios of varying flow hydrograph shapes, where a predominance of the medium hazard class can be observed, which is also the case for the other simulation scenarios. This is due to the hydraulic model output variables – water depth and water velocity specific to the case study area and the approach used for hazard classification, in which the medium flood hazard class includes the area which is estimated to be inundated by a 10-year flood event according to the Slovenian legislation.

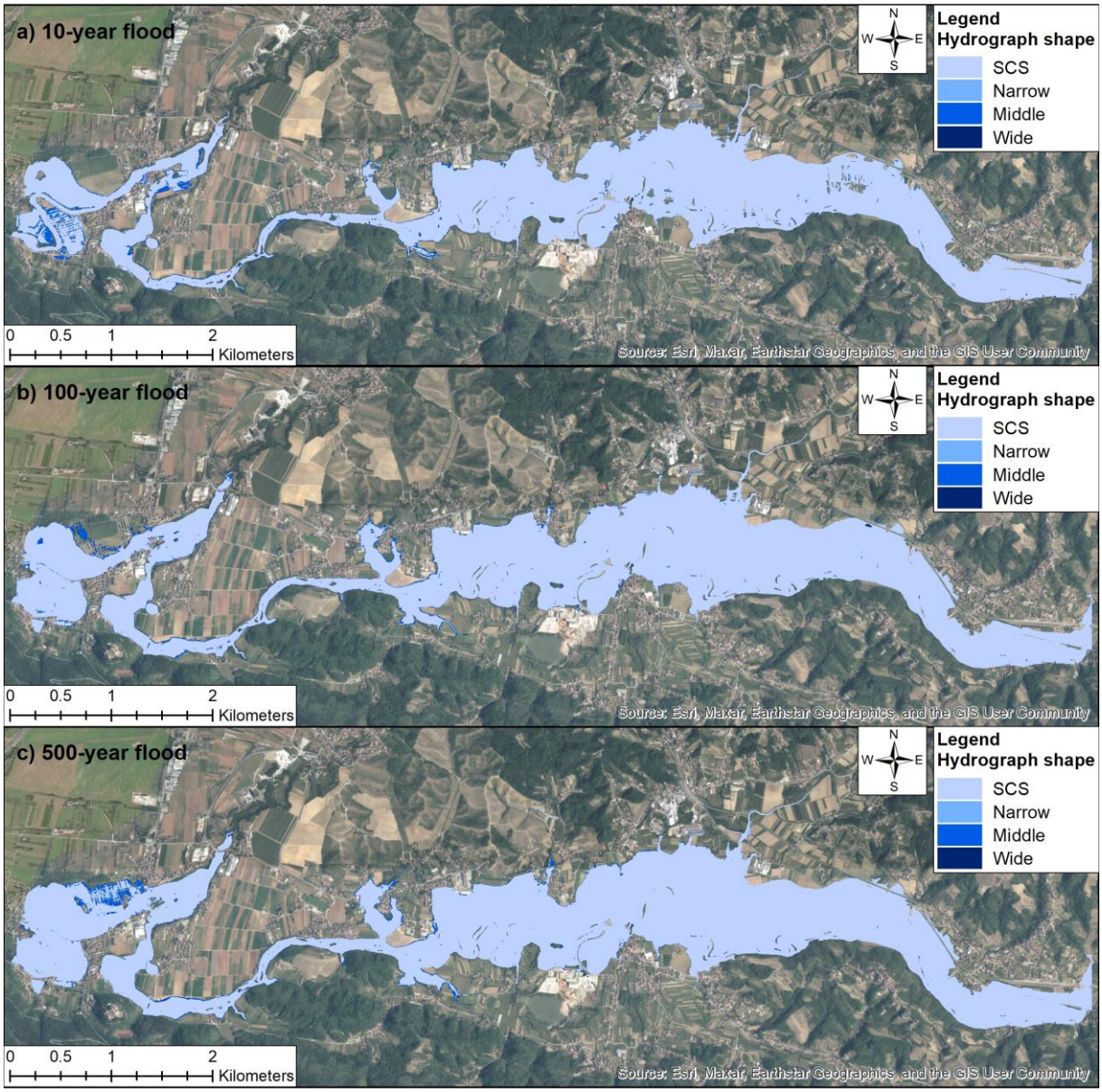

Figure 17. Flood inundation maps for scenarios S1a – different flow hydrograph shapes

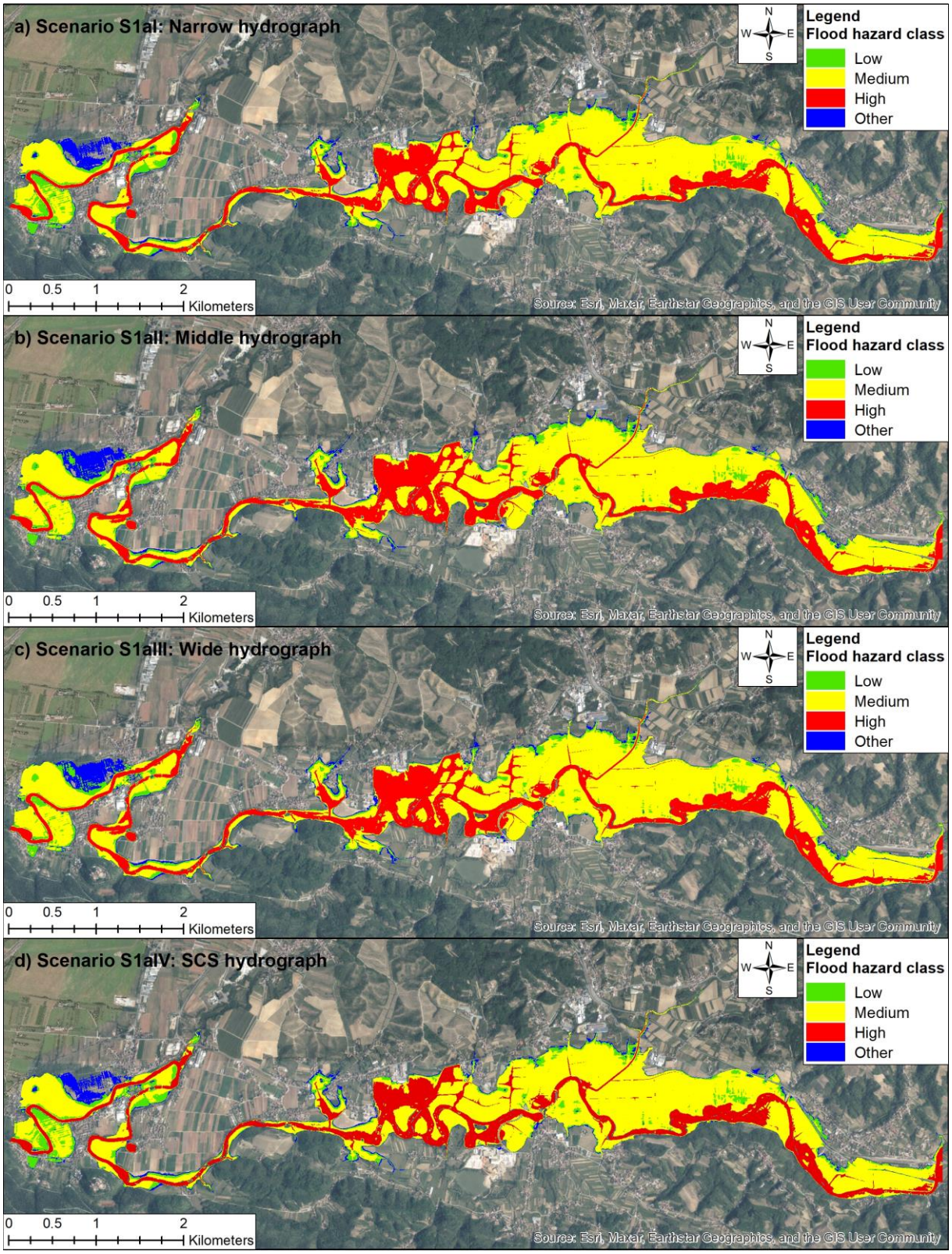

Figure 18. Flood hazard maps for scenarios S1a – different flow hydrograph shapes

Figure 19. Comparison of the flood extension for scenarios S1a – different flow hydrograph shapes

The results show minor differences in the flood extension derived using the different flow hydrograph shapes for all analyzed flood return periods. One should note, that the use of different hydrograph shapes considerably influences the inundation times along the investigated river section, however, the differences in the inundation times were not further investigated, since this is not a criterion used in flood hazard classifications. The increase in the flood inundation area is depicted with "+" and the decrease is depicted with "–" in all graphs showing the flood extent percentage difference. As shown in Figure 19, the inundated area slightly increases as the flow hydrograph becomes wider. The highest difference is observed when comparing the results associated with the narrow and middle hydrograph shapes, up to 3%, which can be considered insignificant. Apart from the three hydrograph shapes from the hydrological study of the Vipava River (Anzeljc, 2021), the scenario with the SCS unit hydrograph also shows very similar results, with a difference in the flood extension of less than 1% with respect to the narrow hydrograph. Therefore, the SCS unit hydrograph was used for all further analyses to optimize the hydraulic simulations and reduce the simulation times.

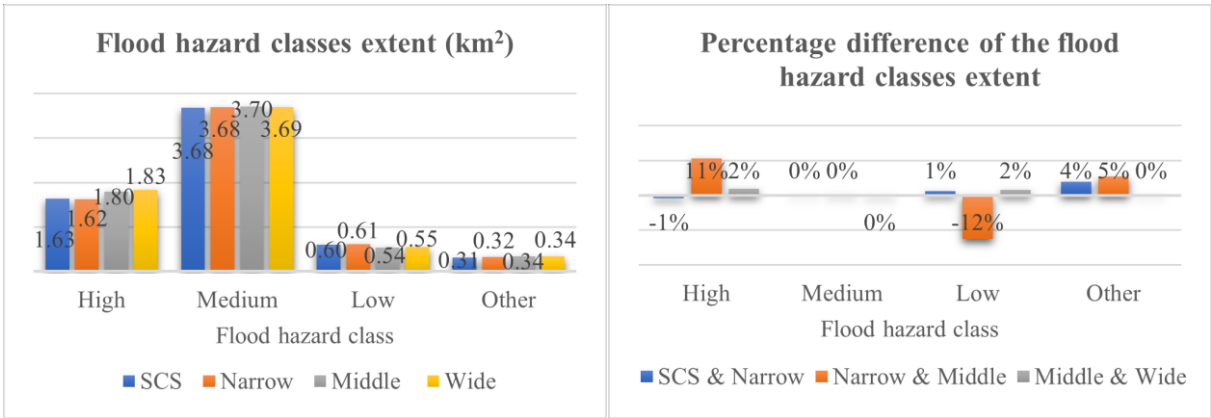

Figure 20. Comparison of the spatial distribution of flood hazard classes for scenarios S1a – different flow hydrograph shapes

The spatial extent of the high hazard class shows a similar trend as the overall inundated area, with a maximum increase of 11% when comparing the results associated with the narrow and the middle hydrographs. The medium flood hazard class extent shows almost no differences when considering all scenarios in this analysis, however, it shifts at the expense of the high hazard class increment. Furthermore, the spatial extent of the low flood hazard class shows an opposite trend, with a maximum decrease of 12% between the narrow and the middle hydrograph shape scenarios. The reason is that some parts of the inundated area which belong to the lower hazard class when considering the narrow hydrograph shape will be classified in the higher hazard class when considering the middle hydrograph

shape. The other flood hazard class shows a slight increase of about 4% between the SCS and the narrow hydrograph scenarios and about 5% between the narrow and the middle hydrograph scenarios.

b) Influence of peak discharges confidence intervals - statistical estimates (10%, middle, 90% confidence intervals)

This section shows the results of the sensitivity analysis considering the different peak discharge confidence intervals from the FFA. In statistical terms, such an analysis could be considered as more classical "probabilistic" flood mapping. The flood extension increases with the peak discharge, as illustrated in Figure 21, which is further reflected in the spatial distribution of flood hazard classes (Figure 22).

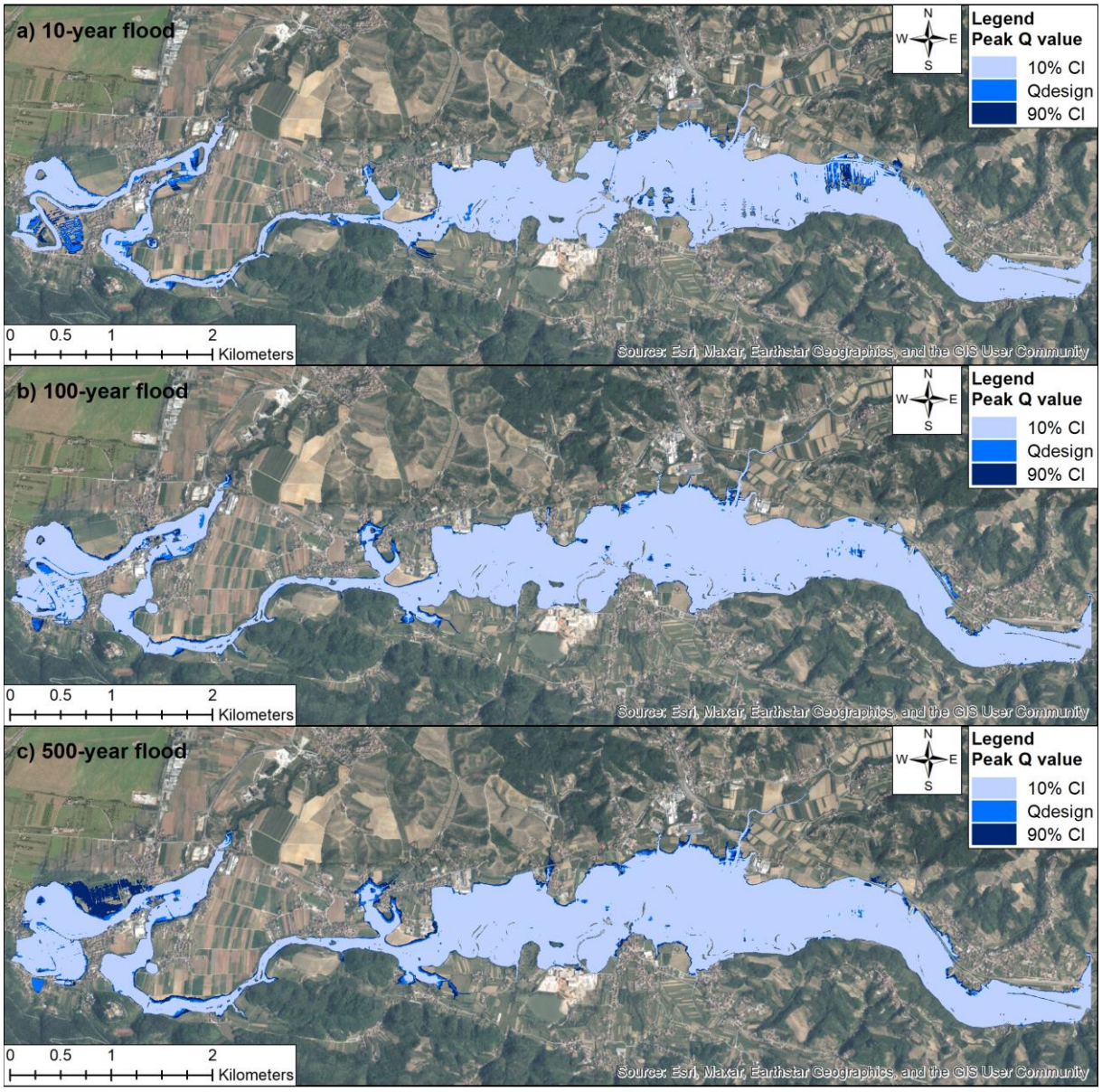

Figure 21. Flood inundation maps for scenarios S1b – different peak discharge confidence intervals

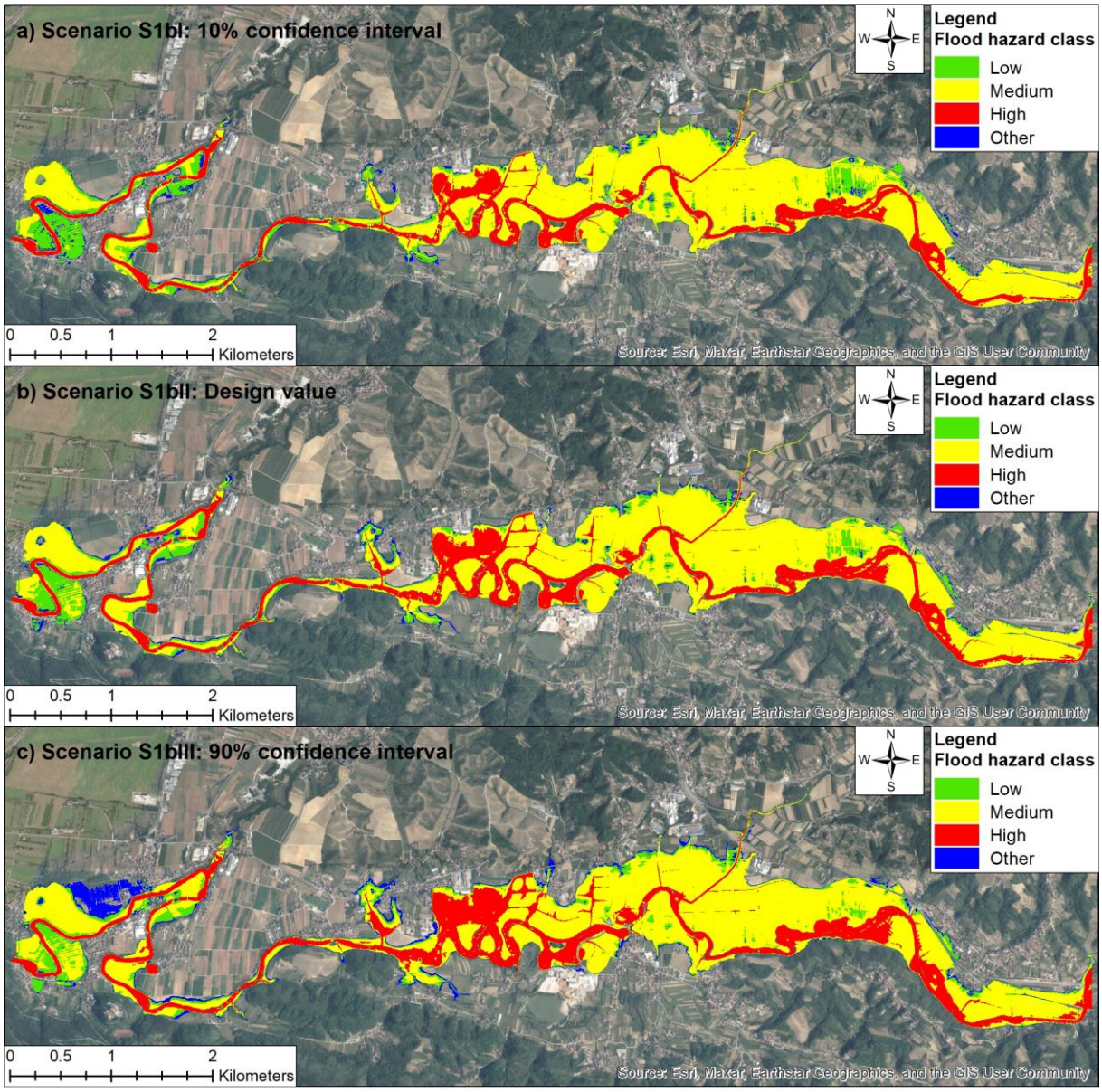

Figure 22. Flood hazard maps for scenarios S1b – different peak discharge confidence intervals

Figure 23. Comparison of the flood extension for scenarios S1b – different peak discharge confidence intervals

As expected, the flood extent increases with the peak discharge for all analyzed flood return periods, showing the largest range of variability when compared to the scenarios which analyze the uncertainties in the hydrograph shape and floodplain Manning's coefficients. The increase in the flood inundation area when comparing the results associated with the 10% confidence interval value and the design discharge peak value is 5-6%, while the difference in the flood extension between the design discharge value and the 90% confidence interval value is 4-7%. The difference in the flood extent between the scenarios of 10% and the 90% confidence interval values is about 11%, 9%, and 12% for 10-, 100-, and 500-years return periods, respectively (Figure 23).

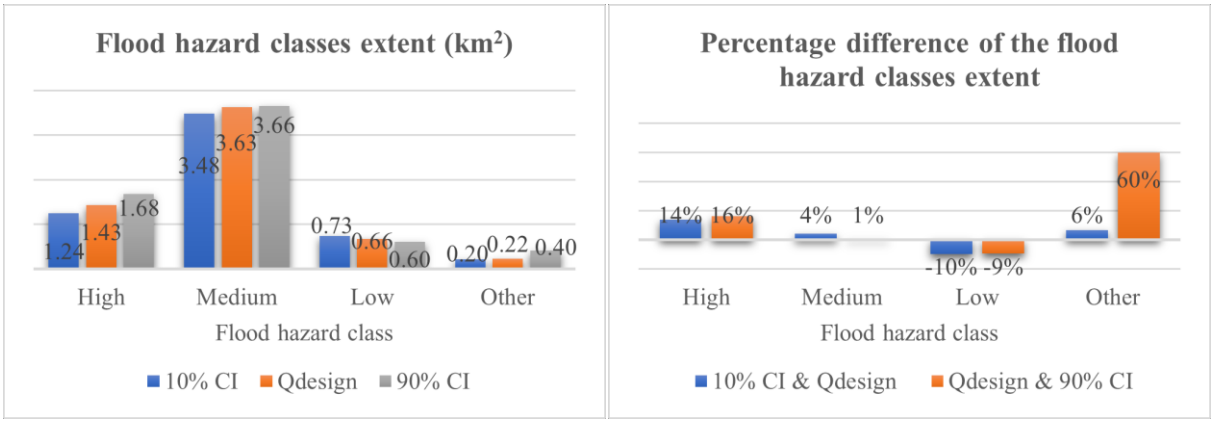

Figure 24. Comparison of the spatial distribution of flood hazard classes for scenarios S1b – different peak discharge confidence intervals

The increase in the overall flood-prone area promotes the spatial expansion of the high flood hazard class, which is about 30% when comparing the scenarios of 10% and 90% confidence interval discharge values. The medium flood hazard class area slightly increases as well, whereas the low hazard class area decreases at the expense of higher hazard classes expansion. The spatial expansion of the other flood hazard class largely increases with the peak discharge (60% between the design and 90% confidence interval values), mainly on the right bank downstream where the floodplain is relatively flat, which can be perceived in Figure 21.

5.2 S2) Influence of floodplain Manning's roughness coefficient variations

This section shows the results of the sensitivity analysis by varying the floodplain Manning's roughness coefficients according to the particular land use in the catchment, showing an expected increase in the flood extent with Manning's coefficients (Figure 25). It should be noted that some small parts downstream show an opposite trend in the inundated area with regard to Manning's coefficients (not shown). However, this trend is observed very locally, hence, can be neglected. It could be associated with the particular topography and land use characteristics, the variability of the overland flow depth, velocity, and direction with changing roughness characteristics, or numerical instability of the hydraulic model. Usually, the flow velocity decreases, and the floodwater depth increases with higher surface roughness. However, the flow velocity may increase with increasing roughness due to the local topography, higher water depths where the effect of the hydraulic roughness could become reduced and other factors. For instance, in steep-slope terrains, the slope highly affects the flow velocities and patterns. Also, the presence of rills, tillage marks, field borders, and infrastructure can change the overland flow pathways (Darboux, 2011; Govers et al., 2000).

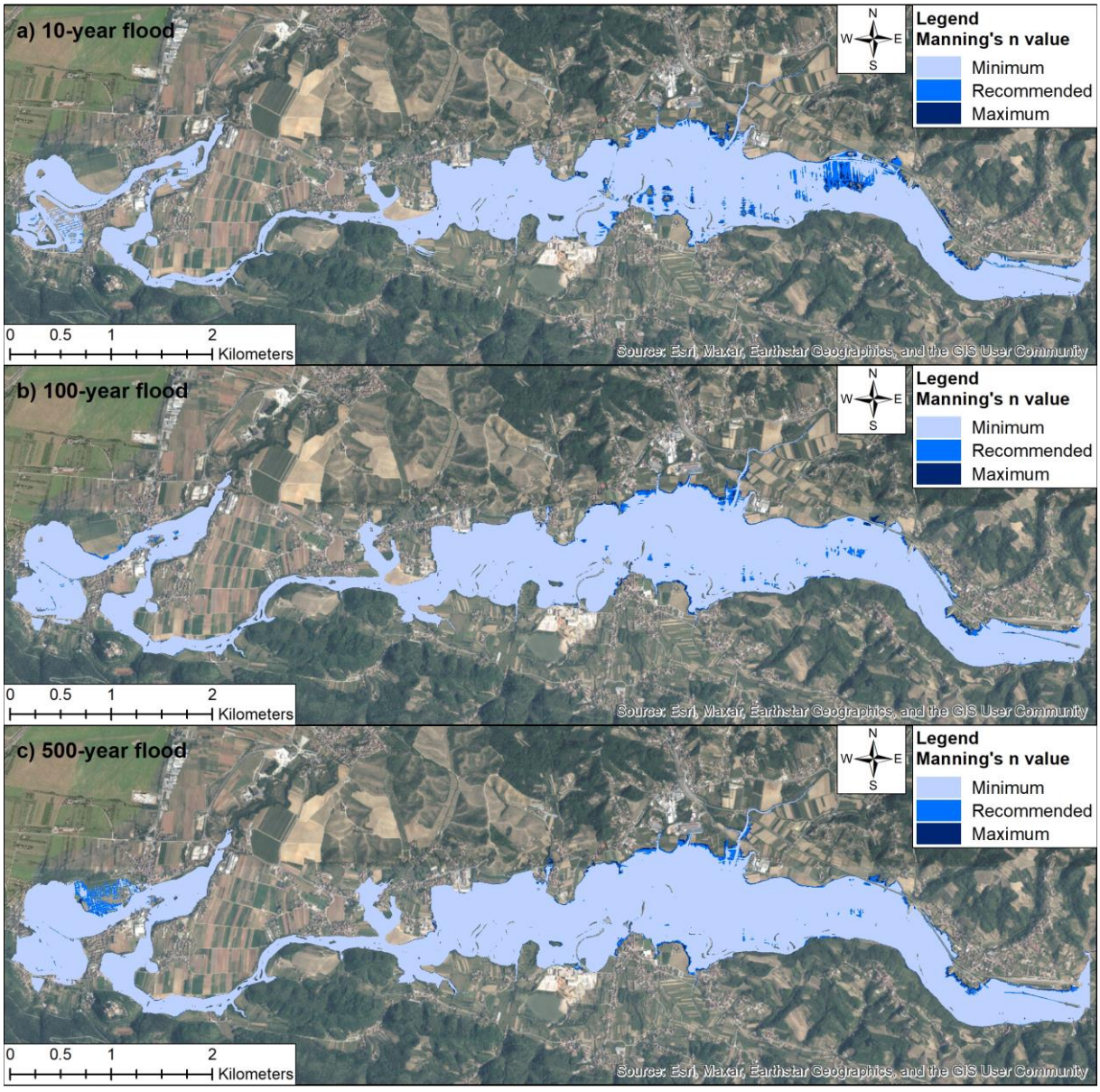

Figure 25. Flood inundation maps for scenarios S2 – different floodplain Manning's coefficient values

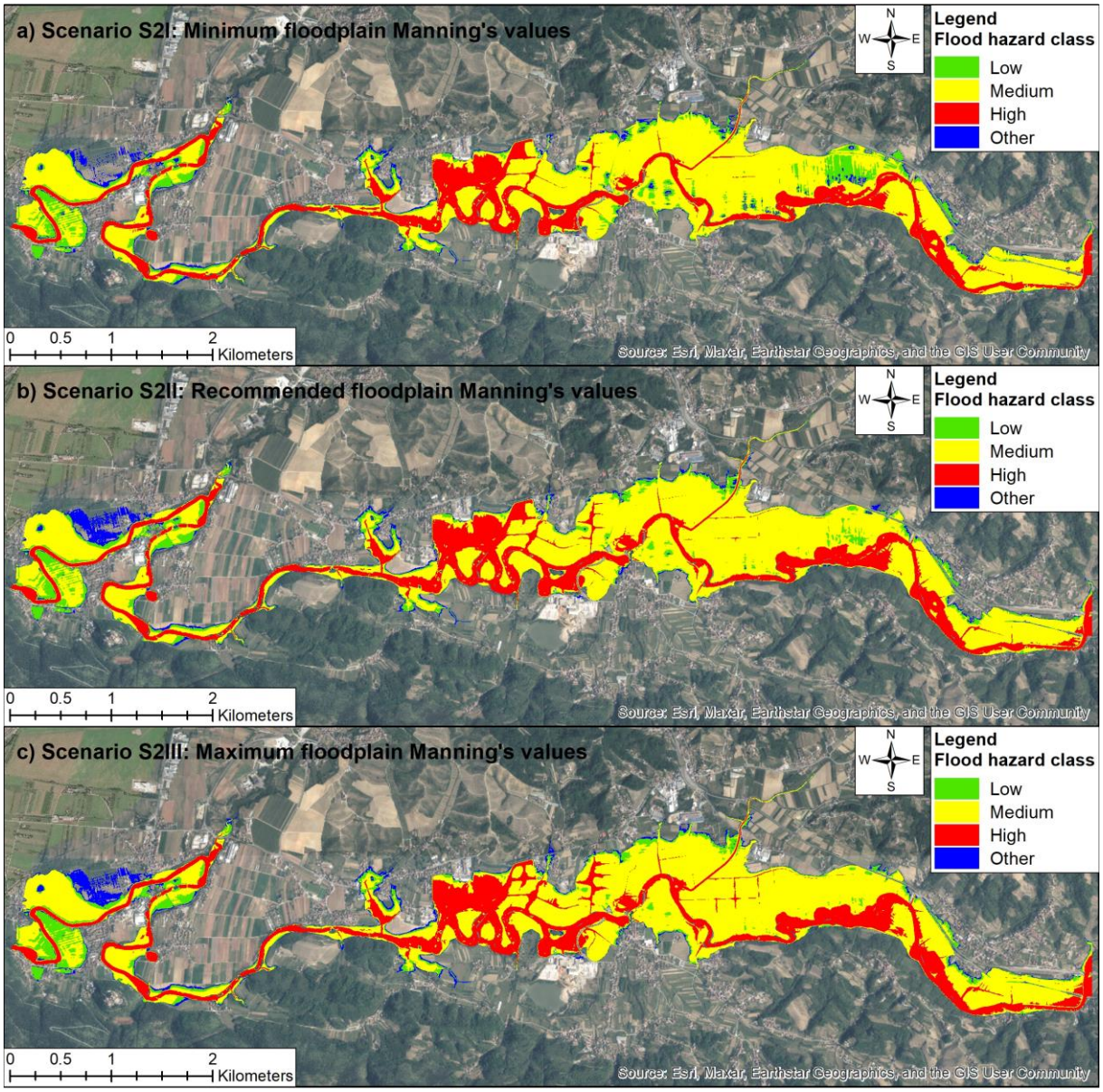

Figure 26. Flood hazard maps for scenarios S2 – different floodplain Manning's coefficient values

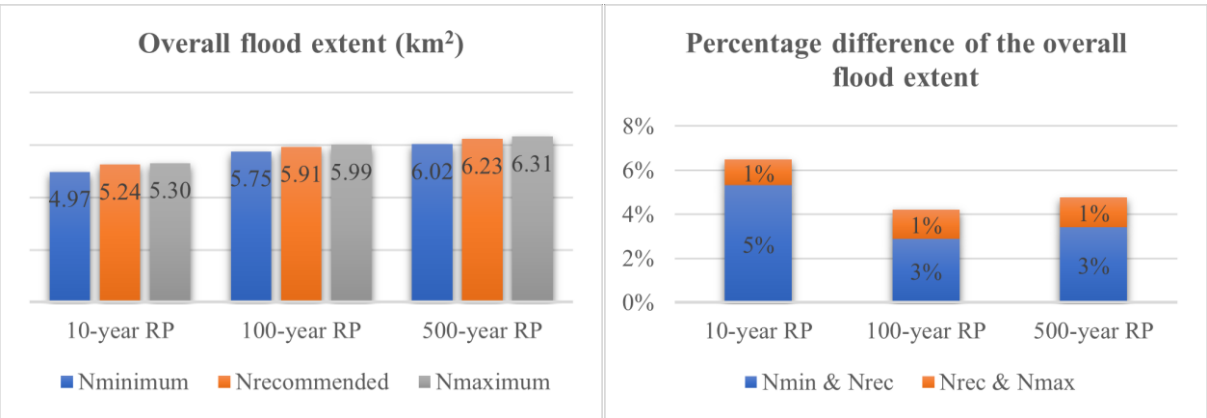

Figure 27. Comparison of the flood extension for scenarios S2 – different floodplain Manning's coefficient values

In general, the flood inundation area grows with increasing floodplain Manning's coefficients for all analyzed return periods, which is shown in Figure 27. This is owing to the fact that the higher roughness of the surface decreases the water velocity, consequently, the water depth increases, expanding the inundated areas. Overall, we can conclude that Manning's roughness coefficients of the floodplain do not significantly influence the flood extension looking from the spatial perspective of the whole analyzed Vipava river reach. The difference in the flood extension when comparing the scenarios of minimum and maximum Manning's values is about 6% for a 10-year flood and about 4% for 100- and 500-year floods. These variations are more noticeable in the areas with gentle slopes, mostly on the right bank where the floodplains are more extensively developed, which can be observed in Figure 25.

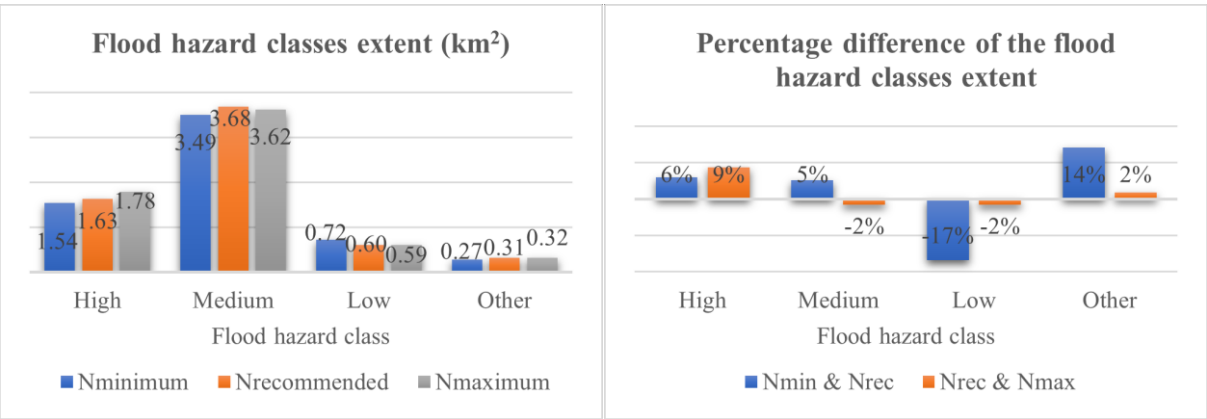

Figure 28. Comparison of the spatial distribution of flood hazard classes for scenarios S2 – different floodplain Manning's coefficient values

Similar to the flood extension, the high flood hazard class expands with increasing floodplain Manning's roughness coefficients. The medium flood hazard class also increases its extension by increasing Manning's coefficients from the minimum to the recommended values. However, with increasing Manning's coefficients from the recommended to the maximum values, the medium flood hazard class decreases. The low flood hazard class also decreases as Manning's coefficients increase. This is because some parts of the flood inundation area which belong to the lower hazard class when considering lower Manning's values will be classified in the higher hazard class for larger Manning's values. The other flood hazard class increases with Manning's roughness coefficients. The highest is the variation in the low flood hazard class spatial extent, amounting to 19% between the scenarios of minimum and maximum Manning's coefficients, depicted in Figure 28.

5.3 S3) Influence of channel Manning's roughness coefficient variations

When some sections of the Vipava river were regulated and widened several decades ago, the design Manning's values of the river channel were in the range of 0.030 to 0.035. However, there have been some local man-made interventions in the river channel and generally, the channel cross-section became successively overgrown by the riparian vegetation since then, and the recent flood events evinced an increase in the channel hydraulic roughness. In this analysis, the flood extension and hazard classes obtained from the simulation with the foreseen channel Manning's coefficient value, which was taken to be 0.035, and the calibrated values against past flood events, which are in the range of 0.03 to 0.078, are compared. Figure 29 shows a relatively larger variation of flood inundation area for a recurrence interval of a 10-year return period when compared to the previously analyzed scenarios, demonstrating a significant sensitivity of the results to the channel roughness for more frequent floods. Namely, higher Manning's values of the main channel considerably reduce the channel hydraulic conductivity, consequently, the flow overtops the channel banks more intensively already during discharges with a lower return period - Q10.

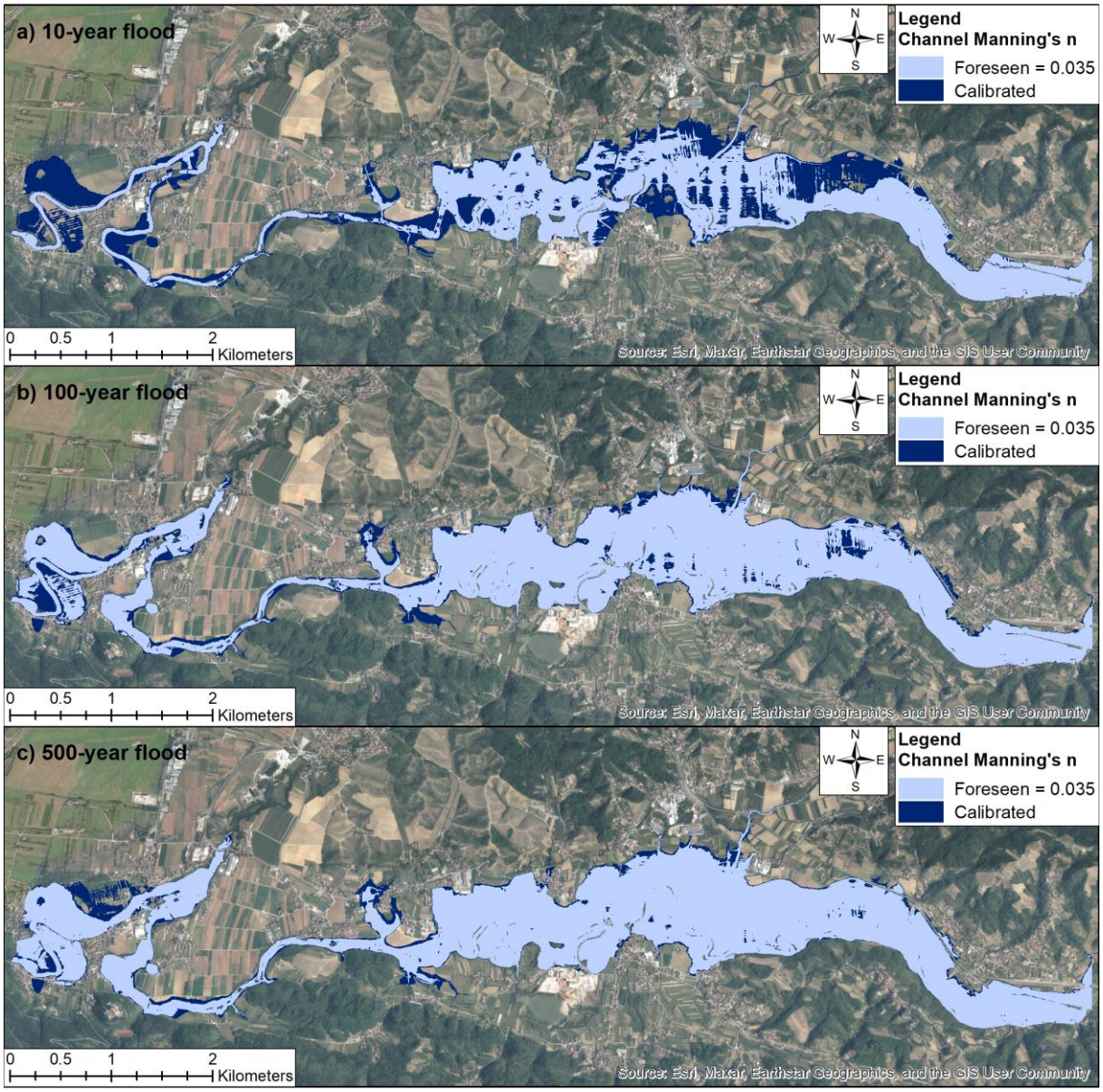

Figure 29. Flood inundation maps for scenarios S3 – different channel Manning's coefficient values

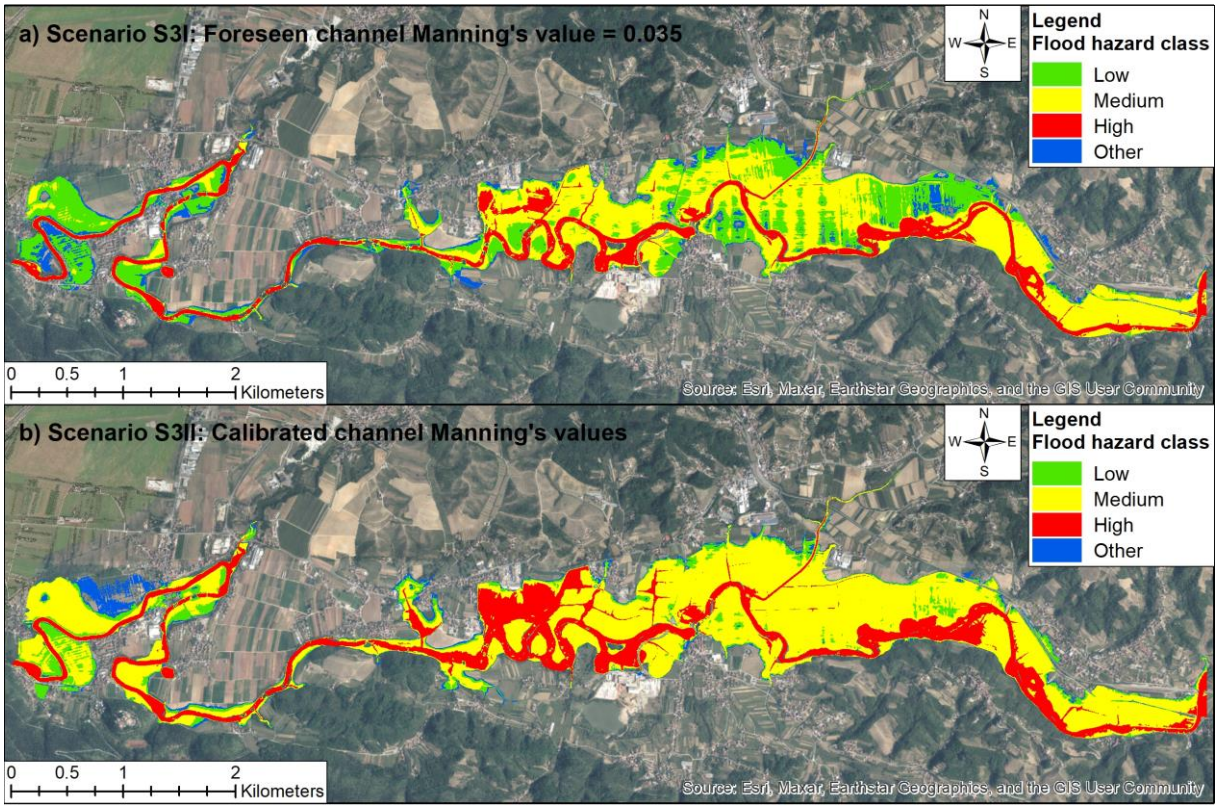

Figure 30. Flood hazard maps for scenarios S3 – different channel Manning's coefficient values

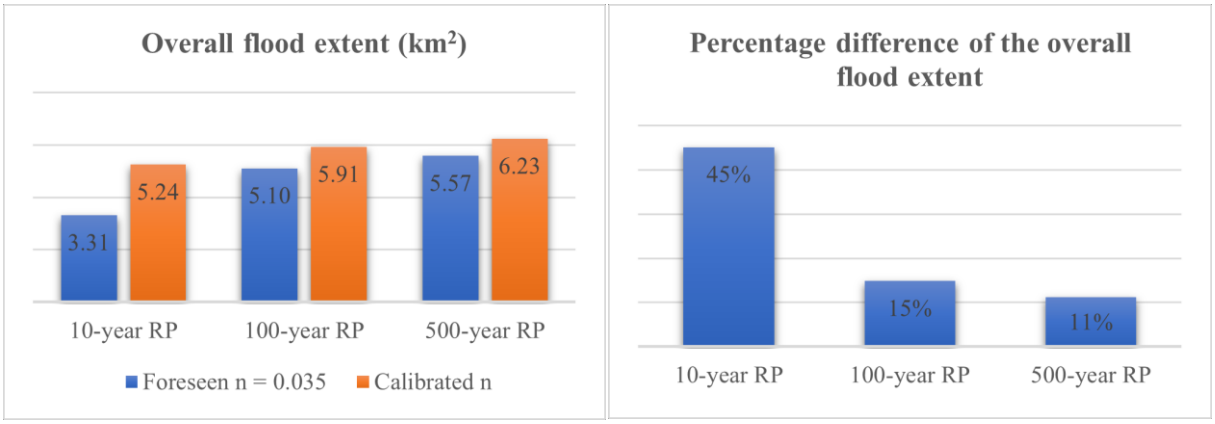

Figure 31. Comparison of the flood extension for scenarios S3 – different channel Manning's coefficient values

Changes in the channel Manning's roughness coefficient produced a noticeable increase in the flood extension and spatial expansion of higher flood hazard classes. The difference in the inundated area when comparing the results associated with the foreseen and the calibrated channel Manning's coefficients is highest for a 10-year flood return period, amounting to 45%. For 100- and 500-year flood events, the flood extension increased by about 15% and 11%, respectively.

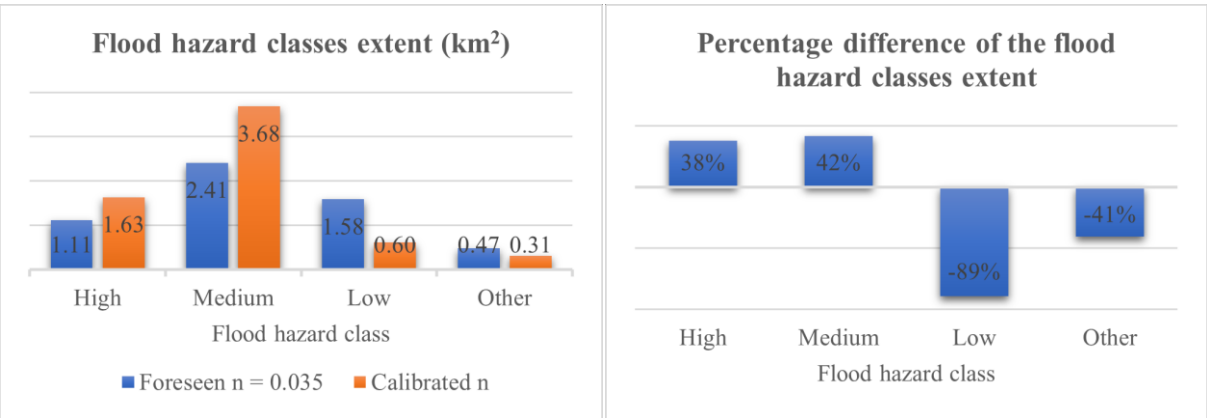

Figure 32. Comparison of the spatial distribution of flood hazard classes for scenarios S3 – different channel Manning's coefficient values

The increase in flood-prone areas is further reflected in the flood hazard classes extent. The spatial distribution of the high and the medium flood hazard class shows an increasing trend of 38% and 42%, respectively, whereas a decreasing trend of 89% and 41% is perceptible for the low and the other flood hazard class, respectively. It should be noted that the lower hazard classes shift at the expense of the higher hazard classes increase (Figure 30), which also causes this decreasing trend in the areas occupied by the lower flood hazard classes.

5.4 Maximum difference in the flood extension considering all scenarios S1-S3

The maximum variation in the flood extent considering all scenarios S1-S3 is perceived between Scenario S1aIII (wide flow hydrograph shape) and Scenario S3I (foreseen channel Manning's coefficient = 0.035) and illustrated in Figure 33. However, as beforementioned, the sensitivity of the flood extension with respect to variations in the flow hydrograph shape is negligible. Consequently, this supports the finding that changes in the channel Manning's coefficients produce the largest variations in the flood-prone area for this specific case, especially for a 10-year flood, with regard to scenarios S1a and S2. However, it cannot be visually directly compared with scenarios S1b, which assess the uncertainty in the peak discharge values, due to the different discharge values as input for the hydraulic model. As beforementioned, in all analyses, the peak discharge values from the official hydrological study of the Vipava river (Anzeljc, 2021) were taken, except for scenarios S1b, which consider other peak discharge values from a master's thesis at UL FGG (Piry, 2020) due to the availability of different confidence intervals of those design values.

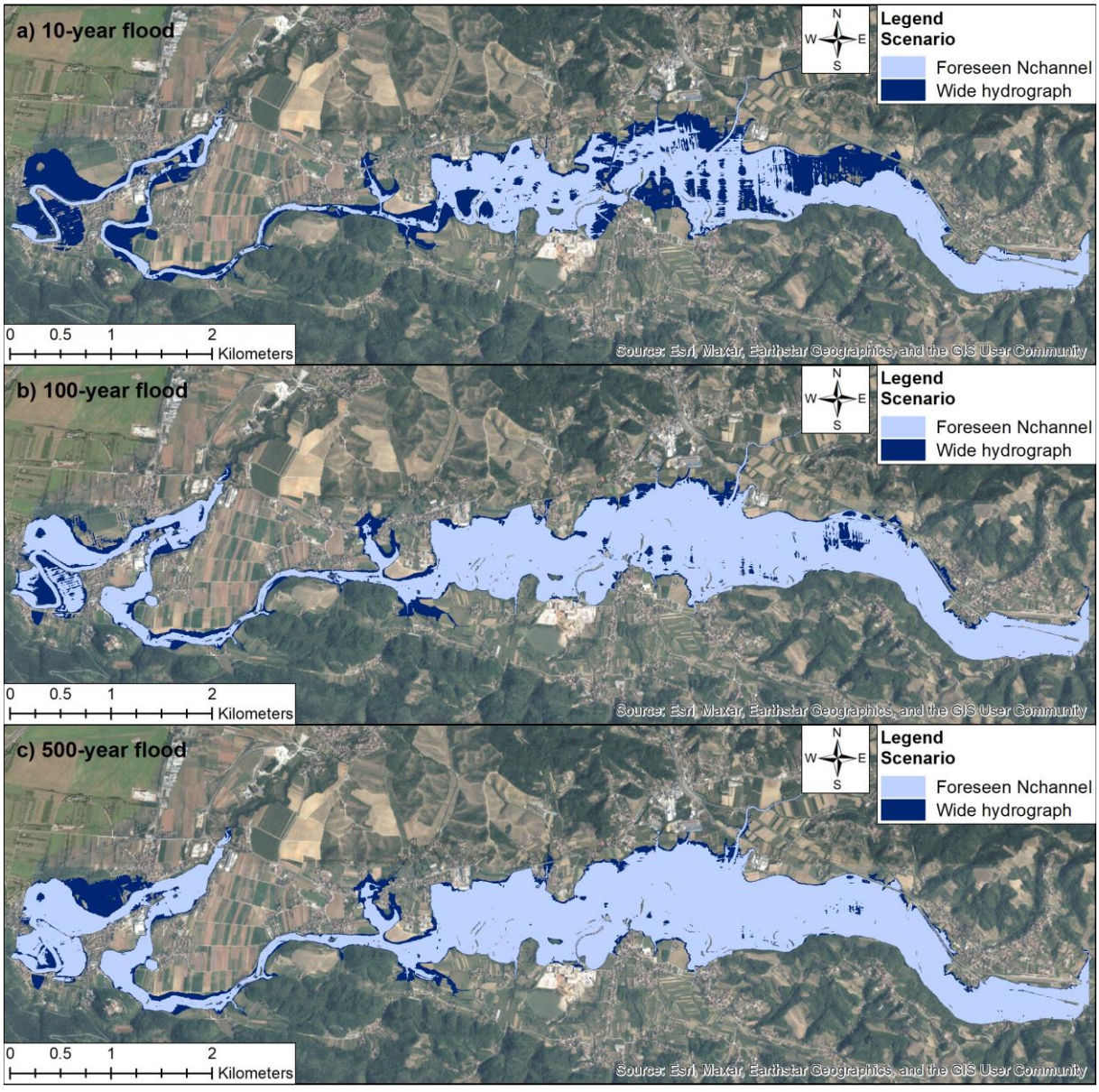

Figure 33. Maximum differences in the flood extension considering all scenarios S1-S3

5.5 Land use in flood-prone areas

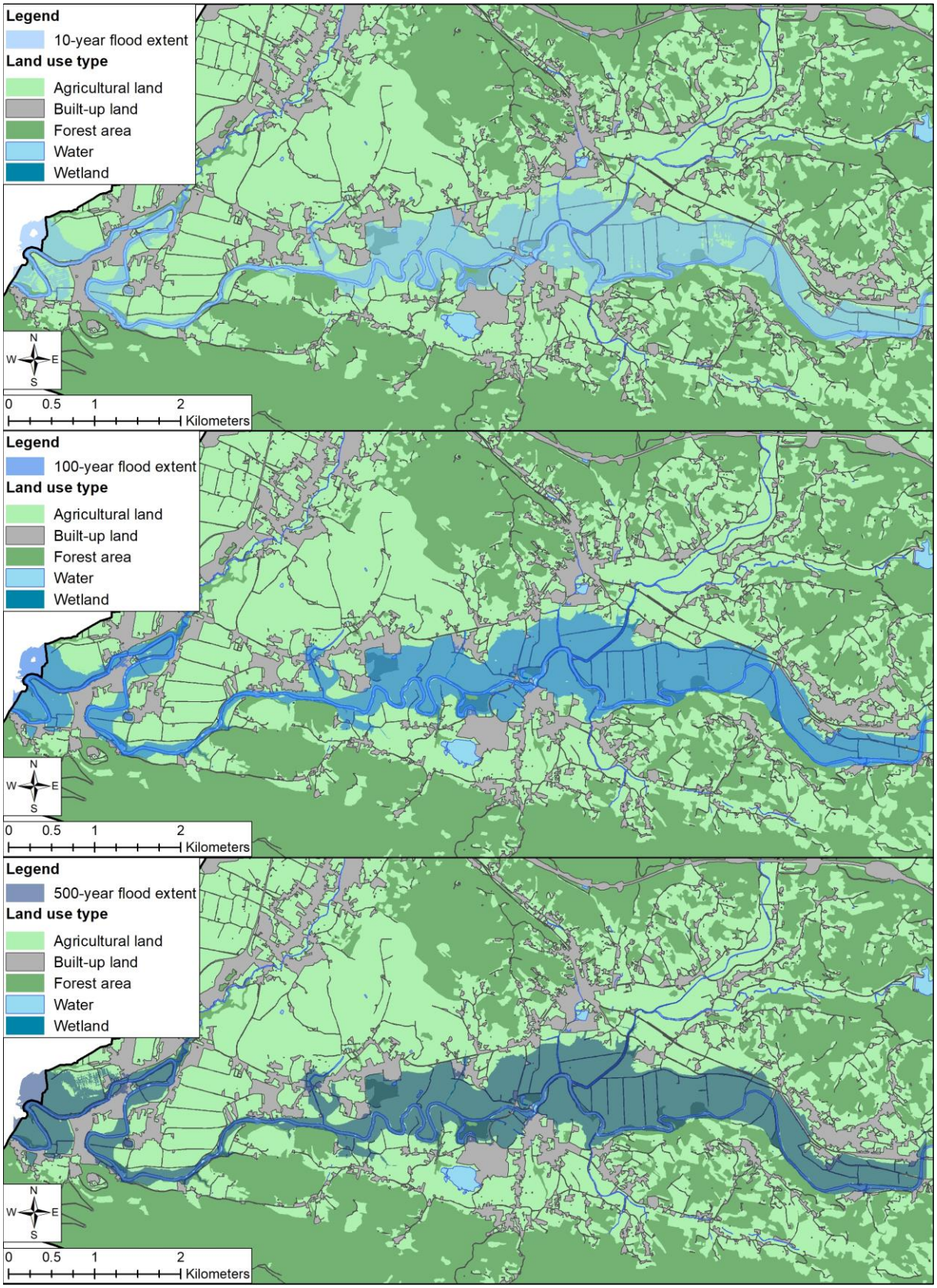

Figure 34. Affected land use for Scenario S2II for 10-, 100-, and 500-year return periods (source: MKGP)

As illustrated in Figure 34, the agricultural land comprises the largest part of land use located in flood-prone areas, which for Scenario S2II is 4.05 km^2, 4.60 km^2, and 4.85 km^2 for 10-, 100-, and 500-year floods, respectively. Most of the forest area is not within the floodplains due to its location at higher altitudes. Moreover, it is worth noting that built-up areas cover a relatively small part of the catchment compared to other land use types and are very dispersed. From the built-up land, the most vulnerable to floods is the road infrastructure. A very small portion of buildings is within the flood inundation area due to the recent flood control measures – sediment cleaning in the downstream area, which has to a certain extent increased the river channel hydraulic conveyance, preventing water to overflow from the river channel. Accordingly, changes in flood-prone areas of the agricultural and built-up land were analyzed for the scenarios S2 – variations in the floodplain Manning's coefficients, for each return period, and presented in Figure 35 and Figure 36.

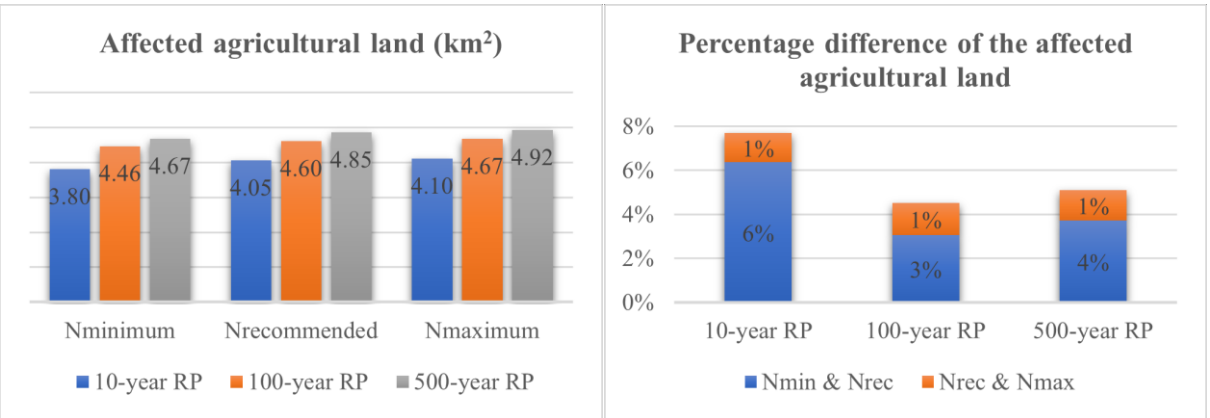

Figure 35. Comparison of the affected agricultural land for scenarios S2 – different floodplain Manning's values

The changes in the affected agricultural area due to variations of the floodplain Manning's coefficient are not significant, showing similar percentage differences as the overall flood extent for all return periods due to the predominance of the agricultural land in the flood-prone zone. The increase in the affected agricultural area between the minimum and maximum floodplain Manning's coefficient scenarios is 7%, 4%, and 5% for 10-, 100-, and 500-year flood return periods, respectively (Figure 35).

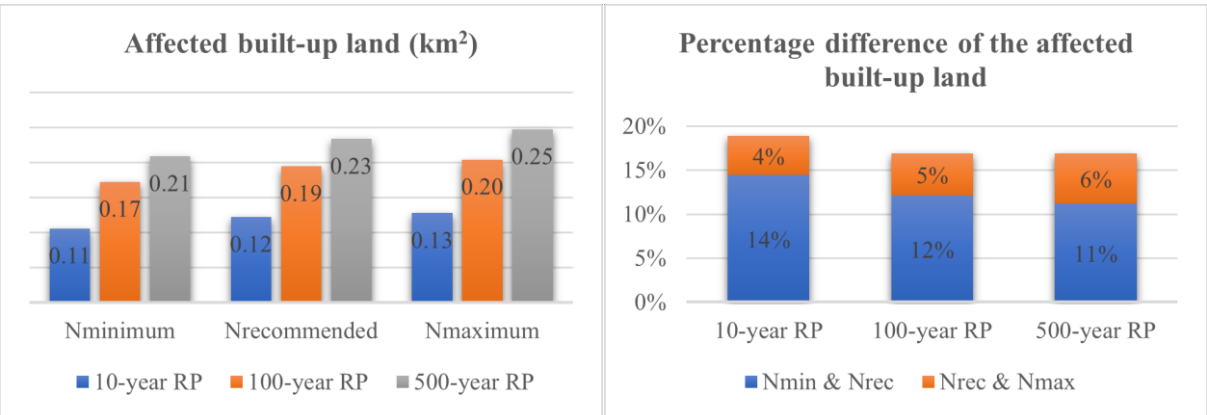

Figure 36. Comparison of the affected built-up land for scenarios S2 – different floodplain Manning's values

The inundated built-up area increases by about 18% for a 10-year flood event and 17% for 100- and 500-year events when comparing the scenarios of minimum and maximum floodplain Manning's coefficients (Figure 36). This difference is more noticeable when compared to the affected agricultural area because the built-up land comprises a much smaller portion of the flood-prone area.

5.6 Comparison of the results with similar studies

The study findings were compared to some similar studies from the literature accounting for different uncertainties in the hydrological and hydraulic inputs and parameters. A study of the Marta river catchment in Italy by Annis et al. (2020) which quantified hydrological uncertainty mostly related to limited precipitation time series of 50 years and uncertainty in hydraulic roughness show higher sensitivity of the flood extension related to the hydrological uncertainty with respect to floodplain Manning's values, which is also the case in this analysis. The study area is characterized by relatively flat terrain, a meandering river channel, and mainly agricultural land use as well.

Furthermore, a study of the Douro river reach in the Spanish city of Zamora done by Garrote et al. (2021) revealed a much higher increase in the overall flood-prone area associated with the FFA amounting to 41% when comparing the results associated with the peak flow quantile with the 99% confidence interval value for a 500-year return period flood. The left river bank is characterized by relatively flat terrain, whereas the right river bank has a steep-slope terrain and is largely urbanized due to the location of the Zamora city center, depicting different land use compared to the Vipava river case study. A similarity in the results in regards to the topography can be observed, i.e., higher uncertainties are denoted in the flatter areas of the Douro river catchment as well. Moreover, the increase in the spatial extent of the high hazard class for the Douro river case study is estimated at approximately 20%, which is half of the overall flood extent increase, and all other flood hazard classes show a decreasing trend. However, it should be also noted that different approaches for flood hazard classification were used in the two studies. Apart from the different water depths and flow velocities specific to the study areas, the different hazard classification approaches could be another reason for the lower percentage increase in the high hazard areas with respect to the overall inundated area. Douro river catchment show predominance of the higher hazard class for a 500-year flood return period, whereas for the Vipava river catchment all return periods are incorporated into a single hazard map for each simulation scenario, and the medium hazard class dominates, as previously mentioned.

6 CONCLUSIONS

6.1 Summary

As there are many potential sources of uncertainty in the hydrological and hydraulic monitoring, calculations, and modelling, the flood hazard assessment procedures cannot avoid the introduction of different uncertainties. This study explored hydrological and hydraulic uncertainties affecting flood inundation and sensitivity of hydraulic simulation results and flood hazard class changes by investigating the potential variability caused by the flow hydrograph shape, peak discharge associated with different return periods, and Manning's roughness coefficients of the channel and floodplain, applied for the case study of Vipava river catchment. The study was driven by the need to adequately address the uncertainty associated with the peak discharge derived through probability distributions fitting a relatively short discharge time series for modelling extreme floods and assess the sensitivity of flood hazard mapping on changing roughness characteristics since they vary largely in time and space. Quantifying these uncertainties through a combined 1D/2D hydraulic model in HEC-RAS 6.2, flood inundation and flood hazard maps were proposed, providing more comprehensive outcomes as compared to the deterministic approach. The outcomes of this research could be highly beneficial for the improvement of spatial planning in the area in order to minimize flood-related losses and improve the life of local people. Engineers and experts should particularly take great care when planning some critical infrastructure such as health centers, schools, etc. in the urban areas of the floodplain, and avoid the worst-case flood inundation zones if possible or plan appropriate flood protection. Additionally, insurance companies could use the results of this sensitivity analysis and incorporate them in the insurance policies.

6.2 Conclusions

The results show the greatest sensitivity of the flood extension associated with variations in the channel Manning's coefficients for a 10-year return period flood, with an increase of 45% between Scenario S3I (foreseen channel Manning's coefficient) and Scenario S3II (calibrated channel Manning's coefficients). For 100- and 500-year flood events, the increase in the flood extent is smaller, amounting to 15% and 11%, respectively. The significant increase in the flood extent is propagated in the flood hazard maps, depicting the largest variability in the spatial distribution of flood hazard classes of scenarios S3 when compared to the other uncertainty analyses. Furthermore, the results confirm the higher impact of the uncertainty in the peak discharge with respect to the impact of varying floodplain Manning's coefficients. The uncertainty in the peak discharge estimates is largely influenced by the length of the recorded discharge time series used to determine the peak discharge quantiles, which in this case is 69 years (1950-2018), and the selection of probability distribution to fit the recorded data. Longer measured discharge data allows for a more credible probabilistic analysis, decreasing the discharge quantile variability, and consequently the uncertainty in the flood prediction. In addition, the credible estimation of the peak discharge distribution is crucial for more accurate flood estimates and hazard assessments. The uncertainties in the peak discharge were delimited through the 10% and 90% confidence intervals, and the results reveal a maximum increase in the flood extension of 11%, 9%, and 12% when considering the flood occurrence probabilities of 10-, 100-, and 500-year return periods, respectively. Moreover, the sensitivity analysis of the floodplain roughness shows that the flood inundation extent grows with the floodplain Manning's coefficients, approaching the largest flood-prone area for maximum Manning's roughness values. The variations in the flood extent between the considered Manning's coefficient limits are 6% for a 10-year flood event and 4% for 100- and 500-year events. Lastly, the impact of the flow hydrograph shape variations on flood inundation and hazard maps

is the lowest, showing its lower significance in flood hazard analysis. However, the flow hydrograph is an important factor to consider when planning and designing structural flood protection measures such as dry retention areas as a prevention measure of lowland floods, which have to ensure enough capacity to lower the hydrograph peaks (Brunner et al., 2018). The flow hydrograph changes depict a maximum increase in the flood-prone area of 3% when considering a 10-year return period and 2% for 100- and 500-year return periods. All these changes in the overall flood extent are further reflected in variations of flood hazard classes, which are not uniform and not equally distributed for all but depend on the water depth distribution which is considered the dominant criterion for flood hazard classification. The higher hazard areas show a similar trend to the overall flood extent, with a higher or lower percentage increase, whereas, the lower hazard areas shift at the expense of higher classes increase and show an increasing or decreasing trend, depending on the analyzed scenario and associated water depth values.

These findings are typical for the case study of the Vipava river catchment due to its specific topography, hydrometeorological conditions, and hydraulic properties. The floodplain morphology affects the inundation extension for different return periods as it bounds the maximum flood extent at some parts of the floodplain. Hence, the differences in the spatial extension of the flood-prone areas are less evident in the steep-slope parts of the floodplain. On the contrary, the flatter areas with wider floodplains, which are more pronounced on the right bank, denote more noticeable uncertainty effects, which are reflected in the greater spatial variability of flood extent and hazard classes. As the results show a significant sensitivity of the inundated areas attributed to the channel Manning's values, especially for more frequent floods, any changes in the river channel impacting its roughness should be carefully considered and incorporated in the flood hazard assessment and further spatial planning in the area. Furthermore, the results of the sensitivity analysis of peak discharge highlight the importance of critical decision-making when planning and designing hydraulic structures, flood protection measures, or other infrastructures within the floodplain.

Additionally, affected land use and associated uncertainties related to simulations S2 – varying floodplain Manning's coefficients were analyzed, which may be useful for the improvement of the land use planning from a flood risk perspective. Results point out the predominance of agricultural land in flood-prone areas, with maximum uncertainty of 7%, 4%, and 5% for 10-, 100-, and 500-year floods, respectively. The second largest portion of land use located in the flood-prone areas comprises built-up land, mainly road infrastructure, depicting an uncertainty of 18% for a 10-year flood, and 17% for 100- and 500-year floods when comparing the floodplain Manning's coefficient lower and upper boundaries. It is worth mentioning that a very small portion of buildings is within the flood-prone area due to the effective recent flood control measures – sediment cleaning in the downstream area, which increased the river channel hydraulic conveyance to a certain extent.

The uncertainty analysis could be further expanded by generating a large number of uncertain model inputs/parameters and multiple simulation runs e.g., by using the Monte Carlo or other sampling methods, which provide more detailed information regarding the inundation probability of a certain area. However, such analysis requires enormous amounts of computational cost and time. Nonetheless, the presented results are adequate to quantify the sensitivity of the flood extent and spatial distribution of different flood hazard classes and confirm the dominant sources of uncertainty affecting flood inundation and flood hazard maps for the Vipava river catchment. To sum up, this study highlighted the importance of quantifying the potential uncertainties affecting the whole chain of flood hazard assessment and incorporating them in flood hazard mapping in order to have more detailed information about the potential hazards for further effective flood risk assessment, spatial planning decisions, and management strategies.

7 REFERENCES

Ahmadisharaf, E., Kalyanapu, A. J., & Bates, P. D. (2018). A probabilistic framework for floodplain mapping using hydrological modeling and unsteady hydraulic modeling. *Hydrological Sciences Journal, 63*(12), 1759-1775. doi:10.1080/02626667.2018.1525615

Alfonso, L., Mukolwe, M., & Di Baldassarre, G. (2016). Probabilistic Flood Maps to support decision-making: Mapping the Value of Information. *Water Resources Research, 52*(2), 1026-1043. doi:10.1002/2015wr017378

Alfonso, L., & Tefferi, M. (2015). Effects of Uncertain Control in Transport of Water in a River-Wetland System of the Low Magdalena River, Colombia.

Annis, A., Nardi, F., Volpi, E., & Fiori, A. (2020). Quantifying the relative impact of hydrological and hydraulic modelling parameterizations on uncertainty of inundation maps. *Hydrological Sciences Journal, 65*(4), 507-523. doi:10.1080/02626667.2019.1709640

Anzeljc, D. (2021). Hidrološka študija Vipave. In: Ministrstvo za okolje in prostor - Direkcija Republike Slovenije za vode.

Apel, H., Merz, B., & Thieken, A. (2008). Quantification of uncertainties in flood risk assessment. *International Journal of River Basin Management Intl. J. River Basin Management, 6*, 149-162. doi:10.1080/15715124.2008.9635344

Apel, H., Thieken, A., Merz, B., & Blöschl, G. (2004). Flood Risk Assessment and Associated Uncertainty. *Natural Hazards and Earth System Science, 4*. doi:10.5194/nhess-4-295-2004

Arcement, G. J., & Schneider, V. R. (1989). *Guide for selecting Manning's roughness coefficients for natural channels and flood plains* (2339). Retrieved from http://pubs.er.usgs.gov/publication/wsp2339

Aronica, G., Bates, P., & Horritt, M. (2002). Assessing the uncertainty in distributed model predictions using observed binary pattern information within GLUE. *Hydrological Processes, 16*, 2001-2016. doi:10.1002/hyp.398

Aronica, G., Hankin, B., & Beven, K. (1998). Uncertainty and equifinality in calibrating distributed roughness coefficients in a flood propagation model with limited data. *Advances in Water Resources, 22*(4), 349-365. doi:https://doi.org/10.1016/S0309-1708(98)00017-7

Azizian, A. (2018). *Advanced 1D-2D Unsteady Flow Modeling by HEC-RAS 5.0*. https://www.researchgate.net/publication/325107047_Advanced_1D-2D_Unsteady_Flow_Modeling_by_HEC-RAS_50

Baghel, D. (2018). Methodologies for Flood Hazard Mapping: A Review. *41*, 22-29. https://www.researchgate.net/publication/343761957_Methodologies_for_Flood_Hazard_Mapping_A_Review

Bales, J. D., & Wagner, C. R. (2009). *Sources of uncertainty in flood inundation maps*. Paper presented at the 4th International Symposium on Flood Defence, Toronto, Canada.

Bates, P. D., Horritt, M. S., Aronica, G., & Beven, K. (2004). Bayesian updating of flood inundation likelihoods conditioned on flood extent data. *Hydrological Processes, 18*(17), 3347-3370. doi:https://doi.org/10.1002/hyp.1499

Bessar, M. A., Matte, P., & Anctil, F. (2020). Uncertainty Analysis of a 1D River Hydraulic Model with Adaptive Calibration. *Water, 12*(2), 561. doi:10.3390/w12020561

Beven, K., Lamb, R., Leedal, D., & Hunter, N. (2014). Communicating uncertainty in flood inundation mapping: A case study. *International Journal of River Basin Management, 13*, 1-11. doi:10.1080/15715124.2014.917318

Brilly, M., Kavčič, K., Šraj, M., Rusjan, S., & Vidmar, A. (2014). Climate change impact on flood hazard. *Proceedings of the International Association of Hydrological Sciences, 364*, 164-170. doi:10.5194/piahs-364-164-2014

Brilly, M., Mikoš, M., & Šraj, M. (1999). *Vodne ujme: varstvo pred poplavami, erozijo in plazovi*: University of Ljubljana, Faculty of Civil and Geodetic Engineering. https://www.unesco-floods.eu/wp-content/uploads/2019/05/Vodne-ujme-1999.pdf

Brunner, M., Sikorska-Senoner, A. E., Furrer, R., & Favre, A.-C. (2018). Uncertainty Assessment of Synthetic Design Hydrographs for Gauged and Ungauged Catchments. *Water Resources Research, 54*. doi:10.1002/2017WR021129

Caro Camargo, C., Pacheco-Merchán, O., & Sánchez-Tueros, H. (2019). Calibration of Manning's roughness in non-instrumented rural basins using a distributed hydrological model •. *Dyna (Medellin, Colombia), 86*, 164-173. doi:10.15446/dyna.v86n210.72506

European Commission. (2007). Directive 2007/60/EC of the European Parliament and of the Council of 23 October 2007 on the Assessment and Management of Flood Risks. Official Journal of European Union. https://eur-lex.europa.eu/legal-content/EN/TXT/?uri=celex:32007L0060

Darboux, F. (2011). Surface Roughness, Effect on Water Transfer. In J. Gliński, J. Horabik, & J. Lipiec (Eds.), *Encyclopedia of Agrophysics* (pp. 887-889). Dordrecht: Springer Netherlands. https://link.springer.com/referenceworkentry/10.1007/978-90-481-3585-1_169

Di Baldassarre, G., & Claps, P. (2010). A hydraulic study on the applicability of flood rating curves. *Hydrology Research, 42*. doi:10.2166/nh.2010.098

Di Baldassarre, G., Schumann, G., Bates, P., Freer, J., & Beven, K. (2010). Flood-plain mapping: A critical discussion of deterministic and probabilistic approaches. *Hydrological Sciences Journal-journal Des Sciences Hydrologiques - HYDROLOG SCI J, 55*, 364-376. doi:10.1080/02626661003683389

Domeneghetti, A., Vorogushyn, S., Castellarin, A., Merz, B., & Brath, A. (2013). Probabilistic flood hazard mapping: Effects of uncertain boundary conditions. *Hydrology and Earth System Sciences, 17*, 3127–3140. doi:10.5194/hess-17-3127-2013

Dottori, F., Martina, M. L. V., & Figueiredo, R. (2018). A methodology for flood susceptibility and vulnerability analysis in complex flood scenarios. *Journal of Flood Risk Management, 11*, S632-S645. doi:10.1111/jfr3.12234

Eleftheriadou, E., Giannopoulou, I., & Yannopoulos, S. (2015). *The European Flood Directive: Current Implementation and Technical Issues*. https://www.researchgate.net/publication/283855269_The_European_Flood_Directive_Current_Implementation_and_Technical_Issues

EXCIMAP. (2007). *Handbook on good practices for flood mapping in Europe*: Ministry of Transport, Public Works and Water Management. https://ec.europa.eu/environment/water/flood_risk/flood_atlas/pdf/handbook_goodpractice.pdf

Foster, L., & Maxwell, R. (2018). Sensitivity analysis of hydraulic conductivity and Manning's n parameters lead to new method to scale effective hydraulic conductivity across model resolutions. *Hydrological Processes, 33*. doi:10.1002/hyp.13327

Gangadhara, K. K., & Vemavarapu, S. V. (2020). *Probabilistic Flood Hazard Maps at Ungauged Locations Using Multivariate Extreme Values Approach*. https://ui.adsabs.harvard.edu/abs/2020EGUGA..22..732K

Garrote, J., Peña, E., & Díez-Herrero, A. (2021). Probabilistic Flood Hazard Maps from Monte Carlo Derived Peak Flow Values—An Application to Flood Risk Management in Zamora City (Spain). *Applied Sciences, 11*(14), 6629. doi:10.3390/app11146629

Glas, H., Deruyter, G., De Maeyer, P., Mandal, A., & James-Williamson, S. (2016). Analyzing the sensitivity of a flood risk assessment model towards its input data. *Natural Hazards and Earth System Sciences, 16*, 2529-2542. doi:10.5194/nhess-16-2529-2016

Glen, S. (2018). Latin Hypercube Sampling: Simple Definition. *From StatisticsHowTo.com: Elementary Statistics for the rest of us!* https://www.statisticshowto.com/latin-hypercube-sampling/ (accessed August, 08-2022)

Govers, G., Takken, I., & Helming, K. (2000). Soil roughness and overland flow. *http://dx.doi.org/10.1051/agro:2000114, 20*. doi:10.1051/agro:2000114

Grünthal, G., Thieken, A. H., Schwarz, J., Radtke, K. S., Smolka, A., & Merz, B. (2006). Comparative Risk Assessments for the City of Cologne – Storms, Floods, Earthquakes. *Natural Hazards, 38*(1-2), 21-44. doi:10.1007/s11069-005-8598-0

Haberlandt, U., & Radtke, I. (2014). Hydrological model calibration for derived flood frequency analysis using stochastic rainfall and probability distributions of peak flows. *Hydrology and Earth System Sciences, 18*(1), 353-365. doi:10.5194/hess-18-353-2014

Hall, J., Tarantola, S., Bates, P., & Horritt, M. (2005). Distributed Sensitivity Analysis of Flood Inundation Model Calibration. *Journal of Hydraulic Engineering-asce - J HYDRAUL ENG-ASCE, 131*. doi:10.1061/(ASCE)0733-9429(2005)131:2(117)

Haque, M. M., Rahman, A., & Haddad, K. (2014). Rating Curve Uncertainty in Flood Frequency Analysis: A Quantitative Assessment *Journal of Hydrology and Environment Research, 2*.

Holmes, R. R. (2016). *River rating complexity*. United States. Conference Paper retrieved from https://pubs.usgs.gov/ja/70193968/70193968.pdf

Kalyanapu, A., Burian, S., & McPherson, T. (2009). Effect of land use-based surface roughness on hydrologic model output. *Journal of Spatial Hydrology, 9*, 51-71.

Khaliq, N., Ouarda, T., Ondo, J. C., Gachon, P., & Bobée, B. (2006). Frequency Analysis of a Sequence of Dependent and/or Non-Stationary Hydro-Meteorological Observations: A Review. *Journal of Hydrology, 329*, 534-552. doi:10.1016/j.jhydrol.2006.03.004

Kidson, R., & Richards, K. (2005). Flood Frequency Analysis: Assumptions and Alternatives. *Progress in Physical Geography - PROG PHYS GEOG, 29*, 392-410. doi:10.1191/0309133305pp454ra

Koivumäki, L., Alho, P., Lotsari, E., Käyhkö, J., Saari, A., & Hyyppä, H. (2010). Uncertainties in flood risk mapping: A case study on estimating building damages for a river flood in Finland. *Journal of Flood Risk Management, 3*, 166-183. doi:10.1111/j.1753-318X.2010.01064.x

Komatina, D., & Branisavljević, N. (2005). *Uncertainty analysis as a complement to flood risk assessment*. Belgrade: University of Belgrade, Faculty of Civil Engineering. http://daad.wb.tu-harburg.de/fileadmin/BackUsersResources/Risk/Dejan/UncertaintyAnalysis.pdf

Leedal, D., Neal, J., Beven, K., Young, P., & Bates, P. (2010). Visualization approaches for communicating real-time flood forecasting level and inundation information. *Journal of Flood Risk Management, 3*(2), 140-150. doi:https://doi.org/10.1111/j.1753-318X.2010.01063.x

Magjar, M., Suhadolnik, P., Šantl, S., Vrhovec, Š., Krivograd Klemenčič, A., & Smolar-Žvanut, N. (2016). Vipava River Basin Adaptation Plan. In: BeWater project.

Makkonen, L. (2008). Problems in the extreme value analysis. *Structural Safety, 30*, 405-419. doi:10.1016/j.strusafe.2006.12.001 https://www.researchgate.net/publication/223865887_Problems_in_the_extreme_value_analysis

Mateo-Lázaro, J., Navarro, J. Á., Garcia-Gil, A., & Romero, V. (2016). Flood Frequency Analysis (FFA) in Spanish Catchments. *Journal of Hydrology, 538*, 598-608. doi:10.1016/j.jhydrol.2016.04.058

McCarthy, S., Beven, K., & Leedal, D. (2014). *Framework for assessing uncertainty in fluvial flood risk mapping*: CIRIA. https://eprints.mdx.ac.uk/13836/1/Framework%20for%20assessing%20uncertainty%20in%20fluvial%20flood%20risk%20mapping%20%282%29%20%281%29.pdf

McMahon, T. A., & Peel, M. C. (2019). Uncertainty in stage–discharge rating curves: application to Australian Hydrologic Reference Stations data. *Hydrological Sciences Journal, 64*(3), 255-275. doi:10.1080/02626667.2019.1577555

Merwade, V., Olivera, F., Arabi, M., & Edleman, S. (2008). Uncertainty in Flood Inundation Mapping: Current Issues and Future Directions. *Journal of Hydrologic Engineering - J HYDROL ENG, 13*. doi:10.1061/(ASCE)1084-0699(2008)13:7(608)

Merz, B., Thieken, A. H., & Gocht, M. (2007). Flood Risk Mapping At The Local Scale: Concepts and Challenges. In S. Begum, M. J. F. Stive, & J. W. Hall (Eds.), *Flood Risk Management in Europe: Innovation in Policy and Practice* (pp. 231-251). Dordrecht: Springer Netherlands.

Ministry of Agriculture, Forestry and Food (MKGP). (2006). Interpretacijski ključ: Podroben opis metodologije zajema dejanske rabe kmetijskih in gozdnih zemljišč. https://gis.si/wp-content/uploads/2020/06/RABA_IntKljuc_20131009.pdf

Mustaffa, N., Ahmad, N., & Razi, M. (2016). Variations of Roughness Coefficients with Flow Depth of Grassed Swale. *IOP Conference Series: Materials Science and Engineering, 136*, 012082. doi:10.1088/1757-899X/136/1/012082

National Oceanic and Atmospheric Administration (NOAA) Coastal Services Center. (2012). LIDAR 101: An Introduction to Lidar Technology, Data, and Applications. https://coast.noaa.gov/data/digitalcoast/pdf/lidar-101.pdf

Neal, J., Keef, C., Bates, P., Beven, K., & Leedal, D. (2013). Probabilistic flood risk mapping including spatial dependence. *Hydrological Processes, 27*(9), 1349-1363. doi:https://doi.org/10.1002/hyp.9572

NOAA Office for Coastal Management. (2016). C-CAP Regional Land Cover and Change. https://coast.noaa.gov/digitalcoast/data/ccapregional.html

NRCS - USDA. (2016). Manning's n Values for Various Land Covers To Use for Dam Breach Analyses by NRCS in Kansas. https://rashms.com/wp-content/uploads/2021/01/Mannings-n-values-NLCD-NRCS.pdf

Ordoñez, J. (2019). *BASIC HYDRODYNAMIC CHARACTERISTICS OF TORRENTIAL FLOW*. https://www.researchgate.net/publication/336196866_BASIC_HYDRODYNAMIC_CHARACTERISTICS_OF_TORRENTIAL_FLOW

Pappenberger, F., Beven, K., Frodsham, K., Romanowicz, R., & Matgen, P. (2007). Grasping the unavoidable subjectivity in calibration of flood inundation models: A vulnerability weighted approach. *Journal of Hydrology, 333*, 275-287. doi:10.1016/j.jhydrol.2006.08.017

Pappenberger, F., Beven, K., Ms, H., & Blazkova, S. (2005). Uncertainty in the Calibration of Effective Roughness Parameters in HEC-RAS Using Inundation and Downstream Level Observations. *Journal of Hydrology, 302*, 46-69. doi:10.1016/j.jhydrol.2004.06.036

Pappenberger, F., Frodsham, K., Beven, K., Romanowicz, R., & Matgen, P. (2006). Fuzzy Set Approach to Calibrating Distributed Flood Inundation Models Using Remote Sensing Observations. *Hydrology and Earth System Sciences, 11*. doi:10.5194/hessd-3-2243-2006

Pappenberger, F., Matgen, P., Beven, K., Henry, J.-B., Pfister, L., & Fraipont, P. (2006). Influence of Uncertain Boundary Conditions and Model Structure on Flood Inundation Predictions. *Advances in Water Resources, 29*, 1430-1449. doi:10.1016/j.advwatres.2005.11.012

Pasquier, U., He, Y., Hooton, S., Goulden, M., & Hiscock, K. M. (2019). An integrated 1D–2D hydraulic modelling approach to assess the sensitivity of a coastal region to compound flooding hazard under climate change. *Natural Hazards, 98*(3), 915-937. doi:10.1007/s11069-018-3462-1

Piry, M. (2020). *Analiza projektnih pretokov z upoštevanjem negotovosti.* (Master's thesis), University of Ljubljana, Faculty of Civil and Geodetic Engineering, Ljubljana. (502/504:556.047/048(497.4)(043.3)) https://repozitorij.uni-lj.si/Dokument.php?id=138645&lang=slv

Poljansek, K., Casajus Valles, A., Marin Ferrer, M., Artes Vivancos, T., Boca, R., Bonadonna, C., Branco, A., Campanharo, W., De Jager, A., De Rigo, D., Dottori, F., Durrant Houston, T., Estreguil, C., Ferrari, D., Frischknecht, C., Galbusera, L., Garcia Puerta, B., Giannopoulos, G., Girgin, S., Gowland, R., Grecchi, R., Hernandez Ceballos, M. A., Iurlaro, G., Kambourakis, G., K arlos, V., Krausmann, E., Larcher, M., Lequarre, A. S., Liberta`, G., Loughlin, S. C., Maianti, P., Mangione, D., Marques, A., Menoni, S., Montero Prieto, M., Naumann, G., Jacome Felix Oom, D., Pfieffer, H., Robuchon, M., Necci, A., Salamon, P., San-Miguel-Ayanz, J., Sangiorgi, M., Raposo De M. Do N. E S. De Sotto Mayor, M. L., Theocharidou, M., Trueba Alonso, C., Theodoridis, G., Tsionis, G., Vogt, J., & Wood, M. (2021). *Recommendations for National Risk Assessment for Disaster Risk Management in EU* (Vol. 1). Luxembourg: Publications Office of the European Union. https://publications.jrc.ec.europa.eu/repository/handle/JRC123585

Romanowicz, R., & Beven, K. (2003). Estimation of flood probabilities as conditioned on event inundation maps. *Water Resources Research - WATER RESOUR RES, 39*. doi:10.1029/2001WR001056

Rusjan, S., Vidmar, A., & Brilly, M. (2012). *The transboundary Soča and Vipava river flood problems*. Paper presented at the EGU Leonardo Conference, Torino.

Sanz-Ramos, M., Bladé, E., González-Escalona, F., Olivares, G., & Aragón-Hernández, J. L. (2021). Interpreting the Manning Roughness Coefficient in Overland Flow Simulations with Coupled Hydrological-Hydraulic Distributed Models. *Water, 13*(23), 3433.

Seewig, J. (2013). *B6.2 - The Uncertainty of Roughness Parameters*. https://www.researchgate.net/publication/347690003_B62_-_The_Uncertainty_of_Roughness_Parameters

Sharafati, A., Khazaei, M. R., Nashwan, M. S., Al-Ansari, N., Yaseen, Z. M., & Shahid, S. (2020). Assessing the Uncertainty Associated with Flood Features due to Variability of Rainfall and Hydrological Parameters. *Advances in Civil Engineering, 2020*, 7948902. doi:10.1155/2020/7948902

Sharifi, M., Majdzadeh Tabatabai, M. R., & Ghoreishi Najafabadi, S. H. (2020). Determination of river design discharge (Tar River case study). *Journal of Water and Climate Change, 12*(2), 612-626. doi:10.2166/wcc.2020.278

Simões, N., Ochoa-Rodríguez, S., Wang, L.-P., Pina, R., Marques, A., Onof, C., & Leitão, J. (2015). Stochastic Urban Pluvial Flood Hazard Maps Based upon a Spatial-Temporal Rainfall Generator. *Water, 7*(12), 3396-3406. doi:10.3390/w7073396

Stephens, T. A., & Bledsoe, B. P. (2020). Probabilistic mapping of flood hazards: Depicting uncertainty in streamflow, land use, and geomorphic adjustment. *Anthropocene, 29*, 100231. doi:https://doi.org/10.1016/j.ancene.2019.100231

Suhadolnik, P. (2016). BeWater Project. Retrieved from http://www.bewaterproject.eu/ (accessed August, 08-2022)

Triglav Čekada, M., Bric, V., Kete, P., Mongus, D., Lukač, N., & Žalik, B. (2015). *Nationwide aerial laser scanning for 3D-acquisition of water surfaces in Slovenia*. Paper presented at the Capturing Reality, Salzburg.

USACE. (2022a). *HEC-RAS 2D User's Manual*. https://www.hec.usace.army.mil/confluence/rasdocs/r2dum/latest (accessed August, 08-2022)

USACE. (2022b). *HEC-RAS User's Manual*. https://www.hec.usace.army.mil/confluence/rasdocs/rasum/latest (accessed August, 08-2022)

Vatanchi, S. M., & Maghrebi, M. F. (2019). Uncertainty in Rating-Curves Due to Manning Roughness Coefficient. *Water Resources Management, 33*(15), 5153-5167. doi:10.1007/s11269-019-02421-6

Vojinović, Z. (2012). *Flood Risk and Social Justice: From Quantitative to Qualitative Flood Risk Assessment and Mitigation* (Vol. 11). London: IWA Publishing.

Wernhart, S., Lenhardt, W., Weginger, S., Pignone, F., Rebora, N., Polese, M., Borzi, B., Faravelli, M., Tocchi, G., Prota, A., Cipranić, I., Ostojić, M., Pejović, J., Serdar, N., Mikoš, M., Rusjan, S., Lebar, K., Vidmar, A., Dolšek, M., Babič, A., Žižmond, J., Sinković, N. L., Doganay, E., Kilic, N., Kadirioğlu, F. T., & Alkan, M. A. (2021). EU project BORIS Deliverable D2.2: Data availability and needs for large scale and cross-border risk assessment, obstacles and solutions.

Westerberg, I., & McMillan, H. (2015). Uncertainty in hydrological signatures. *Hydrology and Earth System Sciences, 19*, 3951-3968. doi:10.5194/hess-19-3951-2015

Wikipedia. (2021). Vipava (river). Retrieved from https://en.wikipedia.org/wiki/Vipava_(river) (accessed August, 08-2022)

Zahmatkesh, Z., Han, S., & Coulibaly, P. (2021). Understanding Uncertainty in Probabilistic Floodplain Mapping in the Time of Climate Change. 13, 1248. doi:10.3390/w13091248

8 APPENDICES

8.1 Appendix A: Comparison of the spatial extent of flood hazard classes for all scenarios

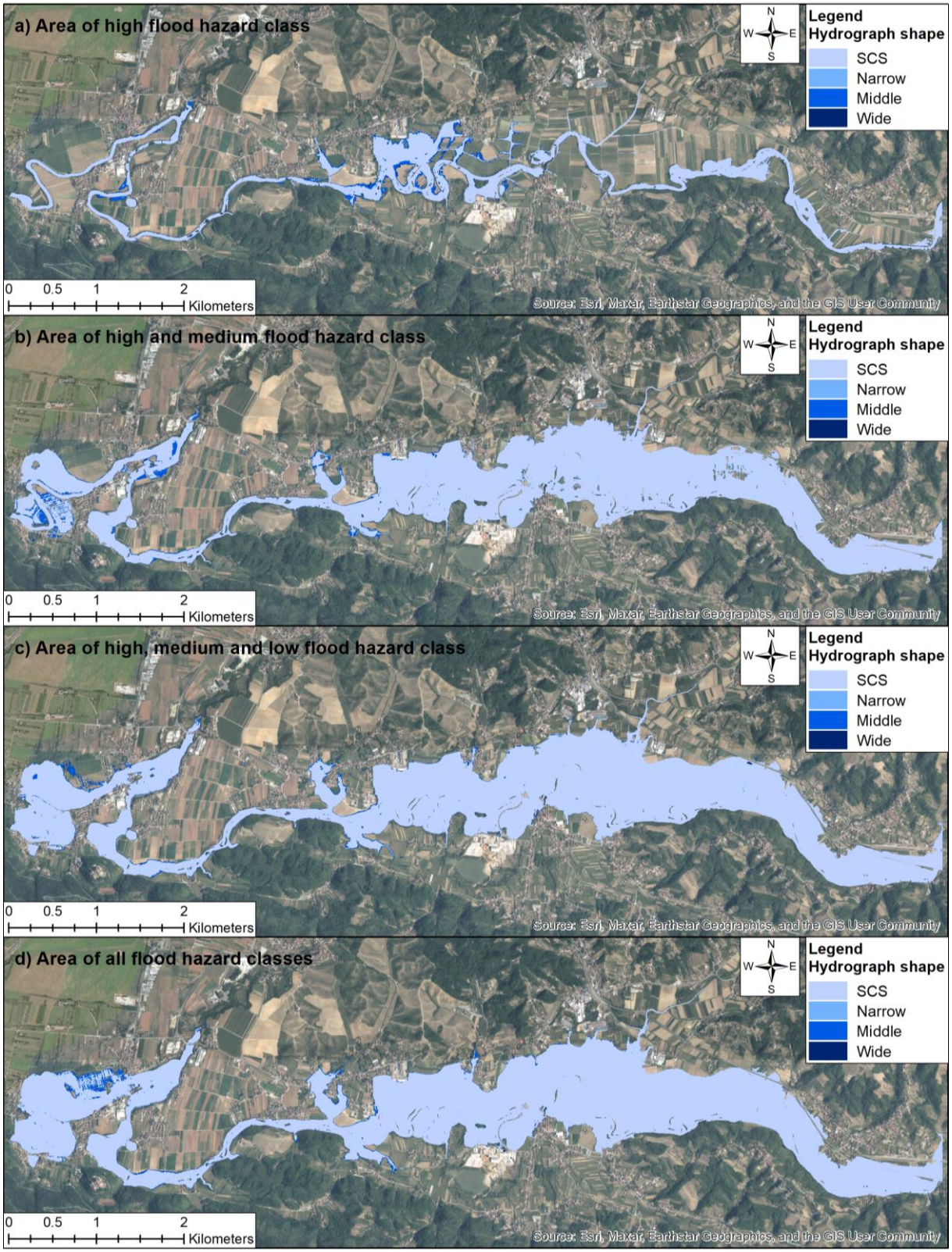

Figure 37. Comparison of the spatial extension of flood hazard classes for scenarios S1a – different flow hydrograph shapes

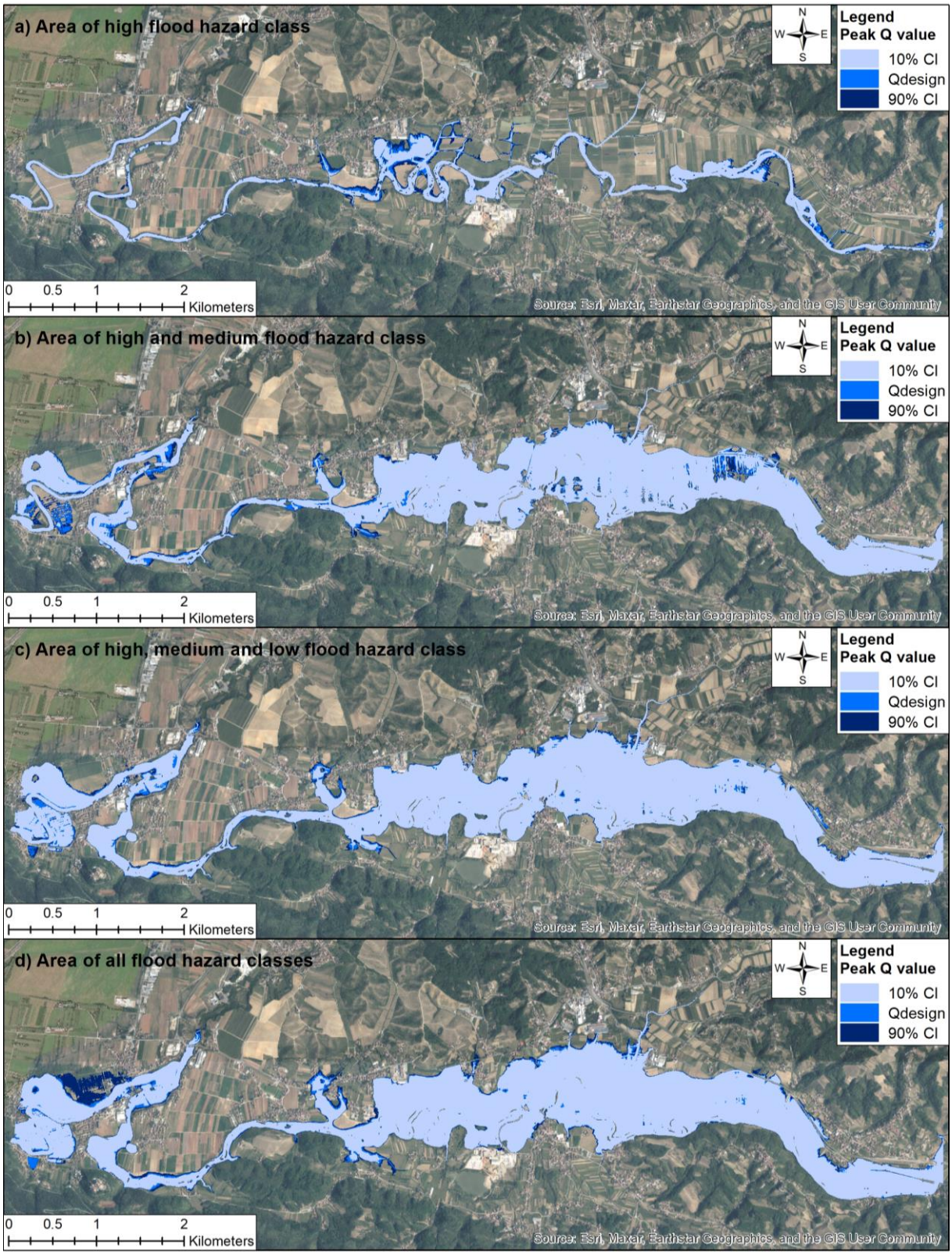

Figure 38. Comparison of the spatial extension of flood hazard classes for scenarios S1b – different peak discharge confidence intervals

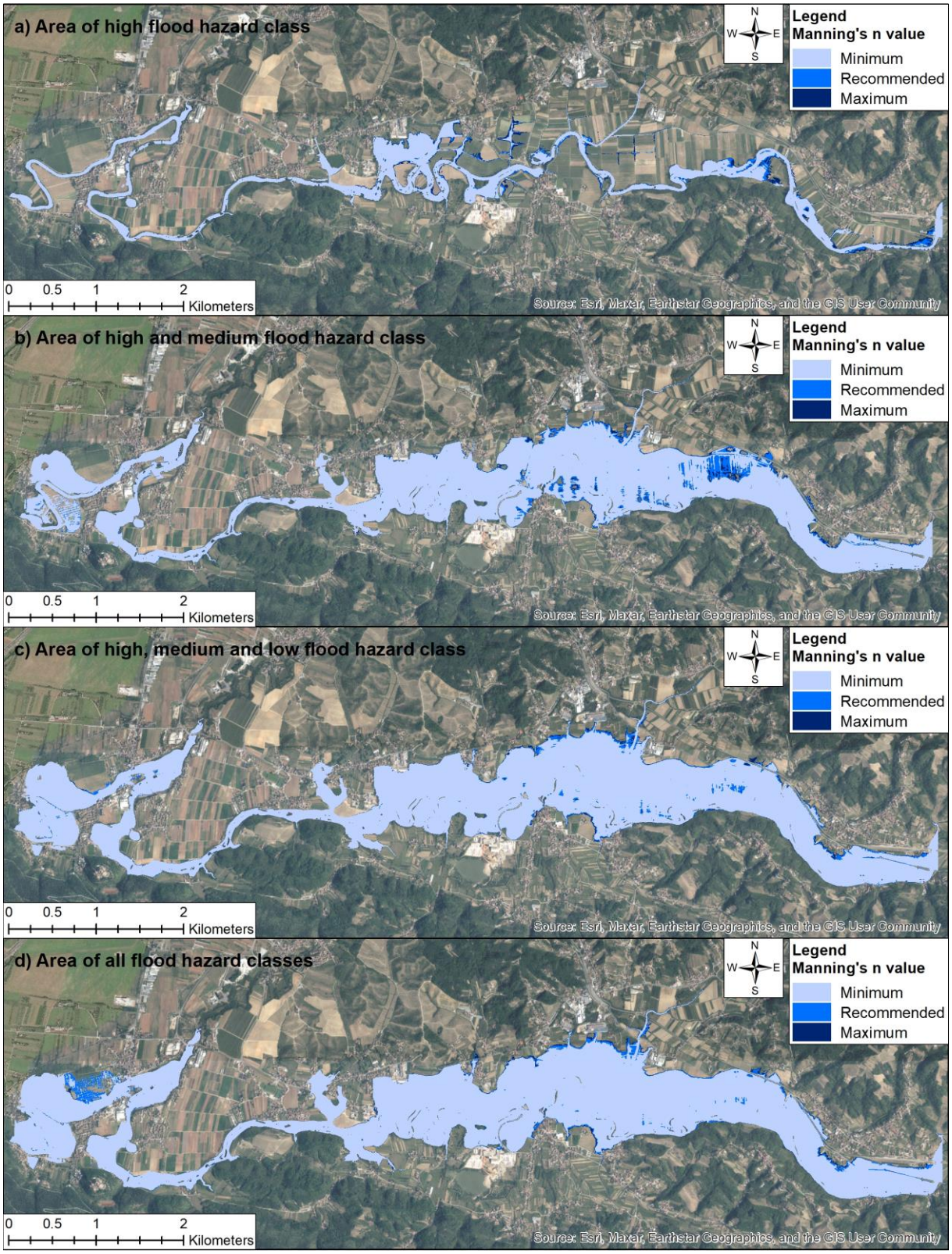

Figure 39. Comparison of the spatial extension of flood hazard classes for scenarios S2 – different floodplain Manning's coefficient values

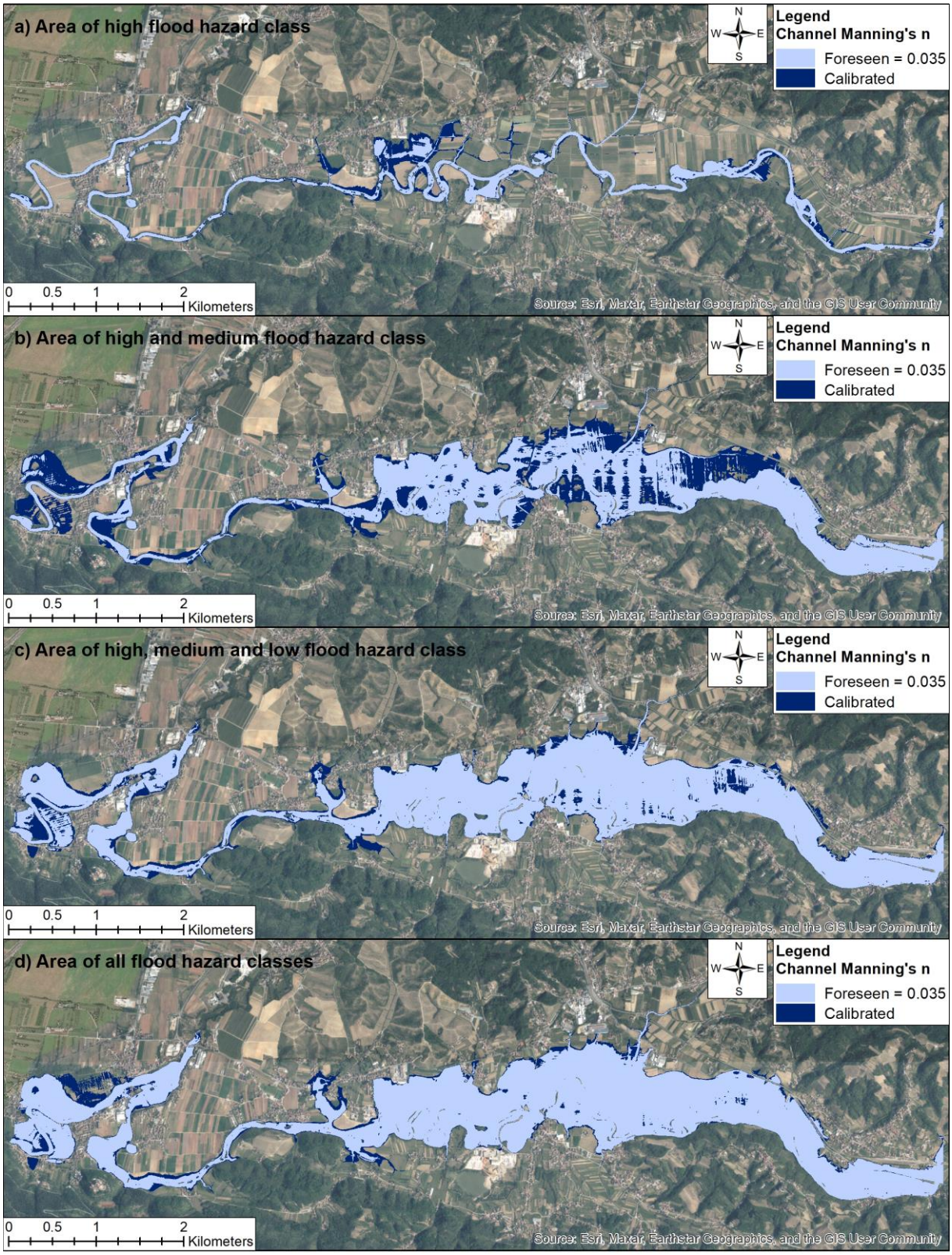

Figure 40. Comparison of the spatial extension of flood hazard classes for scenarios S3 – different channel Manning's coefficient values